SYNTHESIS AND REACTIVITY OF ELECTRON-RICH RUTHENIUM AND IRON HALF-SANDWICH COMPLEXES

Thesis by

Rocco Angelo Paciello

In Partial Fulfillment of the Requirements

for the Degree of

Doctor of Philosophy

California Institute of Technology

Pasadena, California

1987

(Submitted May 13, 1987)

Acknowledgements

It is difficult to acknowledge all of the people that become important to you during five years of your life. Members of the Bercaw group, past and present, have made life interesting, and sometimes amusing. Nancy, Paul, and Greg answered a lot of questions when I first started, or at least stood still long enough so that I could watch. Antonio, Don, and Larry worked on some of the projects in this thesis. Work aside, there have been a lot of hikes, softball, and beers, which have always been fun. Van's always been good for some metaphysical b.s., and numerous book loans. Ray's been a room-mate and a friend. Ramsey made it clear that sometimes life could be very serious. Outside of the group, George "Mama" Spies nagged me through courses and candidacy, and Doug Meinhart helped with the NMR. Bernard Santarsiero pounded out the structure in Chapter 1.

I've been lucky enough to be able to spend some time working at DuPont Central Research during the last two years. This was a lot of fun, and educational too. The education was in large part due to Henry Bryndza, who was kind enough and patient enough to put up with a flaky graduate student for a couple of summers. Chunky and Joe did some of the work, and helped with the fun part, as did Tom, Wilson, and Al. Thanks to these folks, I got to visit some of the finest spots in Wilmington. Serious thanks go to the powers that be at Dupont, Steve Ittel for one, who made it possible for me to spend time there.

The biggest thanks go to John Bercaw, who has had to put up with me for quite some time now. Hopefully, he enjoyed our interactions as much as I did. Groups reflect their advisors, and it's been a great group to be in, intellectually and socially.

A special thanks to my parents who've always been there when I've needed them. And to Lynda, who's put up with far more grad student angst and paranoia than anyone deserves.

Abstract: Late transition metal organometallic complexes, $Cp^*(PR_3)_2MX$ ($Cp^* = \eta^5\text{-}C_5Me_5$), with highly electron donating ligand sets have been synthesized and their reactivity studied. Synthetic routes which allow systematic variation of metal (Ru, Fe), phosphines (PMe_3, PEt_3, P^nBu_3, PMe_2Ph, DMPE), and sigma-bonded ligands (halide, hydride, alkyl, heteroatom) have been developed.

Thermally and photochemically induced ligand loss from these complexes has been studied. Trapping and C-H bond activation chemistry have been observed for the transient $[Cp^*(PR_3)MX]$ complexes produced upon ligand loss. The reactivity of analogous ruthenium and iron complexes is compared and discussed.

The Ru(IV) complex, $Cp^*(PMe_3)RuH_3$, has been prepared and isolated. This complex is found to catalyze H-D exchange, and hydrogenations of unsaturated organic species. The analogous Fe(IV) complex, $Cp^*(PMe_3)FeH_3$, has been prepared and observed spectroscopically. Hydrogen bonding modes in these polyhydrides are discussed. Highly fluxional $Cp^*(PMe_3)FeH_3$ is proposed to be in equilibrium with $Cp^*(PMe_3)Fe(\eta^2\text{-}H_2)H$.

An equilibrium method for the determination of relative Ru-X and Ru-Y bond strengths in $Cp^*(PMe_3)_2RuX$ has been developed. A linear correlation of Ru-X to H-X bond strengths has been found over a wide range of ligands, X. The relationship is found to be general for a number of metal centers.

A study of the kinetics of phosphine exchange for $Cp^*(PMe_3)_2RuX$ has been undertaken. The rate of phosphine loss can be abstracted from a treatment of the kinetics of approach to equilibrium. Lone pairs on X are found to promote ligand dissociation. Dative bond dissociation enthalpies are obtained if small, and constant, barriers for ligand recombination are assumed. The functional group approximation used in solution thermochemical studies is found to break down when large changes are made in the steric constraint at the metal center.

Table of Contents

General Introduction: Transition metal centers have been found to activate small molecules, and to serve as templates for the interactions of these ligands. Such processes form the basis for a number of useful stoichiometric and catalytic transformations.[1] It is therefore of interest to understand such fundamental steps as "simple" ligand addition or loss, and to have some sense of the relative thermodynamics of given transformations, if one is to rationally control the reactivity of a given metal center.

One class of transition metal complexes which show an extraordinarily diverse reaction chemistry are the half-sandwich complexes, CpL_nMX_m ($Cp = \eta^5$-C_5H_5).[2] We have been interested in the synthesis and reactivity of a subclass of these complexes of the type $Cp^*(PR_3)_2MX$ ($Cp^* = \eta^5$–C_5Me_5; M = Fe, Ru). The reaction chemistry of these phosphine complexes has been found to be dependent on the metal used, the steric constraint and basicity of the phosphine ligands, and the identity of the σ-bonded ligand, X. We wish to understand how these factors influence the reactivity of these complexes, with the hope that such an understanding could be generalized to other transition metal complexes.

Initial ligand loss dominates the ligand substitution and oxidative addition reactions of coordinatively and electronically saturated complexes such as $Cp^*(PR_3)_2MX$.[1] Subsequent reactivity then depends on the ligand complement around the metal center in the resultant 16-electron complexes, $[Cp^*(PR_3)MX]$.

Complexes such as $Cp^*(PR_3)_2MX$ possess a highly electron-donating ligand complement. For example, it has been shown that the methyl substituents on the cyclopentadienyl groups in permethylmetallocenes shift the d–ionization energies in the photoelectron spectra down almost one electron volt.[3] The highly basic tertiary phosphines are strong sigma donors with limited π–backbonding character.[4] Electronically, the metal center should be capable of supporting higher formal oxidation states, *ie* Ru(II) $\longrightarrow$ Ru(IV).

Therefore, oxidative addition should be reasonably facile in the unsaturated complexes, [Cp*(PR_3)MX]. Trapping of [Cp*(PR_3)MX] with ligands capable of π-backbonding should occur quite readily. The metal center in Cp*$(PR_3)_2$MX should function as a Lewis base.[5] For example, it should be possible to protonate at the metal center to give $[Cp^*(PR_3)_2MHX]^+$.

The necessity of opening a coordination site on the coordinatively and electronically saturated complex Cp*$(PR_3)_2$MX implies that steric factors, *i.e.*, the size of the phosphine and of X, should be important.[6] Thermolysis and photolysis are possible mechanisms for inducing dative ligand loss. Removal of X^- to form $[Cp^*(PR_3)_2ML]^+$ is also precedented.

In order to test these general assumptions, the synthesis of Cp*$(PMe_3)_2$RuX (X = halide, hydride, and alkyl)[7] has been extended to include a number of phosphines (PEt_3, P^nBu_3, PMe_2Ph), and a wide range of sigma-bonded ligands (OH, OR, NHR, NR_2, SH, SR, CCPh, CH_2COCH_3 etc). A synthetic route to the analogous iron complexes, Cp*L_2FeX (L_2 = PMe_3, DMPE; X = halide, hydride, alkyl) has been devised based on the precursor complex, Cp*(L)Fe(acac).[8] This synthetic flexibility allows the systematic variation necessary for detailed investigation of the basic properties of this system.

We have investigated ligand loss from these ruthenium complexes to generate the 16-electron fragments, [Cp*(PR_3)MX]. This fragment can be trapped by added ligands, L. In particular, the influence of the sigma-bonded ligand X on the rate of phosphine exchange in Cp*$(PMe_3)_2$RuX has been examined by monitoring exchange with $P(CD_3)_3$. The rates of the initial ligand dissociation can be abstracted from an analysis of the kinetics of the approach to equilibrium. Activation parameters have been obtained for this ligand dissociation. Lone pairs on X are found to have an effect on the transition state for ligand loss which is of comparable magnitude to that induced by changing the steric bulk of X.

Thermolysis of ruthenium complexes, Cp*$(PR_3)_2$RuR, in the presence of arenes leads to the loss of RH and the formation of the complexes, Cp*$(PR_3)_2$Ru-Ar. These reactions are

found to proceed *via* a ligand loss mechanism, followed by addition of the arene C-H bond, reductive elimination of RH, and trapping by PR_3. Steric factors on this reaction have been probed by varying ligand size. Thermolysis in alkane solvents leads to metallation of a phosphine ligand to give three- (PR_3 = PMe_3) and four-membered (PR_3 = PEt_3) rings.

The iron complexes, Cp*(PMe_3)FeR, are not observed to activate arene solvents to form Cp*$(PMe_3)_2$Fe–Ar, or to cyclometallate. Cp*$(PMe_3)_2$FeH is found to exchange deuterium from H_2 to perdeuterated solvents, presumably *via* trace amounts of the trihydride complex, Cp*(PMe_3)FeH_3. This reaction is not observed for the analogous ruthenium complex.

Ligand loss in the presence of H_2 allows the preparation of the polyhydrides, Cp*(PMe_3)MH_3. Cp*(PMe_3)RuH_3 is an isolable complex, and is found to be a convenient precursor to the highly reactive hydride fragment, [Cp*(PMe_3)RuH]. [Cp*(PMe_3)RuH] can be generated photochemically and thermally, and is capable of catalyzing the hydrogenation of unsaturated organic substrates. It is also capable of catalyzing H-D exchange between all positions on the complex and perdeuterated alkyl and aryl solvents.

Cp*(PMe_3)FeH_3 can be prepared *in situ* and has been spectroscopically characterized. The polyhydride complex, Cp*(PMe_3)FeH_3, is proposed to be in equilibrium with the dihydrogen hydride complex, Cp*(PMe_3)Fe(η^2-H_2)H. While Cp*(PMe_3)FeH_3 has proven too unstable to isolate, some reaction chemistry has been observed for it. H-D exchange reactions occur with a variety of perdeuterated solvents (C_6D_6, C_6D_{12}, THF-d_8).

As outlined above, the ligand loss chemistry of Cp*$(PR_3)_2$MX and subsequent reaction chemistry of [Cp*(PR_3)MX] have been explored in some detail. The thermochemistry of these complexes is also of interest. The use of solution equilibrium measurements has allowed an investigation of the relative Ru-X bond strengths in these complexes.

The ruthenium complexes, Cp*$(PMe_3)_2$RuX, have been found to equilibrate with HY to yield Cp*$(PMe_3)_2$RuY. This has allowed the determination of relative Ru-X and Ru-Y bond

strengths, where X and Y span a wide range of hydride, alkyl, and heteroatom substituents. A linear correlation between Ru-X and H-X bond strengths is observed. This correlation is found to be general for a number of transition metal complexes. Approximate dative bond dissociation enthalpies have been obtained for a number of these ruthenium complexes. This has allowed an evaluation of the functional group additivity assumption used in the equilibrium sigma bond strength determinations. Large changes in dative ligand bond dissociation enthalpies are found when large steric changes are made in X.

Chapter 1 of this thesis describes the synthesis of a number of Ru(II) complexes and their intra- and intermolecular C-H bond activation chemistry.[9] Ru(IV) complexes such as $Cp^*(PMe_3)RuH_3$ have been synthesized as models of the intermediates in these C-H bond activations. The reaction chemistry of $Cp^*(PMe_3)RuH_3$ is described. Chapter 2 describes the synthesis of the iron complexes, $Cp^*(PMe_3)_2FeX$ and $Cp^*(PMe_3)FeH_3$.[10] The reactivity of these complexes is compared to that of the analogous ruthenium complexes. Chapter 3 describes equilibrium measurements of relative Ru-X and Ru-Y bond strengths in $Cp^*(PMe_3)_2RuX$.[11] Chapter 4 describes studies of the rate of phosphine loss from these Ru(II) complexes.[12]

References

1) Collman, J. P.; Hegedus, L. S. "Principles and Applications of Organotransition Metal Chemistry" University Science Books; Mill Valley, CA; 1980

2) For leading references see: "Comprehensive Organometallic Chemistry", Wilkinson, G.; Stone, F. G. A.; Abel, E. W. eds., Pergamon, Oxford, 1982

3) Green, J. C. *Struct. Bonding (Berlin)*, **1981**, *43*, 37

4) See ref. 1, chapt. 3.2

5) Werner, H. *Ang. Chem. Int. Ed. Eng.*, **1983**, *22*, 927

6) Tolman, C. A. *Chem. Rev.*, **1977**, *77*, 313

7) Tilley, T. D.; Grubbs, R. H; Bercaw, J. E. *Organometallics*, **1984**, *3*, 274

8) Bunel, E. E.; Valle, L.; Manriquez, J. M. *Organometallics*, **1985**, *4*, 1680

9) Tilley, T. D.; Togni, A., Paciello, R. A.; Bercaw, J. E.; and Grubbs, R. H. manuscript in preparation

10) Paciello, R. A.; Bercaw, J. E. manuscript in preparation

11) This work was done as part of a collaborative project with Dr. H. E. Bryndza, Central Research and Development, E. I. DuPont de Nemours and Co., Wilmington, Delaware: Bryndza, H. E.; Fong, L. K.; Paciello, R. A.; Tam, W.; and Bercaw, J. E. *J. Am. Chem. Soc.*, **1987**, *109*, 1444

12) Collaborative project as in ref. 11: Bryndza, H. E.; Domaille, P. J.; Paciello, R. A.; Bercaw, J. E. manuscript in preparation

Synthesis and Reactivity of Electron-Rich Ru(II) and Ru(IV) Organometallic Complexes, $Cp^*(PR_3)_2RuX$ and $Cp^*(PMe_3)RuH_3$

Abstract

The synthesis of a number of Ru(II) complexes, $Cp^*(PR_3)_2RuX$ (R = Me, Et, ^{n}Bu; R_3= Me_2Ph; X = halide, alkyl, hydride), are described. Intermolecular arene C-H bond activation and intramolecular cyclometallation reactions are reported for $Cp^*(PR_3)_2RuR$. A mechanism involving ligand loss to form a highly reactive, 16-electron intermediate, $[Cp^*(R_3)RuR]$, followed by trapping by L or insertion of C–H bonds to yield Ru(IV) complexes is proposed. The synthesis of $Cp^*(PMe_3)RuH_3$ is reported. H–D exchange and hydrogenation reactions are described for this complex. A dihydrogen loss mechanism to generate $[Cp^*(PMe_3)RuH]$, with subsequent trapping by L or oxidative addition is proposed. The structure and hydrogen bonding mode of $Cp^*(PMe_3)RuH_3$ are discussed.

Introduction

The synthesis and reactivity of half-sandwich complexes of the group VIII transition metals have been extensively investigated.[1] Such compounds were initially prepared utilizing cyclopentadienyl groups and carbonyl coligands, *e.g.*, $Cp(CO)_2MX$ (M = Fe[2], Ru[3], Os[4]). These synthesis utilized metal carbonyl complexes as precursors, and have since been generalized to the permethylcyclopentadienyl carbonyl complexes, $Cp^*(CO)_2MX$ (Fe,[5] Ru,[6] and Os[7]).

Complexes with more electron-donating ligand sets have been reported. Initial synthetic attempts involved thermal or photochemical substitution of $Cp(CO)_2MX$ with PR_3, however, such reactions generally yielded monosubstituted complexes.[8] The direct synthesis of the cyclopentadienyl bisphosphine complexes, $Cp(PPh_3)_2MX$ (M = Ru, Os), have been reported, and their reactivity extensively investigated.[9] However, it has not proved possible to generalize these preparative routes to the Cp* complexes.[10] The related arene complexes, $(\eta^6\text{–}C_6H_6)(PR_3)MR_2$ (M = Ru, Os; R = halide, hydride, alkyl) have been reported.[11] These complexes are isoelectronic with, and often display a similar reactivity to the cyclopentadienyl complexes.[12]

We have been interested in the synthesis of complexes with highly electron-donating ligand complements of the form, Cp^*L_2MX ($Cp^* = \eta^5\text{-}C_5Me_5$; L = tri-alkyl phosphine; M = Fe,[13] Ru; X = halide, hydride, alkyl, alkenyl, alkynyl, heteroatom).

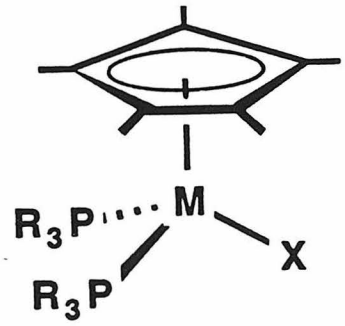

Figure 1

Our studies of the $Cp^*(PMe_3)_2RuX$ system were initiated by the synthesis of $Cp^*(PMe_3)_2RuX$ (X = halide, hydride, alkyl),[10] and by some of the reactivity initially observed for these complexes. Of specific interest was the activation of C-H bonds in arenes intermolecularly, and of a PMe_3 ligand intramolecularly.

Although the reactions of arenes with transition metal complexes[14] and the cyclometallations of metal–bound ligands[15] have been extensively investigated, the continuing interest in C–H oxidative additions[16] prompted us to explore the mechanism of the $Cp^*(PMe_3)_2RuX$ reactions. We now wish to report the preparation of a series of $Cp^*(PR_3)_2RuX$ complexes, where R and X have been varied in order to vary the steric constraint at the metal center. Reactions of these complexes with alkanes, arenes, and trapping ligands, L, are reported. Reaction chemistry of these complexes is proposed to occur *via* ligand loss to yield a highly reactive, 16-electron complex, $[Cp^*(PR_3)RuR]$.

We also wish to report the isolation of the Ru(IV) complex, $Cp^*(PMe_3)RuH_3$, which is proposed to be a model of the intermediates in C–H bond activations. The structure, bonding, and reaction chemistry of this complex are discussed in detail. A highly reactive, 16-electron intermediate, $[Cp^*(PMe_3)RuH]$, is proposed to account for observed reactivity.

Results and Discussion

It is observed that ruthenium alkyl derivatives, $Cp^*(PMe_3)_2RuR$, effect the homogeneous intermolecular activation of arene C–H bonds, see eq. 1.[10]

$$Cp^*Ru(PMe_3)_2R + ArH \xrightarrow{\Delta} Cp^*Ru(PMe_3)_2Ar + RH \qquad (1)$$

The alkyls $Cp^*(PMe_3)_2RuR$ (R = Me, CH_2SiMe_3, CH_2CMe_3) react cleanly with benzene at 80-140 °C to yield $Cp^*Ru(PMe_3)_2Ph$ and RH. The phenyl derivative can be prepared independently from $Cp^*Ru(PMe_3)_2Cl$ and PhMgCl. In C_6D_6, the conversion of $Cp^*(PMe_3)_2RuR$ to $Cp^*(PMe_3)_2RuC_6D_5$ follows pseudo first-order kinetics, and is dramatically inhibited by

PMe_3. The relative rates of phosphine exchange[17] and formation of $Cp^*(PMe_3)_2RuC_6D_5$, see Table 1, follow the same order: $Cp^*(PMe_3)_2RuCH_2CMe_3$ > $Cp^*(PMe_3)_2RuCH_2SiMe_3$ > $Cp^*(PMe_3)_2RuMe$, *i.e.*, ligand loss is more rapid from the bulkier alkyl derivatives.

Table 1. Relative Rates of Benzene C-H Bond Activation by $Cp^*(PMe_3)_2RuR$

Compound	Temp(°C)	$T_{1/2}$(minutes)	k_{obs}(x 10^{-5} sec^{-1})
$Cp^*(PMe_3)_2RuMe$	140	160	8.3
$Cp^*(PMe_3)_2RuCH_2SiMe_3$	95	30	58
$Cp^*(PMe_3)_2RuCH_2CMe_3$	95	10	150

A competition experiment between C_6H_6 and C_6D_6 (1:1 mixture) results in formation of a 2:1 mixture of $Cp^*(PMe_3)_2RuC_6H_5$ and $Cp^*(PMe_3)_2RuC_6D_5$, representing a deuterium isotope effect of 2.0.

The chloride, $Cp^*(PMe_3)_2RuCl$, and hydride, $Cp^*(PMe_3)_2RuH$, do not react according to equation 1. These compounds are stable at 140°C for at least 10 days in C_6D_6. Since these complexes exchange coordinated phosphine with excess $P(CD_3)_3$ within this time, it is presumed that the Ru-Cl and Ru-H bonds are too strong to be broken in this manner.[18]

Thermolysis of $Cp^*(PMe_3)_2RuR$ in C_6D_{12} leads to products indicative of both intramolecular and intermolecular bond activation. For example, heating $Cp^*(PMe_3)_2RuCH_2SiMe_3$ in C_6D_{12} leads to the cyclometallated product $Cp^*(PMe_3)Ru(\eta^2\text{-}CH_2PMe_2)$ and a small amount, *ca.* 20%, of $Cp^*(PMe_3)_2RuH$. Presumably $Cp^*(PMe_3)_2RuH$ is formed by β-hydrogen abstraction in a $Cp^*(PMe_3)RuC_6H_{11}$ intermediate, see Scheme 1.[19]

To evaluate the effects of arene substitution on these C–H bond activation reactions, the trimethylsilylmethyl derivative, $Cp^*(PMe_3)_2RuCH_2SiMe_3$, was reacted with different arenes at 110-120°C. These reactions proceed cleanly in pure arene (*m*-xylene, toluene) or in octane-arene solutions (*p*-xylene, mesitylene, benzaldehyde), affording the aryl derivative and $SiMe_4$ in *ca.* 2 hrs. In the latter reactions, no activation of the octane was observed.

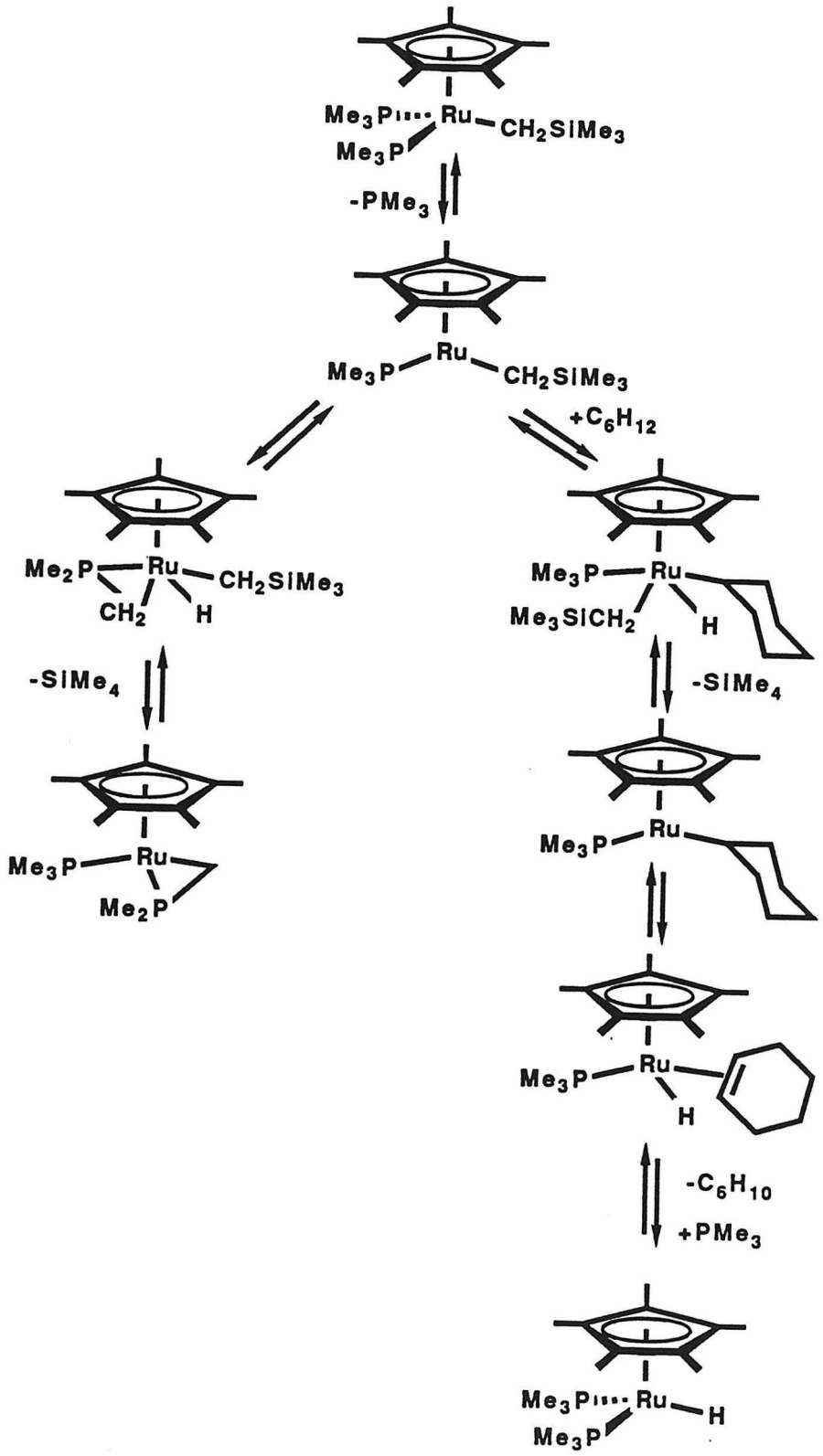
Me3P
Ru
CH2SiMe3
Me3P
-PMe3
Me3P
Ru
CH2SiMe3
+C6H12
Me2P
Ru
CH2SiMe3
CH2
H
Me3P
Ru
Me3SiCH2
H
-SiMe4
-SiMe4
Me3P
Ru
Me2P
Me3P
Ru
Me3P
Ru
H
-C6H10
+PMe3
Me3P
Ru
H
Me3P

Scheme 1

Reaction with benzaldehyde leads to decarbonylation and formation of $Cp^*(PMe_3)(CO)RuPh$. Reaction of *m*-xylene yields substitution only at the position *meta* to both methyl groups. Under similar conditions, no reaction is observed between $Cp^*(PMe_3)_2RuCH_2SiMe_3$ and *p*-xylene or mesitylene, indicating the formation of *o*-substituted aryl derivatives is not sterically favored. Toluene reacts to give a statistical mixture, 2:1, of *m*- and *p*-isomers.

The tolylisomers, *m*- and *p*- $Cp^*(PMe_3)_2RuC_6H_4CH_3$ have been unequivocally identified by comparison with authentic samples. Since the chloride, $Cp^*(PMe_3)_2RuCl$, has proven too unreactive toward tolyl Grignard and lithium reagents, these compounds are prepared by alkylation of the solvated cation, $[Cp^*(PMe_3)_2Ru(Et_2O)]^+OSO_2CF_3^-$, with halide-free[20] *m*- and *p*-tolyl lithium, see eq. 2. The cation can be generated *in situ* by protonation of $Cp^*(PMe_3)_2RuCH_2SiMe_3$ at -78 °C, and subsequent warming of the solution to room temperature.

$$Cp^*(PMe_3)_2RuCH_2SiMe_3 + CF_3SO_3H \xrightarrow{Et_2O} [Cp^*(PMe_3)_2RuHR]^+OSO_2CF_3$$
$$\longrightarrow [Cp^*(PMe_3)_2Ru(Et_2O)]^+OSO_2CF_3 \xrightarrow{CH_3C_6H_4Li} Cp^*(PMe_3)_2RuC_6H_4CH_3 \qquad (2)$$

The observed inhibition of the arene C-H bond activations by added PMe_3, and the dependence on the size of the alkyl group suggests the mechanism shown in Scheme 2, involving ligand loss, possible precoordination of arene, oxidative addition of the arene C-H bond, reductive elimination of alkane, and trapping by phosphine.

Transition state parameters have been obtained for phosphine dissociation from $Cp^*(PMe_3)_2RuR$,[17] this allows calculation of the rate of phosphine dissociation from $Cp^*(PMe_3)_2RuCH_2SiMe_3$ at 95 °C as 4.5×10^{-3} sec^{-1}. While the recombination rates were not obtained in this study, they were restricted to being many orders of magnitude larger than the dissociation rate. Unsaturated intermediates are not observed during $Cp^*(PMe_3)_2RuR$

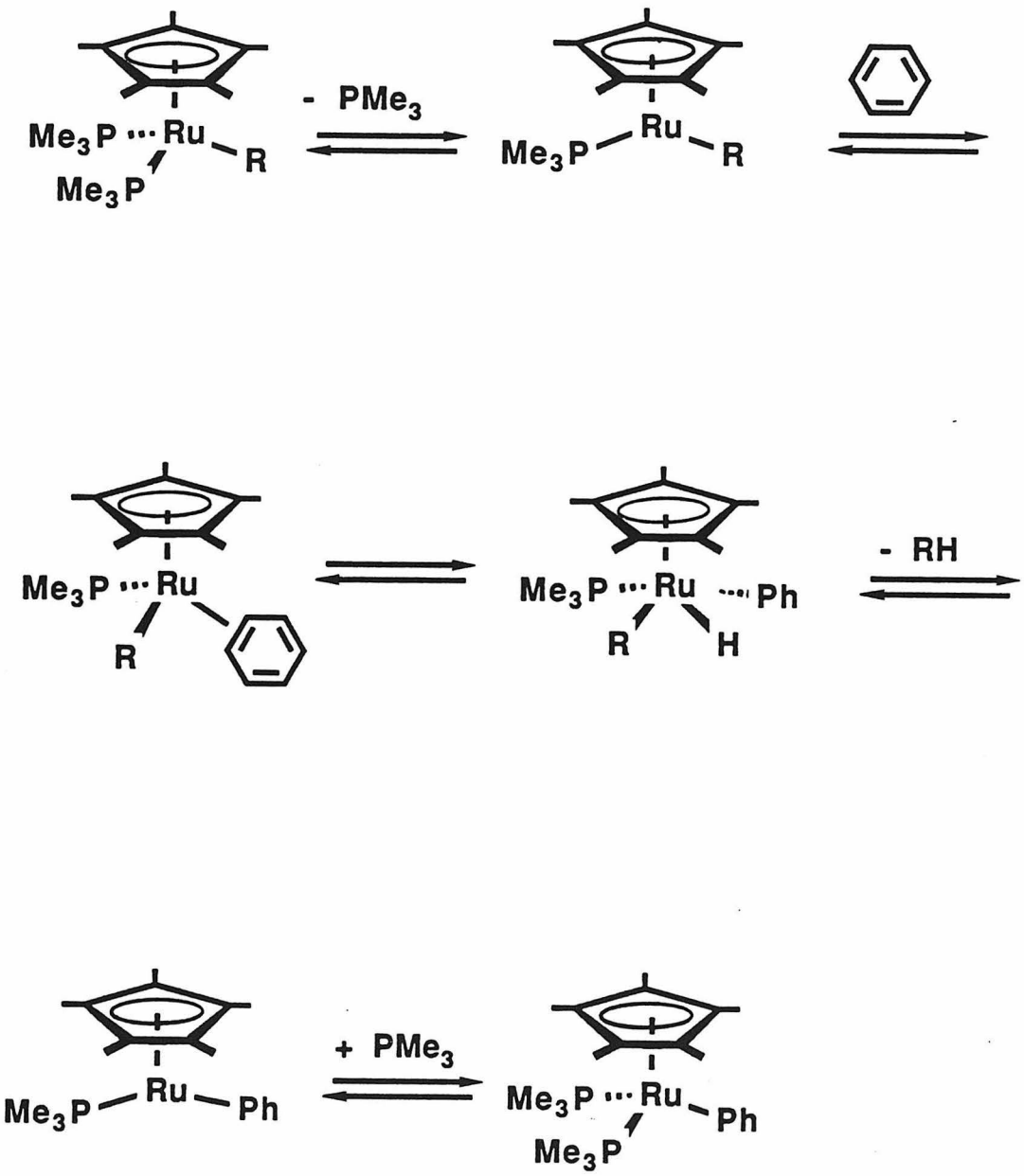
- PMe3
Me3P
Ru
R
Me3P
Me3P
Ru
R
Me3P
Me3P
Ru
R
Me3P
Ru
Ph
R
H
- RH
Me3P
Ru
Ph
+ PMe3
Me3P
Ru
Ph
Me3P
Me3P

Scheme 2

thermolysis, so trapping must also be facile in this case. As the pseudo first-order k_{obs} for the reaction of $Cp^*(PMe_3)_2RuCH_2SiMe_3$ with C_6D_6 at 95 °C is 6.1 X 10^{-4}, Table 1, the phosphine dissociation step is very likely part of a preequilibrium before the rate determining step, as shown in Scheme 2.

There is no direct evidence for the arene precoordination step shown in Scheme 2, nor for the reversibility of the arene C–H bond insertion step. However, η^2-arene complexes have been invoked in a number of arene C–H bond activation reactions. For example, the unsaturated fragment formed upon reductive elimination from $Cp^*(PMe_3)RhHR$ (R = alkyl, H) has been shown to be capable of arene C-H bond insertions. The kinetics of hydrogen scrambling into the perdeuterated phenyl group in $Cp^*(PMe_3)RhH(C_6D_5)$ and the kinetics of tolyl isomer scrambling in $Cp^*(PMe_3)RhH(C_6H_4CH_3)$ have been interpreted as requiring [1,2] shifts, *i.e.,* an η^2-intermediate and reversible insertions.[21] An η^2-adduct, $Cp^*(PMe_3)Rh(\eta^2\text{–}1,4\text{–}C_6H_4(CMe_3)_2)$, has been observed spectroscopically in this system.[22] In addition, the different kinetic isotope effects observed in the activation of arenes by the $[Cp^*(PMe_3)Rh]$ fragment require that direct insertion into the arene C-H bond can not be occurring.[23]

Indirect evidence for arene coordination and reversible C-H bond activation steps is observed when the pure *para*-isomer of $Cp^*(PMe_3)_2RuC_6H_4CH_3$ is heated in toluene (165 °C, 9 h). Formation of the same isomer mixture as that obtained during the much milder $Cp^*(PMe_3)_2RuCH_2SiMe_3$ thermolysis is observed. As hydrocarbon activation is not observed in the $Cp^*(PMe_3)_2RuCH_2SiMe_3$ thermolysis, *i.e.*, the reductive elimination shown in Scheme 2 is irreversible, and scrambling of the pure *para*-isomer is not observed under the same conditions, a reversible step before reductive elimination which allows for production of the thermodynamic product mixture is implied. In a related system, the tolyl isomer ratio in $(PMe_3)_2(P(OMe)_3)_2Os(C_6H_4CH_3)H$, 1:1.75 *meta*:*para*, produced upon reduction of

$(PMe_3)_2(P(OMe)_3)_2OsCl_2$ in toluene changes upon standing to 1:1 *meta*:*para*. Exchange of the coordinated toluene with aromatic solvent is not observed.[24]

The C-H bond activation reactions of the proposed intermediate, $[Cp^*(PMe_3)RuR]$, can be contrasted to those of the $[Cp^*(PMe_3)M]$ fragments generated by the extensively studied iridium and rhodium complexes $Cp^*(PMe_3)MRH$ (M = Ir,[25] Rh;[26] R = H,alkyl,aryl). The $Cp^*(PMe_3)_2RuR$ system differs in that the site of unsaturation leading to oxidative addition of the C-H bond results from ligand dissociation rather than from a reductive elimination step. Therefore, addition of the C-H bond involves a $d^6 \longrightarrow d^4$ ($Ru^{II} \longrightarrow Ru^{IV}$) rather than a $d^8 \longrightarrow d^6$ ($Rh^{I} \longrightarrow Rh^{III}$, $Ir^{I} \longrightarrow Ir^{III}$) oxidative addition.

The reactions of $[Cp^*(PMe_3)RuR]$ can be compared to those of *cis*-$L_4Os(H)R$ (L = PMe_3; R = CH_3, CH_2SiMe_3, CH_2CMe_3). Reactions of these complexes with arene C-H bonds have been investigated, and have been proposed to occur *via* ligand loss to generate highly reactive $[L_3Os(H)R]$ fragments, which then insert C–H bonds to form Os(IV) complexes.[27] This mode of reactivity is surprising; alkane reductive elimination to form an Os(0) intermediate would be expected in such a *cis*-alkyl hydride species. Specifically, this would be similar to the reductive elimination reported in the $(PMe_3)_2(P(OMe)_3)_2Os(C_6H_4CH_3)H$ complexes. However, the mechanism proposed for these C–H bond activations is isoelectronic in all respects (Os(II) $\rightleftharpoons$ 16-electron Os(II) $\rightleftharpoons$ Os(IV)) with the reactions proposed for $Cp^*(PMe_3)_2RuR$.

The steric effects of phosphine ligands on such dissociation processes have been extensively investigated.[28] Increased steric interaction should increase the reaction rates for complexes whose reaction chemistry depends on ligand dissociation. The steric and electronic effects of varying the sigma-bonded ligand, X, in $Cp^*(PMe_3)_2RuX$ have been investigated in some detail and will be reported seperately.[17] The synthesis and reactivity of substituted phosphine complexes, $Cp^*(PR_3)_2RuX$, are outline below.

The synthesis of the trimethylphosphine complexes, $Cp^*(PMe_3)_2RuX$ have been previously reported. The general reaction scheme is outlined in reactions 3-5.

$$RuCl_3 \cdot nH_2O + Cp^*H \xrightarrow{\Delta,\ MeOH} [Cp^*RuCl_2]_x \quad (3)$$

$$[Cp^*RuCl_2]_x + PMe_3 \xrightarrow{RT,\ CH_2Cl_2} Cp^*(PMe_3)_2RuCl \quad (4)$$

$$Cp^*(PMe_3)_2RuCl + RMgCl \longrightarrow Cp^*(PMe_3)_2RuR \quad (5)$$

The necessity of isolating the oligomeric[29] complex, $[Cp^*RuCl_2]_x$, before reaction with phosphine distinguishes the synthetic route in eq. 3-5 from that reported for the normal ring complexes.[30] This oligomeric complex has proved to be a useful precursor in its own right; leading to species such as $[Cp^*RuCl]_4$[31] and $Cp^*RuCl_2 \cdot PR_3$.[32]

The triethylphosphine complex, $Cp^*(PEt_3)_2RuCl$, can be prepared by a straightforward variation of the original $Cp^*(PMe_3)_2RuCl$ synthesis; triethylphosphine being used for the reduction instead of trimethylphosphine. The resulting chloride complex proves to be more easily isolated that the parent PMe_3 complex due to a fortituous absence of the P_4RuCl_2 impurity observed for other phosphines. Alkyl and hydride derivatives can be prepared by treatment of $Cp^*(PEt_3)_2RuCl$ with the appropriate Grignard reagents, RMgCl (R = CH_3, CH_2SiMe_3, ^{t}Bu). See Table 2 for ^{1}H and ^{31}P NMR data.

Other phosphine derivatives such as $Cp^*(P^nBu_3)_2RuCl$ and $Cp^*(PMe_2Ph)_2RuCl$ prove more difficult to isolate cleanly. The n–butylphosphine complex is difficult to obtain free of n-butylphosphine. Approximately 5% phosphine incorporation into the lattice causes crystals grown at low temperature to melt on warming to room temperature. The presence of trace amounts of phosphine does not prevent derivatization with Grignard reagents such as CH_3MgCl. Crystals grown of methyl derivative also melt on warming due to incorporation of *ca* 2-3% free phosphine.

TABLE 2. ^{1}H AND $^{31}P\{^{1}H\}$ NMR DATA

Compound	^{1}H[a] Cp*(J_{P-H})	^{1}H[a] PR_3	^{1}H[a] Other Assignments(J_{P-H})	^{31}P[b]
$Cp^*(PEt_3)_2RuCl$[c]	1.54(1.5)	PCH_2CH_3 1.84 PCH_2CH_3 1.10		21.9
$Cp^*(PEt_3)_2RuMe$[c]	1.70(1.0)	PCH_2CH_3 1.54 PCH_2CH_3 0.95	CH_3 -1.04(*t*, 5.4)	31.0
$Cp^*(PEt_3)_2RuCH_2SiMe_3$[c]	1.69(1.5)	PCH_2CH_3 1.68 PCH_2CH_3 0.97	$CH_2Si(CH_3)_3$ -0.70(t, 5.4) $CH_2Si(CH_3)_3$ 0.43	27.8
$Cp^*(PEt_3)_2RuH$[c]	1.95(1.60) J_{H-H} 0.6 Hz	PCH_2CH_3 1.40 PCH_2CH_3 1.01	H -13.98(t, 37.5)	45.4
$Cp^*(PEt_3)_2RuC_6H_5$[c]	1.60(0.6)	PCH_2CH_3 1.70 PCH_2CH_3 0.90	C_6H_5 7.0(m, 3 H) 7.7 (m, 2 H)	26.9
$Cp^*(PEt_3)Ru(\eta^2\text{-}CH_2CH_2PEt_2)$[c]	1.83(1.6)	1.65(6 H), 1.00(9 H), 0.65(1 H), 2.45(1 H) 1.90(4 H), 0.82(6 H), 1.25(1 H), 3.57(1 H)		38.9 -19.3 J_{P-P} = 34
$Cp^*(P^nBu_3)_2RuCl$	1.66(1.8)	d		15.9
$Cp^*(P^nBu_3)_2RuMe$	1.74(1.0)	d	CH_3 0.01(t, 5.7)	24.8
$Cp^*(PMe_2Ph)_2RuCl$	1.24(1.5)	PCH_3 (vt, 8.4)[e] PCH_3 (vt, 7.8)[e]		12.9
$Cp^*(PMe_3)_2RuC_6H_5$	1.56(1.3)	1.17(vt, 7.5)[e]	C_6H_5 7.6(m, 2 H) 7.18(m, 3 H)	5.6

$Cp^*(PMe_3)_2RuC_6H_4CH_3$	1.60(1.4)	1.20(vt, 7.5)[e]	*CH_3* 2.3 *C_6H_4 meta* H_A 6.46 (d), H_B 6.59 (t), H_C 7.11 (d), H_D 7.19 (s): $^2J_{H-H}$ = 7.5 Hz *C_6H_4 para* H_A, $H_{A'}$ 6.59 H_B, $H_{B'}$ 7.21: $^2J_{H-H}$ = 8.5	5.8
$Cp^*(PMe_3)RuH_3$[g]	1.98(1.6) J_{H-H} = 0.6 Hz	1.22(d, 9.3)	H -11.00(d, 22.5)	17.8
$Cp^*(PMe_3)RuCl_3$	1.45(d, 1.2)	1.33(d, 10.8)		5.7
$Cp^*(PMe_3)(C_2H_4)RuH$	1.8(1.5) J_{H-H} = 0.7	0.90(d, 8.4)	h	18.7
$Cp^*(PMe_3)(C_2H_4)RuEt$	1.5(d, 1.4)	0.75(d, 7.5)	i	21.6
$Cp^*(PMe_3)(CO)RuH$	1.95(d, 1.8) J_{H-H} = 0.4	1.12(d, 9.0)	H -11.8(d, 39.2)	11.5
$Cp^*(PMe_3)(CO)RuPh$	1.63(d, 1.5)	0.90(d, 9.0)	C_6H_6 7.6(m, 2 H) 7.1(m, 3 H)	f
$Cp^*(PMe_3)(CO)RuCH_3$	1.75(d, 1.5)	1.00(d, 8.7)	CH_3 0.05(d, 6.6)	f

a) Shifts in ppm referenced to $SiMe_4$ in C_6D_6, unless noted otherwise, coupling constants in Hz. b) Shifts in ppm referenced to 85% H_3PO_4 at 36.4 MHz in C_6D_6. c) Methylene and methyl protons of phosphine ethyl groups complex multiplets. d) Phosphine n-butyl groups display complex overlapping multiplets from 1-2 ppm. e) Number in parentheses is the separation in Hz between the outer lines of the filled in doublet, $^2J_{P-H} + {}^4J_{P-H}$, unless noted otherwise. f) Not obtained g) Obtained in THF-d_8. h) Four separate overlapping protons in region from 1-2 ppm, obscured by Cp* and PMe_3 peaks. i) Not located.

The complex $Cp^*(PMe_2Ph)_2RuCl$ is initially prepared heavily contaminated with $(PMe_2Ph)_4RuCl_2$. However, the majority of this contaminant can be removed by extended reflux of the reaction mixture in benzene. Such treatment favors the formation and subsequent precipitation of the cationic dimer, $[Ru_2(PMe_2)_8Cl_2]^{2+}2Cl^-$.[33]

The alkyl derivatives of the triethylphosphine complex, $Cp^*(PEt_3)_2RuR$, are found to react with C_6D_6 to give the perdeuterophenyl derivative, $Cp^*(PEt_3)_2RuC_6D_5$. In the case of $Cp^*(PEt_3)_2RuMe$, only CH_3D is observed as the alkane product by ^1H NMR. These reactions occur at lower temperatures than those of their trimethylphosphine analogs. For example, $Cp^*(PEt_3)_2RuCH_2SiMe_3$ thermolyzes slowly at room temperature in benzene to give $Cp^*(PEt_3)_2RuC_6H_5$. The neopentyl derivative is difficult to isolate due to thermal instability. Such increased reactivity is expected on the basis of the increased cone angle of PEt_3 (132°; PMe_3 = 118°),[34] and is consistent with the proposed ligand loss mechanism.

Thermolysis of $Cp^*(PEt_3)_2RuR$ (R = Me, CH_2SiMe_3) in C_6D_{12} gives solely the cyclometallated product, and CH_4 in the case of $Cp^*(PEt_3)_2RuCH_3$, see eq. 6.

$$Cp^*Ru(PEt_3)_2R \longrightarrow Cp^*(PEt_3)Ru(\eta^2\text{-}CH_2CH_2PEt_2) \qquad (6)$$

The observed preference for C-H bond activation in these $Cp^*(PEt_3)_2RuR$ complexes; sp^2 intermolecular > sp^3 intramolecular >> sp^3 intermolecular, is similar to that observed in the isoelectronic $L_4Os(H)R$ complexes.[35]

Intramolecular C-H bond activation in coordinated phosphine ligands to yield four-membered rings has been previously observed.[36] The ^{31}P spectum shows a distinctive upfield shift of the metallated phosphine,[37] and coupling between the now unique phosphines. Treatment of the cyclometallated product with one equivalent of HCl regenerates the starting chloride complex, $Cp^*(PEt_3)_2RuCl$, quantitatively. High field ^1H NMR allows the observation of the four distinct ring protons. Connectivity between these protons can be established by selective homonuclear decoupling experiments, $^1H(^1H)$.

An analogous process has been observed for the complex $(\eta^6\text{–}C_6H_6)(P(CH(CH_3)_2)_3)RuH_2$, which photolyzes in cyclohexane to yield a cyclometallated complex, see eq. 7.

$$(\eta^6\text{–}C_6H_6)(P(CH(CH_3)_2)_3)RuH_2 \xrightarrow{h\nu, C_6H_{12}} (\eta^6\text{–}C_6H_6)Ru(\eta^2\text{-}CH_2CH(CH_3)P(CH(CH_3)_2)_2) \quad (7)$$

This cyclometallated complex reacts at room temperature with C_6H_6 to yield the hydrido phenyl derivative, $(\eta^6\text{–}C_6H_6)(P(CH(CH_3)_2)_3)RuH(C_6H_5)$.[38] In contrast, the cyclometallated ruthenium triethylphosphine complex is stable for days at 80°C.

We were interested in proving the viability of a Ru(IV) center in such reactions, and of exploring the reaction chemistry of such centers. Initial attempts to prepare such complexes were suggested by the reported reaction of $(\eta^5\text{–}C_5Me_4Et)(CO)_2RuBr$ with Br_2 to yield $(\eta^5\text{–}C_5Me_4Et)(CO)RuBr_3$.[39] Attempts to prepare $Cp^*(PMe_3)RuX_3$ by treatment of $Cp^*(PMe_3)_2RuX$ with X_2 ($X_2 = Br_2, Cl_2$) proved unsuccessful. Intractable product mixtures were obtained under all conditions attempted.

An independent route to $Cp^*(PMe_3)RuCl_3$, *via* treatment of $Cp^*(PMe_3)RuH_3$ with exactly three equivalents of HCl, was later found. The compound is found to be thermally sensitive and decomposes after *ca.* 20 minutes at room temperature in C_6D_6.[40] ^1H and ^{31}P NMR spectra of this complex can be obtained, however, which are in accord with the proposed formulation.

A minor hydride product was observed during the hydrogenation of $Cp^*(PMe_3)_2RuCH_2SiMe_3$. This signal appeared as a doublet 13.18 ppm upfield of TMS in the ^1H NMR and was accompanied by loss of an equivalent of PMe_3. As the spectroscopic data suggested formation of $Cp^*(PMe_3)RuH_3$, optimization of the synthesis of this product was then attempted.

$Cp^*(PMe_3)RuH_3$ can be isolated in pure form by using high pressures of H_2 in a Parr reactor, and by removal of the PMe_3 produced, see eq. 8.

$$Cp^*(PMe_3)_2RuCH_2SiMe_3 \xrightarrow{\Delta,\ H_2} Cp^*(PMe_3)RuH_3 + SiMe_4 \qquad (8)$$

Typically, the alkyl, $Cp^*(PMe_3)_2RuCH_2SiMe_3$, is hydrogenated under *ca.* 1500 psi at 60 °C overnight, the solvent and PMe_3 removed, new solvent added, and the mixture hydrogenated again. This process must be repeated three to four times until starting material or $Cp^*(PMe_3)_2RuH$ are no longer visible by ^1H NMR. The reverse reaction is facile as would be expected, *i.e.*, heating $Cp^*(PMe_3)RuH_3$ in the presence of PMe_3 leads to immediate formation of $Cp^*(PMe_3)_2RuH$.

An alternative synthesis of $Cp^*(PMe_3)RuH_3$ has recently been published.[41] It is reported that treatment of an unstable monophosphine adduct of $[Cp^*RuCl_2]_x$, $Cp^*RuCl_2 \bullet PMe_3$, with $LiBHEt_3$ in THF yields the desired complex. This reaction is proposed to involve abstraction of hydrogen from the solvent, presumably by a species such as $Cp^*(PMe_3)RuH_2^-$. The synthesis is similar to that reported for $Cp(PPh_3)_2RuCl$ with $LiAlH_4$ to yield $Cp(PPh_3)RuH_3$.[42] Treatment of $[Cp^*RuCl_2]_2$ with $LiBHEt_3$ in the absence of PMe_3 leads to formation of a tetrameric product, $[Cp^*RuCl]_4$, which has been crystallographically characterized.[43]

The number of neutral organometallic Ru(IV) complexes is quite limited. In addition to $Cp^*(PMe_3)RuH_3$, $(\eta^5\text{-}C_5Me_4Et)(CO)RuBr_3$, and $Cp(PPh_3)RuH_3$, there are the Cp and $Cp^*(\eta^3\text{-allyl})RuX_2$ (X = Cl, Br) complexes[44] and $(PPh_3)_3RuH_4$.[45] A single Ru(VI) complex, $Ru(PCy_3)H_6$ (Cy = cyclohexyl), has been reported.[46]

Upon heating in perdeuterated solvents, $Cp^*(PMe_3)RuH_3$ exchanges all positions with solvent. This H-D exchange occurs with C_6D_6, C_6D_{12}, and THF-d_8, and can be induced thermally and photochemically. Reactions with toluene occur first at the arene positions, then at the methyl positions. It is not clear if exchange of the ring and phosphine methyl groups occurs *via* an inter- or intramolecular process.

The exchange rate for the thermal H-D exchange reaction is observed to be approximately 20 times slower under *ca.* 3 atmospheres of H_2, consistent with H_2 loss as the initial step in these thermal reactions. It is probable that H_2 loss also occurs upon photolysis.[47] However a Ru(VI) polyhydride complex has been reported, $Ru(PCy_3)_2H_6$; and phosphine loss instead of H_2 elimination has been observed upon photolysis of $ReH_5(PMe_2Ph)_3$.[48] In addition, photolysis of $Cp^*(PMe_3)_2RuX$ complexes results in PMe_3 loss.[49] Therefore, while it is possible to propose a H_2 loss mechanism for the thermal reactions, it is not possible to do so with certainty for the photochemical reactions.

Heating $Cp^*(PMe_3)RuH_3$ in the presence of CO at 80°C for 2 hours yields $Cp^*(PMe_3)(CO)RuH$ quantitatively. The reaction occurs in *ca.* 1 hour under photolysis (400 watt medium pressure mercury lamp). If the reactions are continued under either photolytic or thermal conditions, formation of the known complex $Cp^*(CO)_2RuH$ is observed.[50]

Reaction with ethylene under the same thermolysis conditions takes 2-3 days and yields a mixture of $Cp^*(PMe_3)(C_2H_4)RuH$ and $Cp^*(PMe_3)(C_2H_4)RuEt$, *ca.* 5-10%. This reaction takes approximately 1.5 hours under photolysis, the product distributions varying with the temperature of photolysis. After photolysis at 5°C 31% $Cp^*(PMe_3)(C_2H_4)RuEt$ is observed, while photolysis at room temperature yields only 12% $Cp^*(PMe_3)(C_2H_4)RuEt$. No evidence of polymerization has been observed under any set of conditions. The mixture of products can be driven to $Cp^*(PMe_3)(C_2H_4)RuH$ with concomitant formation of ethylene by heating at 80°C in the absence of an ethylene overpressure, see Scheme 3. Reaction of $Cp^*(PMe_3)(C_2H_4)RuH$ with PMe_3 to yield $Cp^*(PMe_3)_2RuEt$ is slow at 80°C (50 % conversion by ^{31}P NMR after 6 hours).

$Cp^*(PMe_3)(C_2H_4)RuH$ has proved difficult to isolate in analytically pure form due to its very high solubility. The ethylene protons in the purest samples obtainable appear as highly coupled individual protons in the same region as the Cp* and PMe_3 peaks. As the hydride is clearly visible, a fluxional process such as that observed

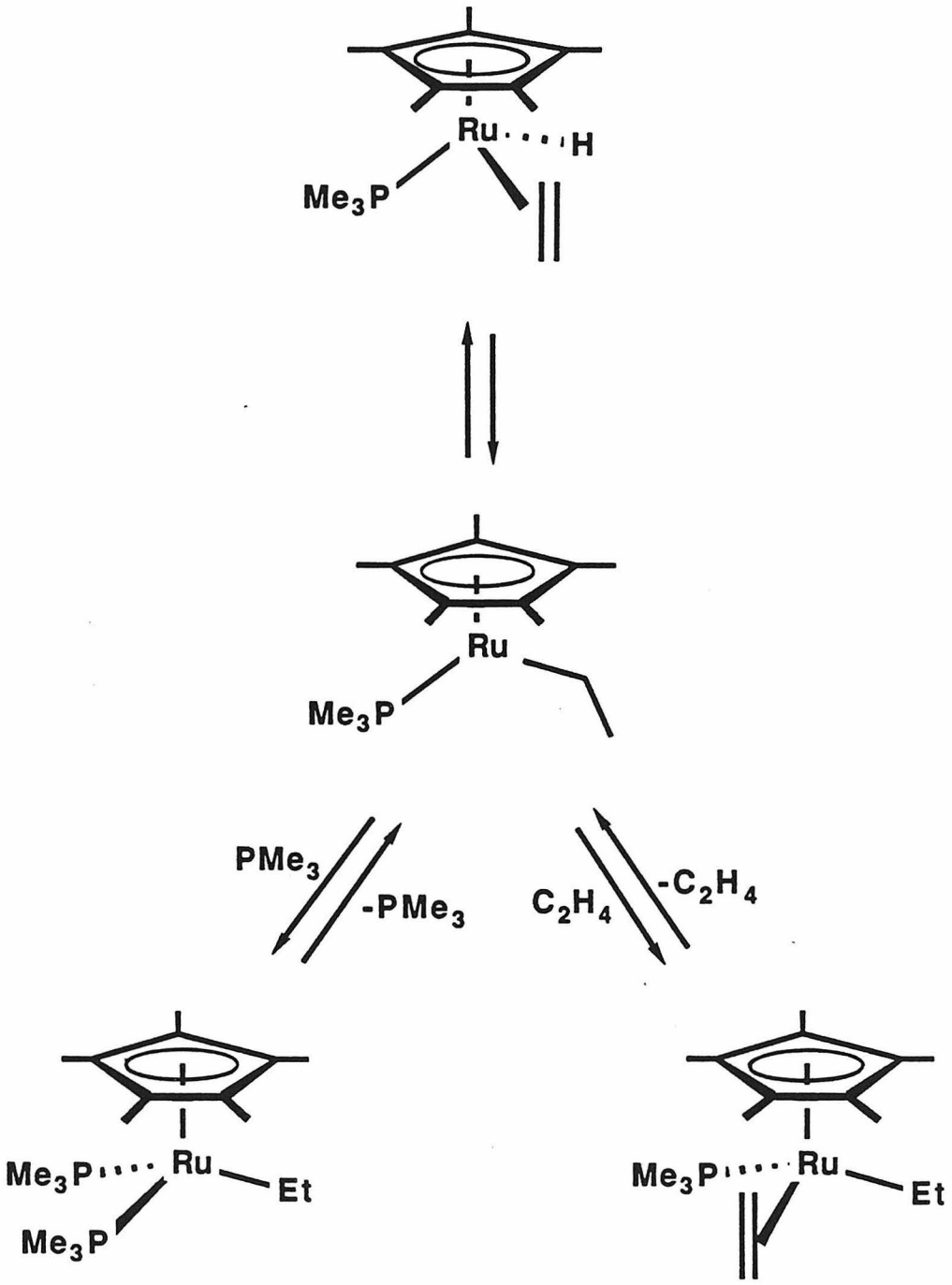

Scheme 3

for $Cp^*(PMe_3)(C_2H_4)FeH$, reversible insertion to give an unsaturated metal alkyl,[51] does not appear to be occurring. A high degree of backbonding to the ethylene from the electron rich metal center is implied by this observation, *i.e.*, a metallacyclopropane-like structure.[52]

Reaction of $Cp^*(PMe_3)RuH_3$ with propyne(80 °C, C_6D_6) leads to catalytic formation of the head to tail dimer of propyne, see eq 9, followed by decomposition of the metal complex.

$$Cp^*(PMe_3)RuH_3 + H\text{-}C{\equiv}C\text{-}CH_3 \longrightarrow CH_2{=}C(Me)\text{-}C{\equiv}C\text{-}Me + \ldots \quad (9)$$

$Cp^*(PMe_3)RuH_3$ hydrogenates C_2H_4 quite efficiently under low pressures of H_2, *ca.* 3 atm, at 80 °C. It will also hydrogenate unsaturated organic species such as ketones catalytically upon photolysis. For example, acetone can be taken to isopropyl alcohol in C_6H_6 under 3 atm. H_2. Acetaldehyde is converted to a mixture 2:1 mixture of ethanol and ethyl acetate. Under thermolytic conditions, few turnovers occur, however the metal product of catalyst decomposition, $Cp^*(PMe_3)(CO)RuMe$, can be observed. Reaction with methyl formate leads to immediate formation of $Cp^*(PMe_3)(CO)RuH$. A representative hydrogenation cycle is outlined for the conversion of acetone to isopropanol, see Scheme 4.

An intermediate, $[Cp^*(PMe_3)RuH_2R]$ (R = alkyl, alkoxide, amide), such as that required for H-D exchange or the hydrogenation reactions has never been directly observed. However, $Cp^*(PMe_3)_2RuOH$ and $Cp^*(PMe_3)_2RuNR_2$ complexes have been shown to undergo facile hydrogenations. Under even moderate pressures of H_2, mixtures of $Cp^*(PMe_3)_2RuH$ and $Cp^*(PMe_3)RuH_3$ are observed.[18]

The isopropoxy intermediates in Scheme 4 are shown bonded *via* the oxygen. This structure is proposed on the basis of steric considerations. Considerations of the thermodynamic bond strengths would imply that the O- and C-bonded species should be isoenergetic.[53] However, the coordination environment around the metal is quite crowded, therefore, the less sterically encumbered species is proposed.

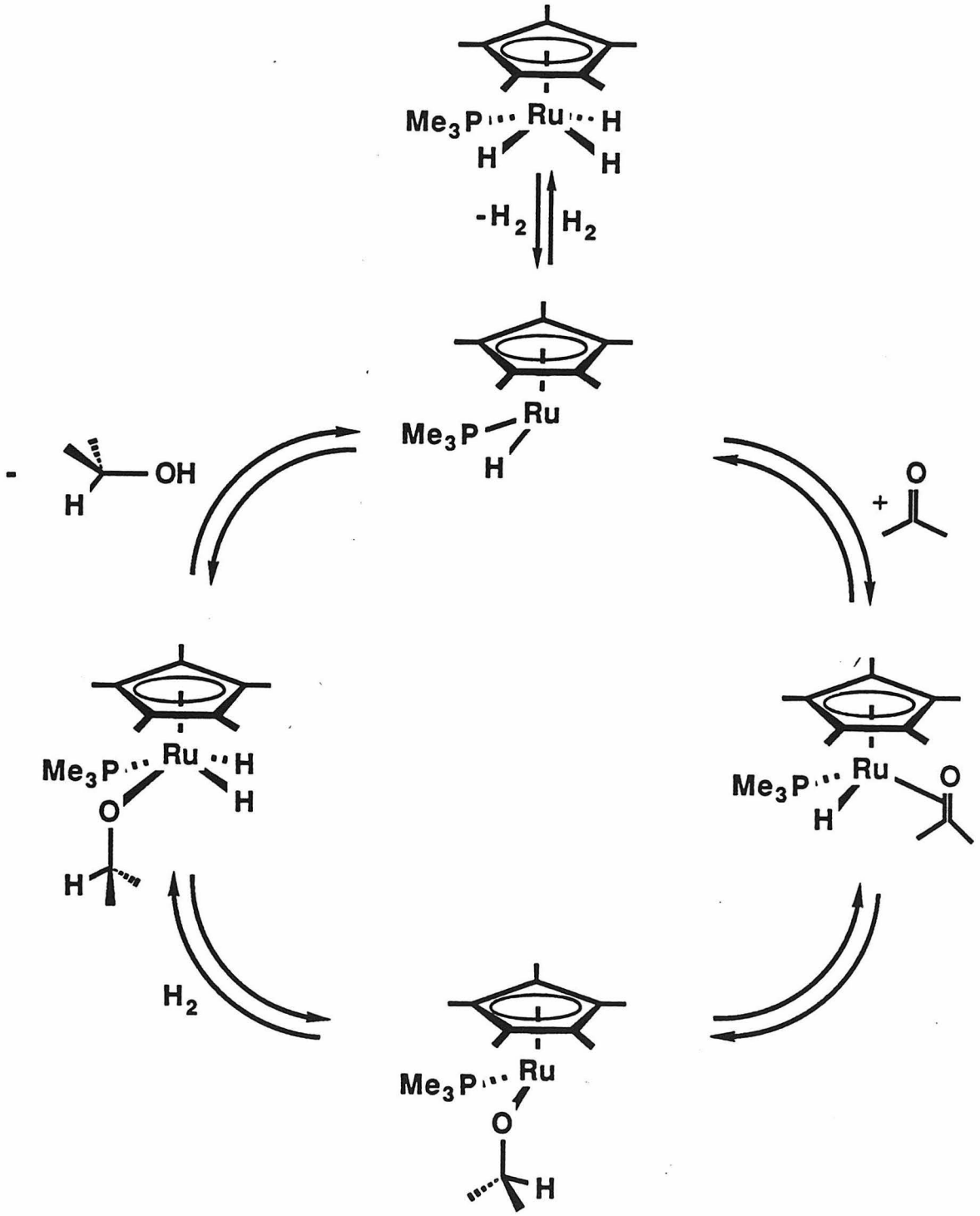
Me3P
Ru
H
H
H
-H2
H2
Me3P
Ru
H
-
OH
H
+
O
Me3P
Ru
H
O
Me3P
Ru
H
H
O
H
H2
Me3P
Ru
O
H

Scheme 4

$Cp^*(PMe_3)RuH_3$ does not react under thermal or photochemical conditions with cyclopropane to give a C-C bond cleavage. Nor does it react with with neohexene and cyclopentane in a manner analogous to that observed for iridium[54] or rhenium[55] polyhydrides to make the mixed ring ruthenocene, Cp*CpRu.

The observed hydrogenation reactions are quite characteristic of a number of transition metal hydride complexes.[56] Of specific note are the anionic ruthenium hydride complexes, $[(PPh_3)_2Ph_2PC_6H_4RuH_2]^-$, which have been shown to be precursors to hydrogenation catalysts for a number of unsaturated organic species such as ketones, aldehydes, and nitriles.[57]

All of the reaction chemistry observed for $Cp^*(PMe_3)RuH_3$ can be most easily explained by a dihydrogen loss mechanism, see Scheme 5. Thermally or photochemically induced H_2 loss opens up a coordination site. This can be followed by either trapping (CO, PMe_3, H_2, R-H), or insertion of an unsaturated ligand into the metal hydride bond (C_2H_4, ketones, aldehydes, nitriles). In the presence of H_2, catalytic hydrogenations occur. As discussed earlier, it is simplest to postulate the same intermediate upon photolysis and thermolysis, but it is not required from the data in hand.

We have examined the spectroscopic data for $Cp^*(PMe_3)RuH_3$ in some detail. This was prompted by the ^1H data for the isoelectronic iridium complex, $[Cp^*(PMe_3)IrH_3]^+BF_4^-$. The low temperature ^1H spectra of the hydride region of this complex exhibits an apparent AB_2 spin system with a J_{A-B} of *ca.* 50 Hz.[58]

Low temperature (-105°C) ^1H spectra of the hydride region of $Cp^*(PMe_3)RuH_3$ can be obtained at 500 MHz. A strongly second order spin coupling pattern is observed. The spectra obtained are not quite at the slow exchange limit as increasing solvent viscosity limited further cooling. In order to simplify the coupling pattern, ^{31}P decoupled spectra can be obtained at the same temperature and field. The observed spectrum is approximately a second order AB_2 spin coupling pattern.[59]

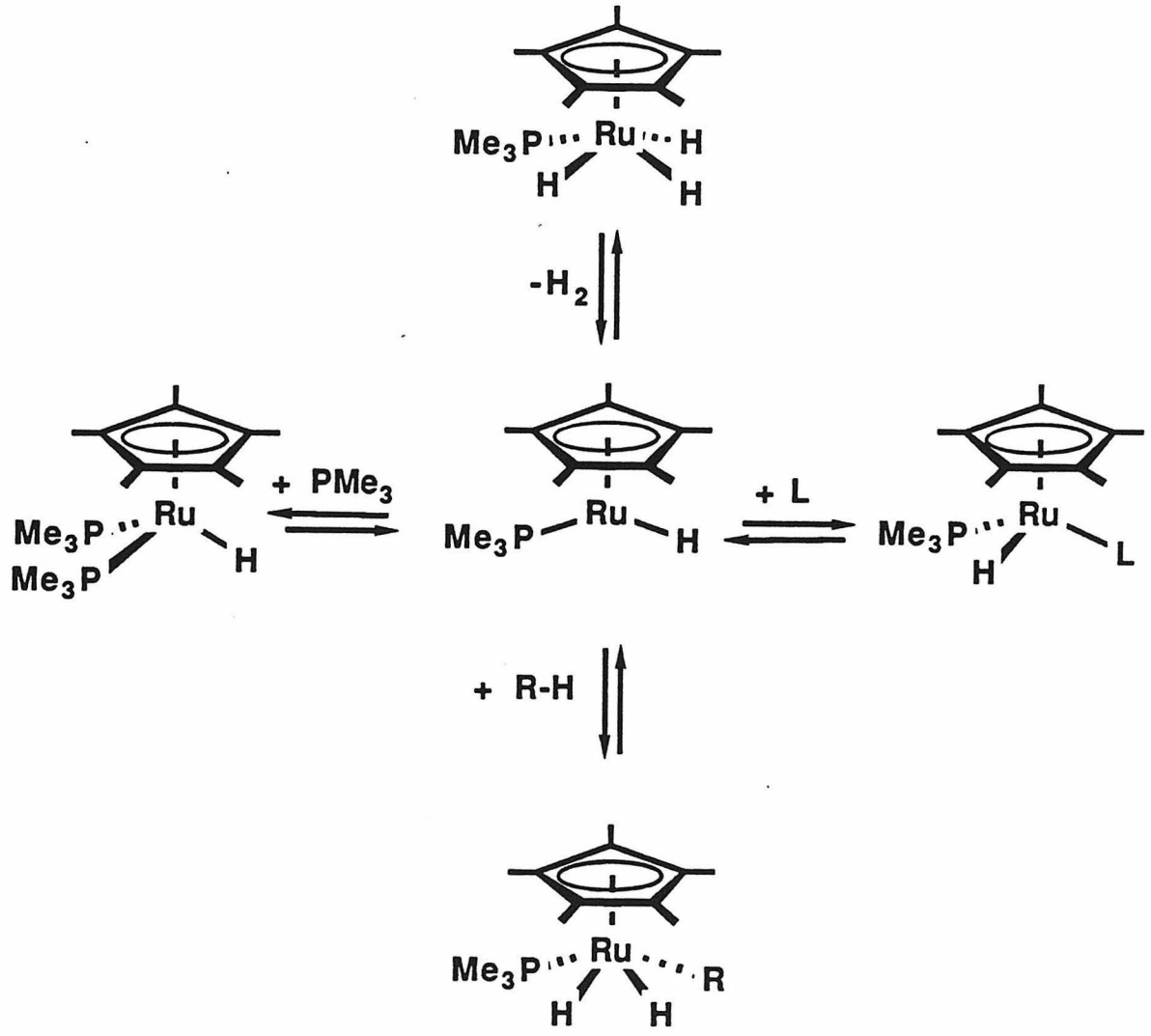
Me3P
Ru
H
H
H
-H2
+ PMe3
Me3P
Ru
Me3P
H
Me3P
Ru
H
+ L
Me3P
Ru
H
L
+ R-H
Me3P
Ru
R
H
H

Scheme 5

The AB_2 spin system can be solved exactly to yield an apparent J_{A-B} of *ca* 206 Hz.[60] A more precise solution in an ABC spin system (B and C almost equal) can be obtained utilizing the standard NMR simulation packages available from Nicolet and Bruker, see Figure 2. The complete ABCX spin system can be simulated by adding in approximately cisoid (*ca.* 5 Hz) and transoid (*ca.* 20 Hz) coupling constants to the best fit H-H coupling constants, see Figure 3.

Such results suggest a dihydrogen adduct such as that proposed initially for $(PR_3)_2(CO)_3W(\eta^2\text{-}H_2)$. One signature of such dihydrogen complexes is the existence of a weak dihydrogen band in the infrared spectrum at 3100-2700 cm^{-1}.[61] Such a band is not observed for $Cp^*(PMe_3)RuH_3$. However, this has also been the case for other dihydrogen adducts.[62]

Yet another criterion is the existence of large H-D coupling constants, *ca.* 30 Hz.[61a,62] A selectively deuterated complex such as $Cp^*(PMe_3)RuH_2D$ could not be prepared. For example, all attempts at deprotonation and quenching with D_2O failed. However, no evidence of a large H-D coupling constant is observed in the ^1H NMR spectrum upon random partial deuteration of the hydride positions of $Cp^*(PMe_3)RuH_3$. The H-D coupling constant must therefore be smaller than the line-width, *ca.* 5 Hz. Partial deuteration of $Cp(PPh_3)RuH_3$ yields a J_{H-D} of 2.78 Hz, which is normal for a terminal metal hydride coupling constant.[63]

T_1s measurements have more recently been proposed as a criterion for the existence of η^2–H_2 metal complexes.[64] However, attempts to measure T_1s of the strongly second order $Cp^*(PMe_3)RuH_3$ hydride coupling pattern at -105 °C did not yield consistent results.

A single crystal X-ray diffraction study was then attempted of $Cp^*(PMe_3)RuH_3$. However, the existence of an intimate twinning disorder prevented location of the hydride ligands. The heavy atoms could be located, see Figure 4. See Table 3 for crystallographic data, Table 4 for atomic coordinates, and Table 5 for selected angles and distances.

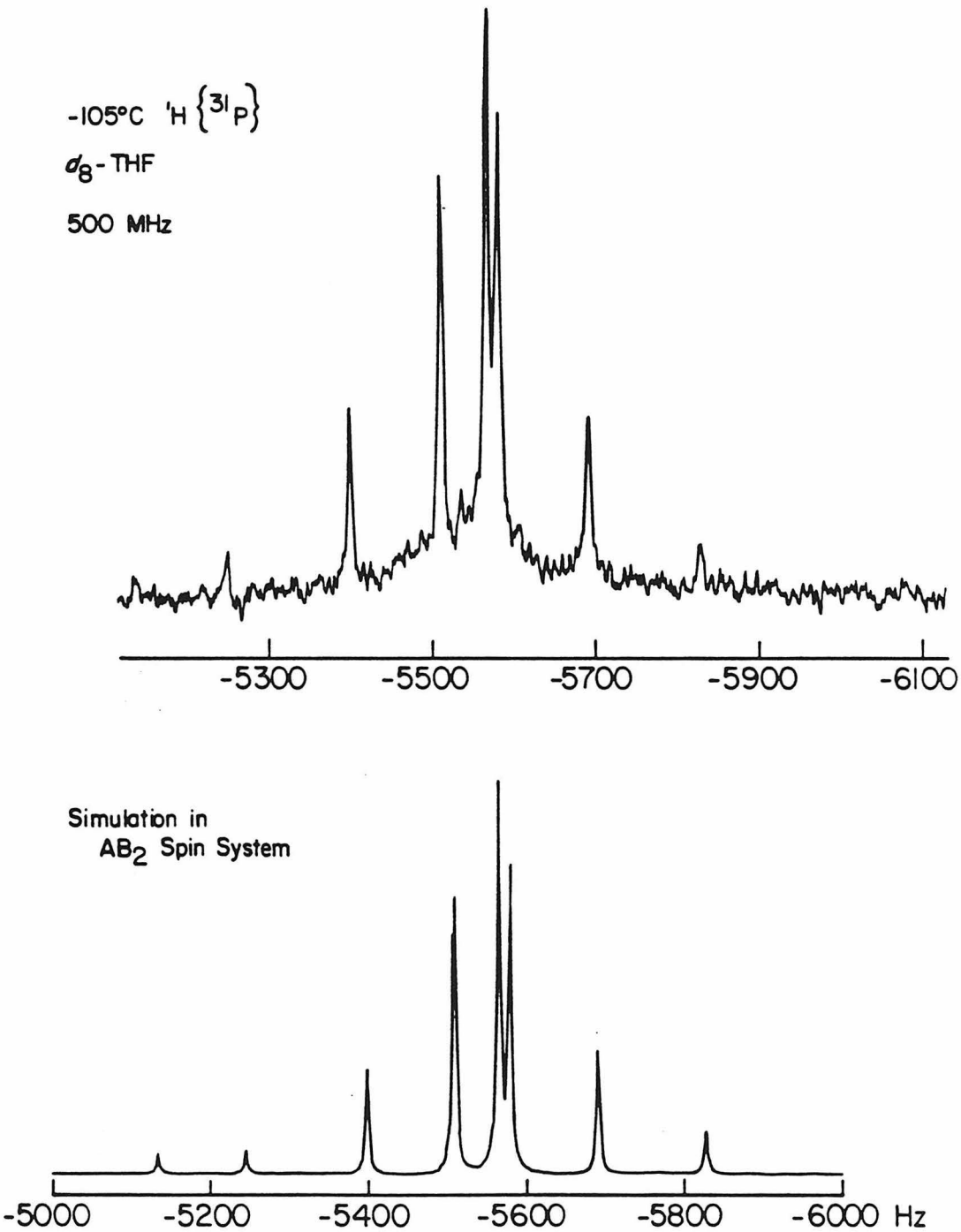

Figure 2. Low temperature 500 MHz $^1H\{^{31}P\}$ NMR spectrum of the hydride region of $Cp^*(PMe_3)RuH_3$. Simulation in AB_2 spin system, J_{A-B} = 206 Hz.

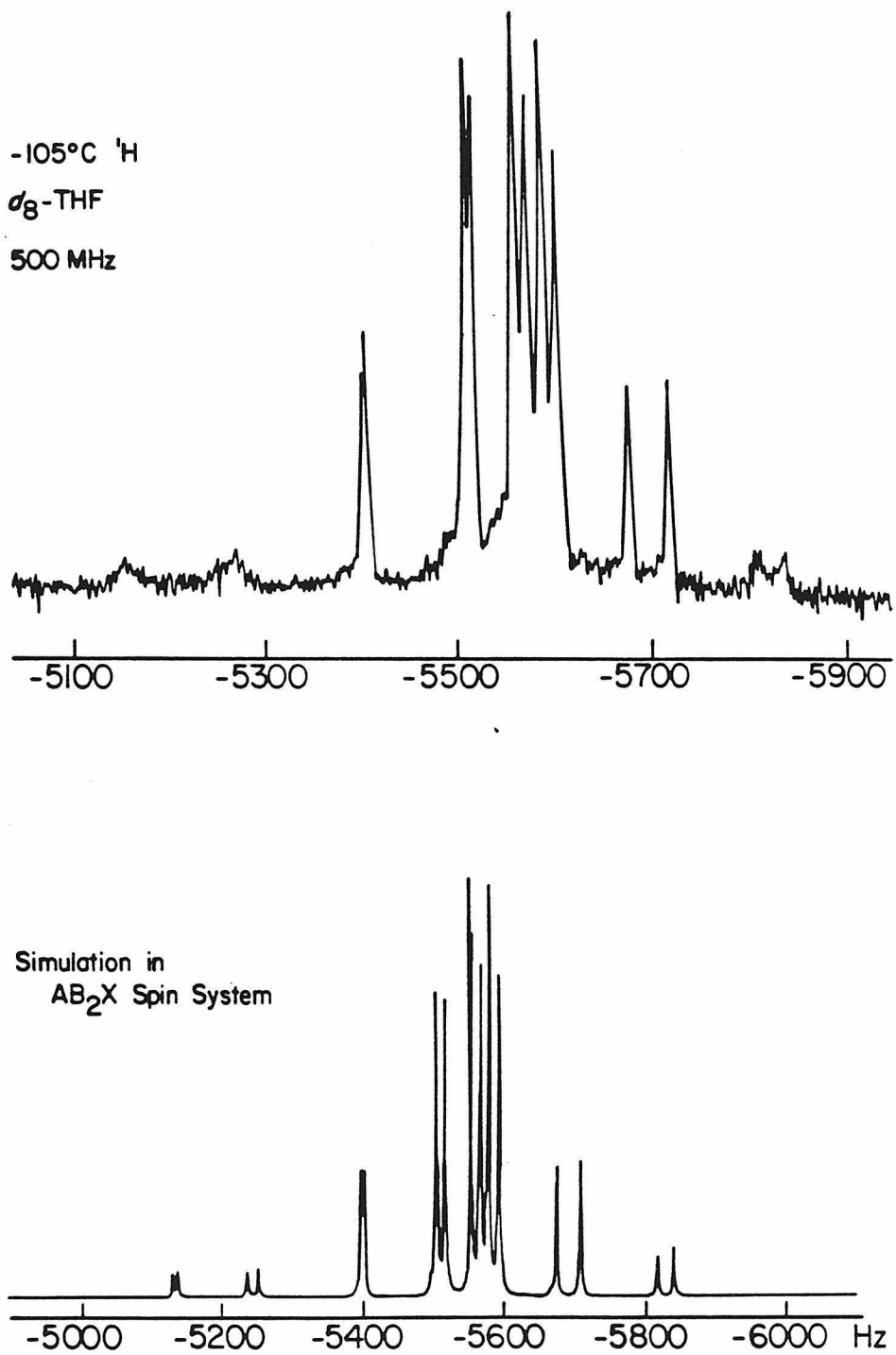

Figure 3. Low temperature 500 MHz ^1H NMR spectrum of the hydride region of $Cp^*(PMe_3)RuH_3$. Simulation in AB_2X spin system, J_{A-B} = 206 Hz.

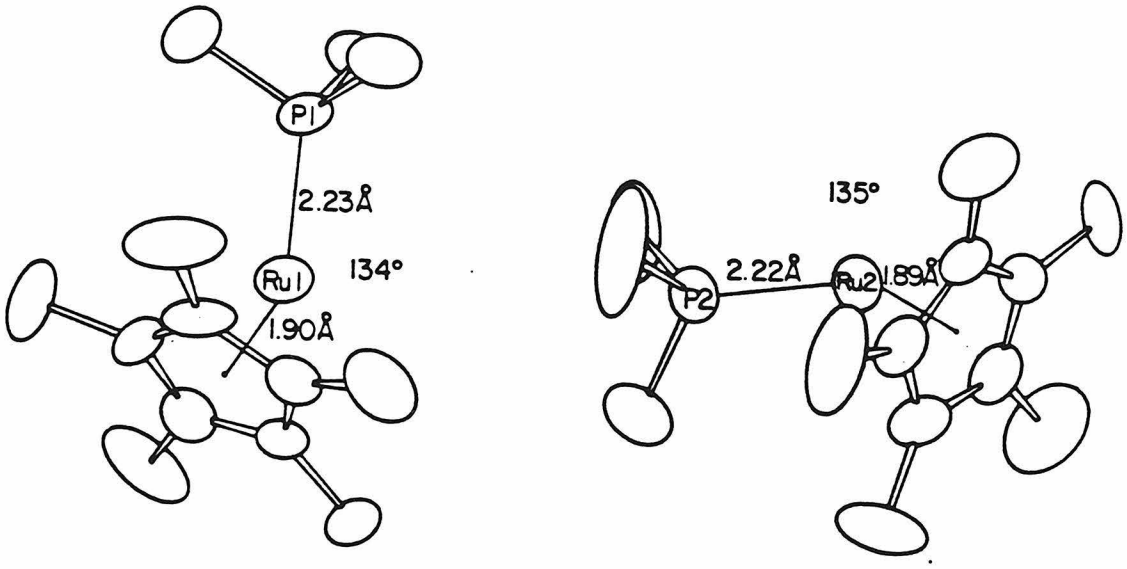

Figure 4. ORTEP drawing of low temperature, -20°C, single crystal structure determination of $Cp^*(PMe_3)RuH_3$. Crystallographic data in Table 3, atomic coordinates in Table 4, selected angles and distances in Table 5.

Table 3. Crystal data for $(\eta^5\text{-}C_5Me_5)(PMe_3)RuH_3$

formula $C_{13}H_{27}PRu$	crystal size 0.40 x 0.35 x 0.15
space group: $P2_1/n$	λ Mo Kα = 0.7107Å
Z = 8	T = -20°C
A = 14.784(10)Å	fw 315.4
B = 14.766(11)Å	V = 3190 Å^3
C = 14.616(9)Å	ρ_c = 1.313 g/cc
α = 90.00	μ = 10.34 cm^{-1}
β = 89.76	$2\theta_{max}$ = 35°
γ = 90.00	

The structure is consistent with a four-legged piano stool in which one ligand, the phosphine, occupies a greater volume around the metal center. The most relevant structure reported, that of $(\eta^5\text{–}C_5Me_4Et)(CO)RuBr_3$,[65] is badly disordered making comparison difficult. A C_{3v} structure with the phosphine trans to the Cp ring plane was proposed for $Cp(PPh_3)RuH_3$ on the basis of a symmetry analysis of the infrared bands.[66] However, no crystal structure was reported for this complex.

Low temperature (-105°C) ^{1}H spectra were then obtained of $Cp^*(PMe_3)RuH_3$ at 400 MHz. These spectra immediately appear anomalous. The 400 MHz spectra are apparently at the slow exchange limit. ^{31}P decoupled spectra were obtained at the same temperature and field. The decoupled spectra can be solved exactly in an AB_2 spin system, or can be modeled in an ABC spin system. However, the H-H coupling constant obtained is 169 Hz, see Figure 5. This field dependence makes it clear that the simulations in an AB_2 spin system are in error. The apparent coupling constant is an artifact of the modeling process.

The modeling programs do suggest that the process which is producing the apparent AB_2 spin coupling pattern has some underlying symmetry, *i.e.*, a mirror plane relating the hydrogens. And the dependence on reaching the apparent slow exchange limit as a function of field implies that this is actually a fast exchange limit for some process with a very low barrier. However, the nature of this process is not known.

Table 4. Atom Coordinates and U_{eq} for $Cp^*(PMe_3)RuH_3$

Atom	x[a]	y	z	U_{eq}[b]
RU1	28017(6)	5500(6)	25882(6)	421(2)
C11	41145(73)	7540(73)	18946(75)	502(28)
C12	42821(62)	6632(71)	28502(71)	433(26)
C13	40294(66)	-2214(81)	31316(76)	512(31)
C14	37045(67)	-6966(70)	23062(85)	524(33)
C15	37596(76)	-778(85)	15755(74)	548(30)
C11M	44048(105)	15457(99)	13173(102)	990(47)
C12M	47622(81)	13340(91)	34682(85)	744(38)
C13M	41393(88)	-6572(108)	40599(86)	899(44)
C14M	34112(97)	-16811(82)	22679(122)	1000(61)
C15M	35673(107)	-3349(126)	5833(88)	1125(57)
P1	14210(19)	-589(21)	26663(20)	471(7)
C16	4636(76)	7358(89)	28122(90)	712(40)
C17	10446(81)	-7284(95)	16586(79)	728(37)
C18	11925(96)	-8995(98)	35692(87)	850(42)
RU2	19021(6)	15477(7)	77023(6)	484(2)
C21	17890(70)	13409(78)	92310(67)	452(26)
C22	25062(89)	19263(76)	90477(76)	567(31)
C23	31923(78)	14575(97)	84783(83)	660(35)
C24	28510(83)	5338(89)	83653(72)	593(30)
C25	19944(79)	4854(86)	88232(71)	541(29)
C21M	10140(89)	15655(114)	98537(78)	875(46)
C22M	26372(137)	28823(106)	94333(116)	1257(65)
C23M	41186(102)	17931(132)	82432(121)	1208(64)
C24M	33229(114)	-2671(100)	79506(89)	1024(50)
C25M	14506(107)	-3506(98)	89472(92)	932(46)
P2	22119(22)	14491(22)	62190(20)	528(8)
C26	22967(170)	3227(99)	57418(88)	1470(86)
C27	32641(119)	19011(161)	57939(108)	1497(79)
C28	14178(113)	19748(120)	54198(81)	1122(60)

[a] x, y and z have been multiplied by 10^4

[b] $U_{eq} = 1/3(U_{11}+U_{22}+U_{33}) \times 10^3$; $\sigma(U_{eq}) = 6^{-1/2}\langle\sigma U_{ii}/U_{ii}\rangle U_{eq}$

Table 5. Selected Distances and Angles for $Cp^*(PMe_3)RuH_3$

Atom	Atom	Distance	σ
RU1	C11	2.2066	0.011
RU1	C12	2.2298	0.010
RU1	C13	2.2880	0.011
RU1	C14	2.3099	0.011
RU1	C15	2.2446	0.012
RU1	P1	2.2329	0.003
C11	C12	1.4258	0.015
C12	C13	1.4189	0.015
C13	C14	1.4776	0.015
C14	C15	1.4076	0.016
C11	C11M	1.5031	0.019
C12	C12M	1.5186	0.016
C13	C13M	1.5111	0.018
C14	C14M	1.5180	0.018
C15	C15M	1.5270	0.020
P1	C16	1.8502	0.013
P1	C17	1.8610	0.013
P1	C18	1.8419	0.014

Atom	Atom	Atom	Angle	σ
11M	11	RU1	127.77	0.849
11M	11	12	124.94	1.028
12M	12	RU1	127.77	0.743
13	12	11	108.90	0.902
12M	12	11	127.22	0.950
12M	12	13	123.45	0.945
14	13	12	106.65	0.906
13M	13	12	128.54	1.016
14M	14	RU1	127.21	0.827
15	14	13	107.05	0.939
14M	14	13	125.36	1.017
14M	14	15	127.54	1.055
15M	15	RU1	127.56	0.883
15M	15	14	123.28	1.084
16	P1	RU1	116.69	0.413
17	P1	RU1	116.73	0.410
18	P1	RU1	118.22	0.452
17	P1	16	101.37	0.564
18	P1	16	101.94	0.595
18	P1	17	98.89	0.592

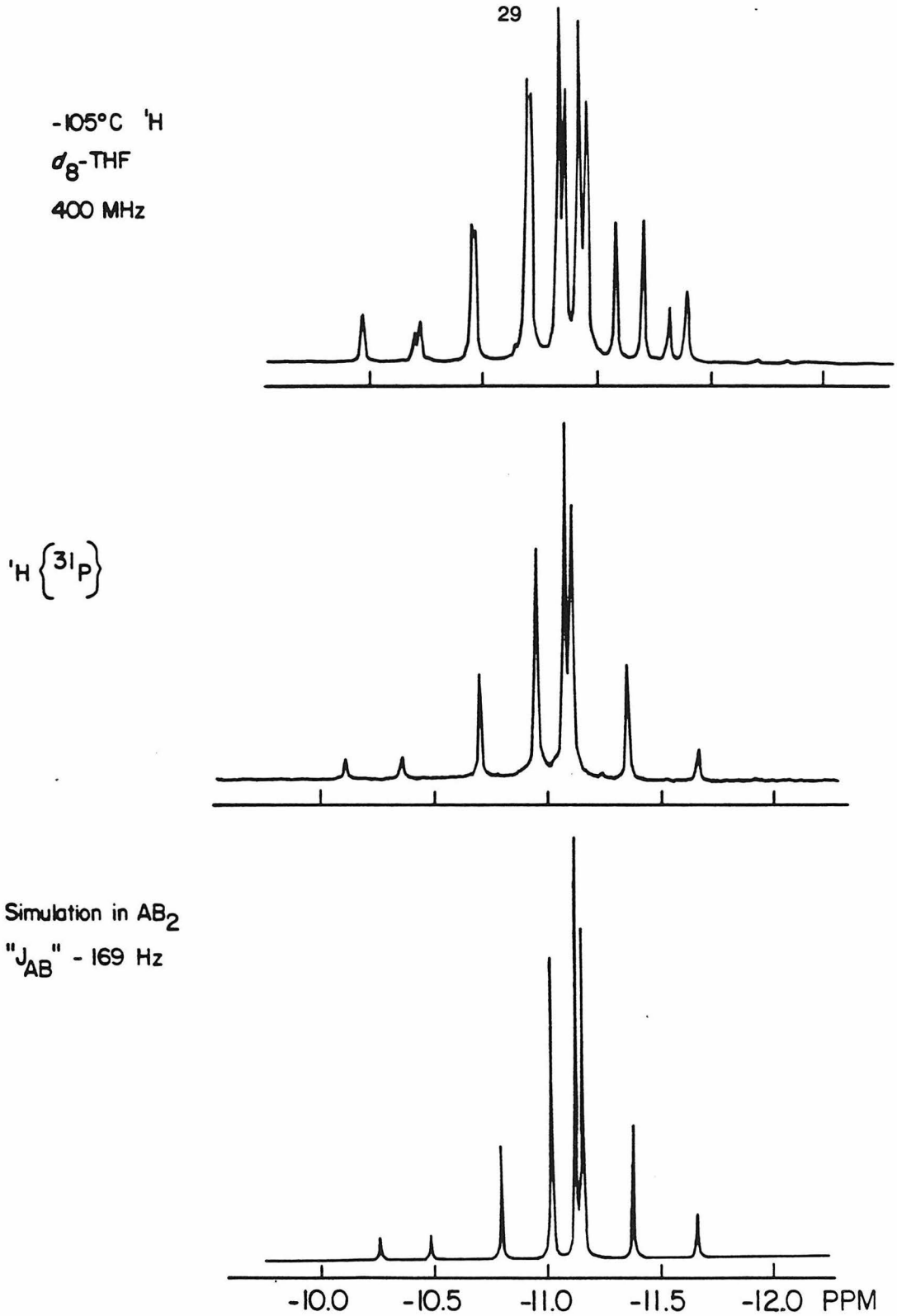

Figure 5. Low temperature 400 MHz ^1H and $^1H\{^{31}P\}$ NMR spectra of hydride region of $Cp^*(PMe_3)RuH_3$. Simulation of $^1H\{^{31}P\}$ spectrum in AB_2 spin system, "J_{A-B}" = 169 Hz

It is interesting to note that other anomalous AB_2 spin coupling patterns exist. For example, Cp_2NbH_3 when treated with aluminum reagents yields an apparent AB_2 spin system with a J_{A-B} of *ca.* 100 Hz. As the alkyl aluminum is proposed to bind to the center hydrogen in the wedge, it is difficult to interpret this result by postulating an η^2-H_2 adduct.[67] The 50 Hz coupling constant observed for $[Cp^*(PMe_3)IrH_3]^+$ is anomalous because of its intermediate size.[58] While equilibrium mixtures of η^2-H_2 adducts and dihydride adducts have been reported for $(PR_3)_2(CO)_3WH_2$,[68] and will be proposed for $Cp^*(PMe_3)FeH_3$ in a later chapter of this thesis; no other intermediate cases of coupling constants than that of the iridium trihydride cation have been reported. To date, complexes have been either dihydrogen adducts, J_{H-H} = *ca* 200 Hz, or dihydrides, J_{H-H} = *ca.* 10 Hz. It is not clear why AB_2 spin systems display such anomalous behavior, but such behavior seems more general than would be expected.

As the previous discussion has made clear, the only criterion for an η^2-H_2 binding mode which is unambiguously absent from $Cp^*(PMe_3)RuH_3$ is the appearance of an extremely large H-D coupling constant. The field dependence of the apparent coupling constants from the low temperature ^1H spectra was only obtained when the instrumentation necessary became available.

A number of fluxional processes could be proposed which would yield the observed NMR behavior in $Cp^*(PMe_3)RuH_3$. Formally seven coordinate species such as $Cp^*(PMe_3)RuH_3$ are often steriochemically nonrigid.[69] Movement of the phosphine to a position trans to the ring would place the three hydrides in equivalent equitorial positions, see Figure 6. Such a conformation has been proposed for the isoelectronic complex, $Cp(PPh_3)RuH_3$.[66] A fast exchange between a rigid terminal trihydride complex and dihydrogen hydride complexes, see Figure 6, would preserve AB_2 symmetry, as observed. Such a fast equilibrium has been proposed for site scrambling in $[IrH(H_2)(PPh_3)_2(C_{13}H_8N)]^+$.[62a] The presence of only a small of amount of dihydrogen hydride would be consistent with the absence of a large H-D

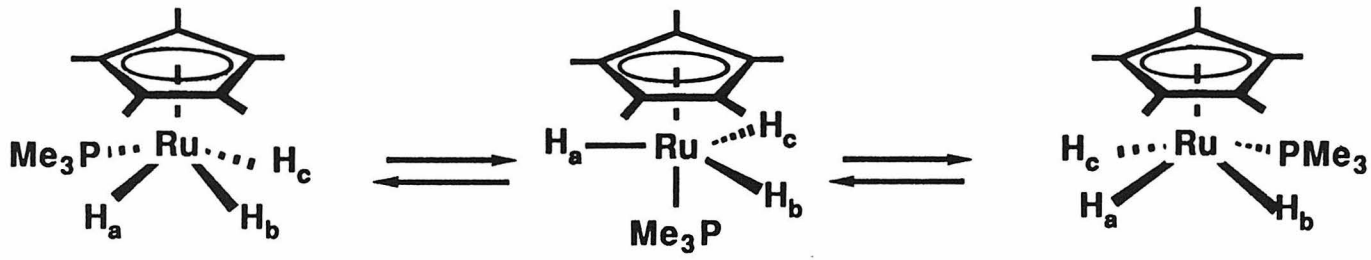

Fast Exchange Process at Room Temperature

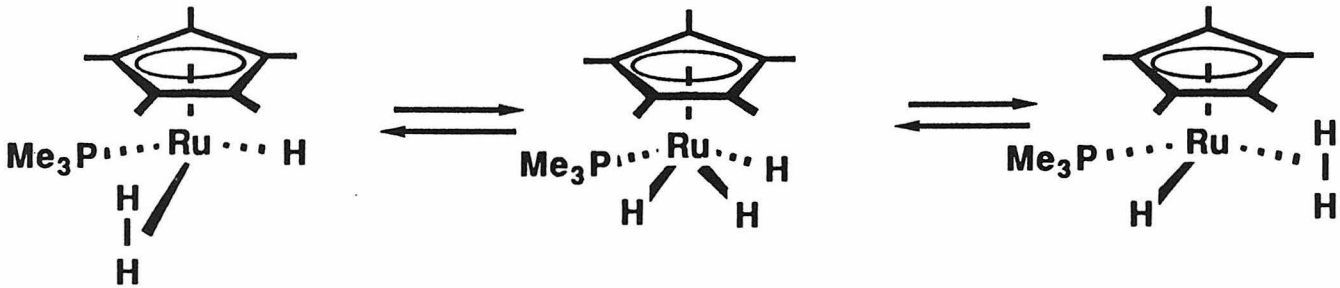

Fast Exchange Process at -105°C

Figure 6

coupling constant upon partial deuteration. However, it must be stressed that these mechanisms are purely speculative.

In summary, it has been shown that the synthesis of $Cp^*(PMe_3)_2RuX$ can be generalized to other phosphines. Inter- and intramolecular C-H bond activations occur for these complexes. The observed reactivity is consistent with a ligand loss model to generate highly reactive 16-electron species, $[Cp^*(PR_3)RuR]$, followed by subsequent oxidative addition to generate Ru(IV) intermediate species. A Ru(IV) complex, $Cp^*(PMe_3)RuH_3$, has been synthesized as a model for these intermediate species. The reactivity of this complex has been explored. Thermal reactions are consistent with a dihydrogen loss model to generate a highly reactive 16-electron species, $[Cp^*(PMe_3)RuH]$. The structure and hydrogen bonding mode on $Cp^*(PMe_3)RuH_3$ have been investigated in some detail. The complex is proposed to have terminal hydride ligands.

Experimental

All syntheses and chemical manipulations were carried out by standard high vacuum and Schlenk techniques. Hydrogen, nitrogen, and argon were purified by passing the streams through MnO on vermiculite followed by activated 4 Å sieves.[70] Benzene, petroleum ether (bp 60-80 °C), THF, diethyl ether and toluene were purified by distillation from purple sodium/benzophenone ketyl solutions under argon, or by vacuum transfer from the same drying and degassing medium or from "titanocene".[71] Benzene, toluene and petroleum ether required the addition of tetraglyme (Aldrich) to effect dissolution of the sodium. Methylene chloride was vacuum transferred from calcium hydride. Methanol was dried by stirring over NaOMe and vacuum transferred. $HBF_4 \cdot Et_2O$ was degassed and used as supplied from Aldrich. Hydrogen, carbon monoxide, and ethylene (freeze-pump-thawed three times) were used as obtained from Matheson. Grignard reagents were used as received from Aldrich. $RuCl_3 \cdot nH_2O$ (Aesar) was obtained commercially and used as received.

IR spectra were recorded as nujol mulls on KBr plates on a Beckman IR 4230 spectrophotometer. Routine ^1H and ^{31}P spectra for characterization were obtained in benzene-d_6 or THF-d_8 with Me_4Si or H_3PO_4 as standard references, on Varian EM-390, Jeol FX-90Q, or Jeol GX-400 spectrometers. T_1s measurements were obtained using standard programs and data analysis packages on the Jeol GX-400. Low temperature spectra were obtained on Brucker WM-500 or Jeol GX-400 instruments.

Routine survey reactions were done in sealed NMR tubes prepared utilizing standard high vacuum techniques for solvent and gas addition. Deuterated solvents were purified and maintained in the same manner as the protonic isotopomers.

High pressure reactions were done in a Parr Stirred Minireactor (Model 4561) using ultra high purity H_2 (Matheson). Photolysis were done using a medium pressure mercury lamp (450 watt, Hanovia) or a mercury/xenon arc lamp (1000 watt, Hanovia) on samples in pyrex NMR tubes or pyrex schlenk tubes. Samples were regulated at 5°C with a water bath cooled by a coil from a circulating constant temperature bath.

The complexes $[Cp^*RuCl_2]_x$ and $Cp^*(PMe_3)_2RuX$ (X = Cl, H, CH_2SiMe_3, CH_3) were prepared as previously reported.[72] Halide free *m*- and *p*-tolyl lithium reagents and phenyl lithium were prepared by literature methods.[73] Satisfactory elemental analysis on new complexes were obtained from the California Institute of Technology analytical service or the Dornis and Kolbe Microanalytical Laboratory.

Thermolysis of $Cp^*(PMe_3)_2RuR$ in C_6D_6: For reactions of $Cp^*(PMe_3)_2RuR$ (R = Cl, H, CH_3, CH_2CH_3, CH_2SiMe_3, CH_2CMe_3) with C_6D_6, the initial concentrations were 0.10-0.15 M. The reactions were carried out in flame-sealed 5 mm NMR tubes in oil baths regulated to the given temperatures (±1°C), and monitored by ^1H NMR after quenching to room temperature. The deuterated product $Cp^*(PMe_3)_2RuC_6D_5$ was identified by comparison of NMR data with that of the unlabeled complex.

Thermolysis of $Cp^*(PMe_3)_2RuCH_2SiMe_3$ in C_6H_6: $Cp^*(PMe_3)_2RuCH_2SiMe_3$ (0.10 g, 0.2 mmol) and C_6H_6 (4 ml) were placed into an ampoule and the ampoule flame-sealed. The ampoule was placed in a 100°C oven for 3 h then cooled to room temperature. The contents were transferred to a Schlenk tube and the volatiles removed leaving yellow crystalline $Cp^*(PMe_3)_2RuC_6H_5$, identified by comparison of ^1H and ^{31}P data with the independently prepared complex.

$Cp^*(PMe_3)_2RuC_6H_5$: To a solution of $Cp^*(PMe_3)_2RuCl$ (1.29 g, 3 mmol) in 20 ml diethyl ether/THF (5:1) was added PhMgCl (1.7 ml of a 2 M sol. in THF, 3.3 mmol). The solution was stirred 12 h, 5 ml H_2O added, and stirring continued 5 min. Removed volatiles from diethyl ether fraction, and extracted the residue with 3x20 ml petroleum ether. Reduced volume to *ca.* 10 ml, heated gently to completely dissolve, and slow cooled to -78°C. Yield 1.202 g, 85% of light yellow crystals. Anal.: calcd. C 56.8, H 8.22, P 13.3; found C 56.7, H 8.18, P 13.0.

$Cp^*(PMe_3)_2RuR$ thermolysis with Ar-H: $Cp^*(PMe_3)_2RuCH_2SiMe_3$ was thermolyzed at 110-120°C in pure arene (*m*-xylene, toluene) or in octane solutions with stoichiometric quantities of the arene (mesitylene, *p*-xylene, benzaldehyde) for *ca.* 2 h. No activation of octane was observed in any thermolysis. Volatiles were removed under vacuum, and ^1H and ^{31}P NMR spectra obtained of the organometallic products in C_6D_6.

Reaction of $Cp^*(PMe_3)_2RuCH_2SiMe_3$ with Toluene: A Carius tube was charged with $Cp^*(PMe_3)_2RuCH_2SiMe_3$ (80 mg, 0.16 mmol) and toluene (2 ml). The tube was then flame-sealed and placed in a 100°C oven for 10 h. The contents of the tube were transferred to a Schlenk flask and the volatiles removed in vacuo leaving a yellow-orange solid. ^1H NMR showed this to be a mixture of the *m*- and *p*-isomers of $Cp^*(PMe_3)_2Ru(C_6H_4Me)$. Spectral data were compared to samples of the pure isomers prepared independently. Anal. for thermodynamic mixture of tolyl isomers: calcd. C 57.6, H 8.41, P 12.92; found C 57.53, H 8.34, P 12.78

Preparation of *m*- and *p*-Cp*(PMe$_3$)$_2$Ru(C$_6$H$_4$Me): To a solution of Cp*(PMe$_3$)$_2$RuCH$_2$SiMe$_3$ (999 mg, 2.1 mmol) in 20 ml diethyl ether was added 1.05 equivalents CF$_3$SO$_3$H (195 μL) at -78°C. The solution was warmed to room temperature and stirred 3 h. A solution of 1.1 equivalents *p*-tolyl lithium (recrystallized from diethyl ether, 125 mg) in 5 ml THF was added to the solution of cation at -78°C, warmed to room temperature and stirred 2 h. Added 5 ml H$_2$O, stirred 15 min, and removed diethyl ether fraction. Dried diethyl ether fraction under high vacuum, extracted 100 ml petroleum ether. Reduced volume and grew yellow orange crystals. The *m*-tolyl isomer was prepared in the same fashion. Anal for *p*-tolyl isomer: calcd. C 57.60, H 8.41; found C 57.29, H 8.63.

Arene Competition Experiments: Cp*(PMe$_3$)$_2$RuCH$_2$SiMe$_3$ was dissolved in a 50:50 mixtures of C$_6$H$_5$/C$_6$D$_6$ and heated at 80°C for *ca.* 2 h. Removal of volatiles under vacuum yielded a mixture of products which could be analyzed by ^{1}H and ^{31}P NMR.

Reaction of Cp*(PMe$_3$)$_2$RuCH$_2$SiMe$_3$ with C$_6$H$_{12}$: A 5 mm NMR tube was charged with Cp*(PMe$_3$)$_2$RuCH$_2$SiMe$_3$ (20 mg) and cyclohexane-d_{12}. The tube was flame-sealed and heated to 140°C for 24 h. Analysis of the reaction was done by ^{1}H NMR and ^{31}P NMR. The hydride, Cp*(PMe$_3$)$_2$RuH, and cyclometallated product, Cp*(PMe$_3$)Ru(η^2-CH$_2$PMe$_2$), have been prepared independently.

Preparation of Cp*(PEt$_3$)$_2$RuCl: Three equivalents of PEt$_3$ (2.9 ml) were added to a solution of [Cp*RuCl$_2$]$_x$ (2 g, 6.5 mmol) in 30 mls CH$_2$Cl$_2$ at room temperature. The solution was allowed to stir for 12 h, volatiles were removed under vacuum, and the resultant green residue extracted with 3X50 ml petroleum ether. The combined extracts were reduced to 50 ml, the solution gently heated to completely dissolve the solid, and cooled to 0°C to yield dark red plates. Yield 68%, 2.245 g. Anal.: calcd. C 52.02, H 8.87; found C 52.04; H 8.87.

Cp*(PEt$_3$)$_2$RuMe: To a solution of Cp*(PEt$_3$)$_2$RuCl (500 mg, 1 mmol) in 30 ml Et$_2$O at -78°C was added MeMgCl (373 μL, 2.9 M sol in THF). The solution was stirred at -78°C for 1 h,

warmed to room temperature, then stirred for 12 hours. Volatiles were removed under vacuum, and the light yellow residue extracted with 2X25 ml petroleum ether. The combined extracts were reduced to 10 ml, the solution cooled to -78°C, and light yellow crystals isolated after *ca.* 6 h. Yield 420 mg, 87.5%. Anal.: calcd. C 56.67, H 9.86; found C 56.67, H 9.51.

$Cp^*(PEt_3)_2RuCH_2SiMe_3$: To a solution of $Cp^*(PEt_3)_2RuCl$ (500 mg, 1 mmol) in 25 ml Et_2O at room temperature was added Me_3SiCH_2MgCl (100 μL, 1 M sol in Et_2O). The solution was stirred for 12 hours, the volatiles removed under vacuum, and the residue extracted with 2X20 ml petroleum ether. Reduced the combined extracts to 5 ml and cooled to -78°C to yield light yellow crystals. Yield 300 mg, 54.5%. Anal.: calcd. C 55.42, H 9.95; found C 55.60; H 9.84.

$Cp^*(PEt_3)_2RuH$: To a solution of $Cp^*(PEt_3)_2RuCl$ (500 mg, 0.9 mmol) in 10 ml Et_2O at -78°C was added $^{t}BuMgCl$ (.54 ml, 2 M sol in Et_2O). The solution was warmed to room temperature and stirred 12 hours. Volatiles were removed under vacuum, the residue extracted with 2X25 ml petroleum ether, the combined extracts reduced to 5 mls, and light yellow cubic crystals were grown at -78°C over an 8 h period. Yield 349 mg, 75%. Infrared (Nujol Mull): 1930 cm^{-1}. Anal.: calcd. C 55.81, H 9.73; found C 55.97, H 9.71.

$Cp^*(P^{n}Bu_3)_2RuCl$: To a solution of $[Cp^*RuCl_2]_x$ (2 g, 6.5 mmol) in 30 ml CH_2Cl_2 was added 3.1 equiv. $P^{n}Bu_3$ (4.82 mls). The solution was stirred at room temperature 16 h. Volatiles were removed and the gummy residue extracted with 3X50 ml petroleum ether. The filtered extracts were combined and reduced to 20 ml. Red crystals could be grown at 0°C in *ca* 12 hours and subsequently washed with petroleum ether at -78°C. Upon warming to room temperature the crystals reverted back to a highly viscous red oil. ^{31}P NMR indicated *ca* 5% free $P^{n}Bu_3$ in the oil. Yield 3.6 g, *ca.* 80%. Compound otherwise pure by ^{1}H and ^{31}P NMR.

$Cp^*(P^{n}Bu_3)_2RuMe$: To a solution of $Cp^*(P^{n}Bu_3)_2RuCl$ (3g red oil, 4.4 mmol) in 50 ml Et_2O at-78 °C was added 1.1 equiv. CH_3MgCl (1.7 ml, 2.9 M sol in THF). The solution was warmed to room temperature and allowed to stir for 12 h. Removed volatiles under vacuum and

extracted with 2X50 ml petroleum ether. Reduced volume to 25 mls after filtration and grew light yellow crystals at -78°C over a 6 h period. Filtered and washed once with petroleum ether at -78°C. Dried thoroughly at 0°C, warmed to room temperature. Crystals reverted back to light yellow oil. ^{31}P NMR indicated 2-3% free phosphine present. Yield 2.3 g, *ca.* 80%. Compound otherwise pure by ^{31}P and ^{1}H NMR.

$Cp^*(PMe_2Ph)_2RuCl$: To a solution of $[Cp^*RuCl_2]_x$ (5.1 g, 16 mmol) in 150 ml CH_2Cl_2 was added 3 equiv. PMe_2Ph (7.2 ml) *via* syringe. The solution was allowed to stir at room temperature for 24 h. The volatiles were removed and the residue thoroughly dried under vacuum (3 days). The resultant mass was broken up and vigorously stirred under 100 ml petroleum ether for 12 h. Removed volatiles under vacuum. Extracted yellow powder with 125 ml petroleum ether using soxhalt apparatus, *ca.* 2 days. Cooled solution to -80°C and filtered. Dried yellow powder, dissolved in C_6H_6 and refluxed *ca* 12 hours. A light yellow precipitate formed. Filtered and removed volatiles from C_6H_6 solution. Dried thoroughly under vacuum. Yield 7.45 g, *ca* 80%. Orange powder contains *ca.* 10% $(PMe_2Ph)_4RuCl_2$ by ^{31}P NMR.

Thermolysis of $Cp^*(PEt_3)_2RuR$ in C_6D_6: Thermolysis of $Cp^*(PEt_3)_2RuCH_3$ and $Cp^*(PEt_3)_2RuCH_2SiMe_3$ were conducted by NMR in flame sealed 5 mm NMR tubes, initial concentration 0.10-0.15 M. The reactions were carried out in an 80°C oil bath (±1°C), and monitored by quenching to room temperature and recording the ^{1}H NMR spectrum. The trimethylsilylmethyl derivative was observed to thermolyze slowly at the temperature of the NMR probe-*ca.* 30°C. Only CH_3D was observed by ^{1}H NMR upon thermolysis of the methyl derivative. The triplet for $(CH_3)_3SiCH_2D$ could be observed but could not be sufficiently resolved for quantitation. $Cp^*(PEt_3)_2RuC_6D_5$ was identified by comparison of ^{1}H and ^{31}P NMR data with those of the unlabelled species.

$Cp^*(PEt_3)_2RuC_6H_5$: To a solution of $Cp^*(PEt_3)_2RuCl$ (240 mg, 0.47 mmol) in diethyl ether/THF (5:1) was added PhMgCl (.35 ml of a 2 M sol. in THF, .7 mmol). The solution was

stirred 12 h, 5 ml H_2O added, and stirring continued 5 min. Removed volatiles from diethyl ether fraction and extracted the residue with 10 ml petroleum ether. Reduced volume to *ca.* 2 ml, heated gently to completely dissolve, and slow cooled to -78°C. Yield 197 mg, 76% of light yellow crystals. Anal.: calcd. C 61.7, H 9.16; found C 61.24, H 8.71.

Thermolysis of $Cp^*(PEt_3)_2RuR$ in C_6D_{12}: Thermolysis of $Cp^*(PEt_3)_2RuCH_3$ and $Cp^*(PEt_3)_2RuCH_2SiMe_3$ were conducted by NMR in flame sealed 5 mm NMR tubes, initial concentration 0.10-0.15 M. The reactions were carried out in 80°C and 120°C oil baths (±1°C), and monitored by quenching to room temperature and recording the ^1H NMR spectrum. Only CH_4 and Me_3SiCH_3 were detected by ^1H NMR. Only the cyclometallated species, $Cp^*(PEt_3)Ru(\eta^2\text{-}CH_2PEt_2)$, was detected by ^1H and ^{31}P NMR. Treatment of a sample of cyclometallated complex with exactly one equivalent of HCl yielded the chloride derivative, $Cp^*(PEt_3)_2RuCl$.

$Cp^*(PEt_3)Ru(\eta^2\text{-}CH_2CH_2PEt_2)$: A solution of $Cp^*(PEt_3)_2RuCH_2SiMe_3$ (500 mg, 0.9 mmol) in 10 ml cyclohexane in a small glass bomb was stirred at 80°C for 75 min. The red solution was then transferred to a 25 ml rb flask on a small frit. The volatiles were removed under vacuum, and the resultant red oil was rigorously dried under high vacuum. 5 ml Et_2O were added at -78°C, and the solution vigorously stirred. A bright yellow powder was isolated on the frit at low temperature, and washed three times with petroleum ether. The yellow powder was then recrystallized by slow cooling of an Et_2O solution. Yield 177 mg, 41%. Anal.: calcd C 56.03 H 9.40 ; found C 55.83 H 9.13.

$Cp^*(PMe_3)RuH_3$: A solution of $Cp^*(PMe_3)_2RuCH_2SiMe_3$ (7.8 g, 16 mmol) in 300 mls pentane was heated at 60°C and stirred 12 h under *ca* 1300 psi of H_2 in a Parr reactor. The solution was transferred to a rb flask under N_2, and the volatiles removed under vacuum. The crude product was dissolved in 300 mls pentane and hydrogenated again under the same conditions. This cycle was repeated three times until no starting material or $Cp^*(PMe_3)_2RuH$ was observed in the crude product by ^1H NMR. The solution from the last hydrogenation was

transferred under inert atmosphere to a rb on a frit, and the volatiles then removed under vacuum. The brown oil remaining was frozen at -78°C, then broken up under petroleum ether at this temperature to yield a light yellow powder. This powder was filtered on a cold frit and dried under vacuum. Recrystallization from petroleum ether by slow cooling to -78°C yielded crystalline $Cp^*(PMe_3)RuH_3$ as off-white rectangular cubes. Yield 2.36 g, 44%. Infrared (Nujol Mull) 1960 cm^{-1}. Anal.: calcd. C 49.52, H 8.57; found C 49.68, H 8.50.

Structure Determination for $Cp^*(PMe_3)RuH_3$: A single crystal grown from petroleum ether at -78°C over 2 days was cleaved lengthwise with a razor blade, and the resultant 0.40 x 0.35 x 0.15 mm fragment mounted in a glass capillary under N_2. The crystal was centered on a modified Syntex $P\bar{1}$ diffractometer with graphite monochromated Mo Kα radiation.[74] A monoclinic cell was found, and cell dimensions obtained from a least-squares fit to the setting angles of 15 reflections (various forms of 6 independent reflections) with $20° < 2\theta < 26°$. Systematic absences observed in the data at 0k0, k = 2n+1 and h0l, h+l = 2n+1 are unique to space group no. 14, $P2_1/n$. One quadrant of data to $2\theta = 35°$ was collected, and the check reflections removed giving 7402 reflections. No decay was observed. All 7402 reflections had $F_0^2 > 0$ and 4327 had $F_0^2 > 3\sigma(F_0^2)$. The least-squares refinement used all 7402 reflections and minimized the quantity $\Sigma w(F_0^2 - F_c^2)^2$, where $w = 1/\sigma^2(F_0^2)$. No absorption correction was made. A Patterson map gave the ruthenium coordinates, and successive structure factor-Fourier calculations located the remaining heavy atoms. An intimate twin was discovered. Subtraction of the twin allowed location of the heavy atoms but limited the refinement to a final R of 0.112 for the data where $F_0^2 > 3\sigma(F_0^2)$. The goodness of fit was S = 3.05 where n = number of data = 7402 and p = number of parameters. In the final refinement no parameter shifted more than 0.02 of its standard deviation. Hydrogen atoms including the metal hydride ligands could not be located due to the presence of the twin. Crystal data are given in Table 3, atom coordinates and U's in Table 4, and selected angles and bond lengths in Table 5. Calculations were done using the programs of the CRYM crystallographic computing system[75] on a VAX 11/750 computer; the final drawing was done using ORTEP.[76]

$Cp^*(PMe_3)RuH_3$ + HCl: $Cp^*(PMe_3)RuH_3$ (50 mg, 0.2 mmol) was dissolved in 0.3 ml C_6D_6 in a 5 mm NMR tube, exactly three equivalents of anhydrous HCl added at -78 °C, and the tube sealed at low temperature. Upon warming, an immediate color change to dark red was observed. ^1H and ^{31}P NMR spectra were consistent with the formulation as $Cp^*(PMe_3)RuCl_3$. A dark red insoluble precipitate began to form after *ca.* 30-40 min. at room temperature.

$Cp^*(PMe_3)RuH_3$ H-D Exchange Reactions: Experiments were conducted with 0.15-0.20 M solutions of $Cp^*(PMe_3)RuH_3$ in the appropriate deuterated solvent; C_6D_6, C_6D_{12}, C_7D_8, THF–d_8, in 5 mm NMR tubes. The tubes were sealed under vacuum and heated in regulated oil baths (±1 °C) or broadband photolyzed using a 400 watt medium pressure lamp or a 1000 watt high pressure lamp. The reactions were monitored by ^1H NMR. As internal standards are also H-D exchanged, comparison could only be attempted by utilizing identical spectrometer settings for a given thermolysis. Thermolysis of $Cp^*(PMe_3)RuH_3$ in C_7D_8 was observed continuously by ^1H NMR, no evidence was observed for the appearance of an H-D coupling greater than the linewidth of the hydride peaks upon loss of signal intensity.

H_2 Inhibition of $Cp^*(PMe_3)RuH_3$ H-D Exchange: $Cp^*(PMe_3)RuH_3$ (20 mg, 0.1 mmol) was dissolved in 0.3 ml C_6D_6 in a 5 mm NMR tube and the tube sealed under 700 torr pressure H_2 at -196 °C. The tube was heated to 80 °C in an oil bath for 24 h. ^1H NMR showed negligible exchange of the Cp* or PMe_3 peaks, no line broadening observed. A small amount of deuteration was observed for the hydride positions. Comparison to reference thermolysis spectra in the absence of H_2 showed a *ca.* 20 fold rate decrease.

$Cp^*(PMe_3)RuH_3$ + CO: $Cp^*(PMe_3)RuH_3$ (20 mg, 0.1 mmol) was taken up in 0.3 ml C_6H_6 in a 5 mm NMR tube. Thermolysis, 80 °C, or broadband photolysis yielded $Cp^*(PMe_3)(CO)RuH$. Identified by comparison of ^1H and ^{31}P NMR data with an authentic sample prepared by thermolysis $Cp^*(PMe_3)_2RuH$ in the presence of CO.

$Cp^*(PMe_3)RuH_3 + C_2H_4$: Took up $Cp^*(PMe_3)RuH_3$ (380 mg, 1.2 mmol) in 5 ml pentane in a small glass bomb fitted with a teflon Kontes valve. Approximated 8 atm. of freeze-pump-thawed ethylene (Matheson) were added. The solution was photolyzed for 18 h while at 5 °C utilizing a 1000 watt lamp. Removed the volatiles *in vacuo* and extracted residue with petroleum ether. The resultant light brown oil showed clean conversion by ^1H NMR to two new products. Heated NMR sample and one product cleanly converted to the other with concomitant evolution of an equivalent of C_2H_4. The resultant oil was *ca.* 95 % $Cp^*(PMe_3)(C_2H_4)RuH$ by ^1H and ^{31}P NMR. The mixture of products was consistant with 2:1 mixture of $Cp^*(PMe_3)(C_2H_4)RuH$ and $Cp^*(PMe_3)(C_2H_4)RuEt$. All attempts to crystallize $Cp^*(PMe_3)(C_2H_4)RuH$ failed. Heating mixtures of C_2H_4 and H_2 with *ca.* 1% $Cp^*(PMe_3)RuH_3$ showed catalytic hydrogenation of the ethylene to give ethane. No evidence for polymerization was observed.

$Cp^*(PMe_3)RuH_3 + R(CO)R' + H_2$: To solutions of $Cp^*(PMe_3)RuH_3$ (0.15-0.20 M) in C_6H_6 in sealable 5 mm NMR tubes were added *ca.* 10 equivalents of CH_3COCH_3, CH_3COH, or CH_3CO_2Me. The tubes were then sealed under *ca.* 3 atm H_2 (*ca.* 7 equivalents) and either heated (80 °C) or photolyzed (1000 watt lamp). Products were analyzed by ^1H NMR and infrared. Typically, volatile components would be vacuum transferred to a new NMR tube, the ^1H NMR spectrum obtained followed by the solution infrared spectrum. Non-volatile components, including the metal containing products, would be redissolved in C_6D_6 and their ^1H and ^{31}P NMR spectra obtained. Hydrogenation of CH_3CN under thermal conditions showed conversion of *ca.* 3-4 equivalents to $CH_3CH_2NH_2$.

References

1) For leading references see "Comprehensive Organometallic Chemistry" Wilkinson, G.; Stone, F. G. A.; Abel, E. W. ed., vol. 4, Pergamon Press, Oxford, 1982

2) a) Piper, T.S.; Cotton, F. A.; Wilkinson, G. *J. Inorg. Nucl. Chem.*, **1955**, *1*, 165: b) Piper, T. S.; Wilkinson, G. *Ibid.*, **1956**, *2*, 39: c) Coffey, C. E. *J. Inorg, Nucl. Chem.*, **1963**, *25*, 179: d) King, R. B.; Bisnette, M. B. *J. Am. Chem. Soc.*, **1964**, *86*, 1267

3) a) Haines, R. J.; duPreeze, A. L. *J. Am. Chem. Soc.*, **1971**, *93*, 2820: b) Haines, R. J.; duPreeze, A. L. *JCS Dalton*, **1972**, 944: c) Blackmore, T.; Cotton, J. D.; Bruce, M. I.; Stone, F. G. A. *J. Chem. Soc (A)*, **1968**, 2931

4) Fischer, E. O.; Bittler, K. *Z. Naturforsch.; Teil B,* **1962**, *17*, 274

5) a) Catheline, D.; Astruc, D. *Organometallics*, **1984**, *3*, 1094: b) Guerchais, V.; Astruc, D. *J. Chem. Soc.,Chem. Commun.*, **1985**, 835

6) Nelson, G. O. *Organometallics*, **1983**, *2*, 1474

7) Pourreau, D. B.; Geoffroy, G. L.; Rheingold, A. L.; Geib, S. J. *Organometallics*, **1986**, *5*, 1337

8) For $Cp(CO)_2FeX$ complexes, see a) Treichel, P. M.; Shubkin, R. L.; Barnett, K. W.; Reichard, D. *Inorg. Chem.*, **1966**, *4*, 1177: b) Brown, D. A.; Lyons, H. J.; Manning, A. R.; Rowley, J. M. *Inorg. Chim. Acta*, **1969**, *3*, 346: c) Haines, R. J.; Du Preez, A. L.; Marais, I. L *J. Organomet. Chem.*,**1971**, *28*, 405: d) Cullen, W. R.; Sams, J. R.; Thompson, J. A. *Inorg. Chem.*, **1971**, *10*, 843: e) Treichel, P. M.; Komar, D. A. *J. Organomet. Chem.*, **1981**, *206*, 77

9) a) Blackmore, T.; Bruce, M. I.; Stone, F. G. A. *JCS Dalton Trans.*, **1974**, 106: b) Abu Salah, O. M.; Bruce, M. I. *Ibid.*, **1975**, 2311: c) Bruce, M. I.; Gardner, R. C. F.; Stone, F. G. A. *Ibid.*, **1976**, 81; d) Bruce, M. I.; Gardner, R. C. F.; Howard, J. A. K.; Stone, F. G. A.; Wellington, M.; Woodward, P. *Ibid.*, **1977**, 621: e) Bruce, M. I.; Wallis, R. C. *J. Organomet. Chem.*, **1978**, *161*, C1: f) Ashby, G. S.; Bruce, M. I.; Tomkins, I. B.; Wallis, R. C. *Aust. J. Chem.*, **1979**, *32*, 1003: g) Bruce, M. I.; Wallis, R. C. *Ibid.*, **1979**, *32*, 1471: h) Bruce, M. I.; Swincer, A. G. *Ibid.*, **1980**, *33*, 1471: i) Bruce, M. I.; Wong, F. S.; Skelton, B. W.; White, A. H. *JCS Dalton*, **1981**, 1398: j) Bruce, M. I.; Humphrey, M. G.; Swincer, A. G.; Wallis, R. C. *Aust. J. Chem.*, **1984**, *37*, 1747

10) T. D. Tilley, R. H. Grubbs, and J. E. Bercaw, *Organometallics*,**1984**, *3*, 274

11) a) Werner, H.; Kletzin, J. *J. Organomet. Chem.*, **1982**, *228*, 289: b) Werner, H.; Kletzin, J. *Ibid.*, **1983**, *243*, C59

12) Werner, H. *Ang. Chem. Int. Ed. Eng.*, **1983**, *22*, 927

13) Paciello, R. A.; Bercaw, J. E. manuscript in preparation. See also Paciello, R. A. PhD Thesis California Institute of Technology, 1987, chapt. 2

14) For leading references see a) Green, M. L. H. *Pure Appl. Chem.*, **1978**, *50*, 27: b) Diamond, S. E.; Szalkiewicz, A.; Mares, F. *J. Am. Chem. Soc.*, **1979**, *101*, 490: c) Werner, R.; Werner, H. *Ang. Chem. Int. Ed. Eng.*, **1981**, *20*, 793: d) Green, M. A.; Huffman, J. C.; Caulton, K. G. *J. Am. Chem. Soc.*, **1981**, *103*, 695: e) Bradley, M. G.; Roberts, D. A.; Geoffroy, G. L. *Ibid.*, **1981**, *103*, 379: f) Green, M. L. H.; Izquierdo, J. *JCS Chem. Commun.*, **1981**, 186: g) Gell, K. I.; Schwartz, J. *J. Am. Chem. Soc.*, **1981**, *103*, 2687: h) Gustavson, W. A.; Epstein, P. S.; Curtis, M. D. *Organometallics*, **1982**, *1*, 884

15) Bruce, M. I. *Ang. Chem. Int. Ed. Eng.*, **1977**, *16*, 73

16) For leading references see a) Crabtree, R. H. *Chem. Rev.,* **1985**, *85*, 245: b) Green, M. L. H.; O'Hare, D. *Pure Appl. Chem.*, **1985**, *57*, 1897: c) Halpern, J. *Inorg. Chim. Acta*, **1985**, *100*, 41

17) A study of transition state parameters for phosphine dissociation from $Cp^*(PMe_3)_2X$ is in preparation: Bryndza, H. E.; Domaille, P. J.; Paciello, R. A.; Bercaw, J. E.. See also Paciello, R. A. Thesis California Institute of Technology, 1987, chapt. 4

18) Bryndza, H. E.; Fong, L. K.; Paciello, R. A.; Tam, W.; Bercaw, J. E. *J. Am. Chem. Soc.*, **1987**, *109*, 1444.

19) $Cp^*(PMe_3)Ru(\eta^2\text{-}CH_2PMe_2)$ can be independently synthesized by metathesizing $Cp^*(PMe_3)_2RuCl$ with LiNH(*tert*-Bu), see ref. 18.

20 It was observed that the solvated cation preferentially abstracts halogen from Grignard reagents. Presence of halide salts also leads to formation of the ruthenium halide species.

21) Jones, W. D.; Feher, F. J. *J. Am. Chem. Soc.*, **1984**, *106*, 1650

22) Jones, W. D.; Feher, F. J. *J. Am. Chem. Soc.*, **1984**, *106*, 1650

23) Jones, W. D.; Feher, F. J. *J. Am. Chem. Soc.*, **1986**, *108*, 4814

24) Werner, H.; Goetzig, J. *J. Organomet. Chem.*, **1985**, *284*, 73

25) a)Janowicz, A. H.; Bergman, R. G. *J. Am. Chem. Soc.*, **1982**, *104* 352: b) Janowicz, A. H.; Bergman, R. G. *Ibid.*, **1982**, *105*, 3929: c) Janowicz, A. H.; Periana, J.; Buchanan, M.; Kovac, C. A.; Stryker, J. M.; Wax, M. J.; Bergman, R. G. *Pure and Appl. Chem.*, **1984**, *56*, 13

26) a) Jones, W. D.; Feher, F. J. *J. Am. Chem. Soc.*, **1982**, *104*, 4240: b) Jones, W. D.; Feher, F. J. *Organometallics*, **1983**, 2, 562: c) Jones, W. D.; Feher, F. J. *Ibid.*, **1983**, 2, 686: Jones, W. D.; Feher, F. J. *J. Am. Chem. Soc.*, **1984**, *106*, 1650: d) Jones, W. D.; Feher, F. J. *Ibid.*, **1985**, *107*, 620

27) a) Desrosiers, P. J.; Shinimoto, R. S.; Flood, T. C. *J. Am. Chem. Soc.*, **1986**, *108*, 1346: b) Desrosiers, P. J.; Shinimoto, R. S.; Flood, T. C. *Ibid.*, **1986**, *108*, 7964

28) Tolman, C. A. *Chem. Rev.*, **1977**, *77*, 313

29) It was not possible to solve the crystal structure of $[Cp^*RuBr_2]_x$ (Single crystal grown by A. Togni), however preliminary results suggested that the structure is trimeric. Bernard Santarsiero personal communication

30) Bruce, M. I., Windsor, N. J. *Aust. J. Chem.*, **1977**, *30*, 1601

31) Fagan, P. J. Personal Communication

32) Arliguie, T.; Chaudret, B. *JCS Chem. Commun.*, **1986**, 985

33) Jones, R. A.; Mayor Real, F.; Wilkinson, G.; Galas, A. M. R.; Hursthouse, M. B.; Abdul Malik, K. M. *JCS Dalton*, **1980**, 511

34) Tolman, C. A. *Chem. Rev.*, **1977**, *77*, 313

35) Desrosiers, P. J.; Shinimoto, R. S.; Flood, T. C. *J. Am. Chem. Soc.*, **1986**, *108*, 1346

36) a) Clark, H.; Goel, A.; Goel, S. *Inorg. Chem.*, **1979**, 2803; b) Goel, R.; Montmayor, R. *Ibid.*, **1977**, *16*, 2184: c) Hietkamp, S.; Stufkens, D.; Vrieze, K. *J. Organomet. Chem.*, **1977**, *139*, 189

37) Garrou, P. *Chem. Rev.*, **1981**, *81*, 229

38) Kletzin, H.; Werner, H. *Ang. Chem. Int. Ed. Eng.*, **1983**, *22*, 873

39) Nowell, I. W.; Tabatabaian, K.; White, C. *JCS Chem. Commun.*, **1979**, 547

40) It is very likely that one product is the tetrameric species, $[Cp^*RuCl]_4$

41) Arliguie, T.; Chaudret, B. *JCS Chem. Commun.*, **1986**, 985

42) Baird, G. J.; Davies, S. G.; Moon, S. D.; Simpson, S. J.; Jones, R. H. *JCS Dalton Trans.*, **1985**, 1479

43) Fagan, P. J. personal communication

44) Nagashima, H.; Katsunori, M.; Kenji, I. *Organometallics*, **1984**, *3*, 1314

45) a) Knoth, W. *J. Am. Chem. Soc.*, **1972**, *94*, 104: b) Harris, R. O.; Hota, N. K.; Sadavoy, L.; Yuen, J. M. C. *J. Organomet. Chem.*, **1973**, *54*, 259

46) Chaudret, B.; Poilblanc, R. *Organometallics*, **1985**, *4*, 1722

47) Geoffroy, G. L.; Wrighton, M. S. "Organometallic Photochemistry", Academic Press, New York, 1983

48) Green, M. A.; Huffman, J. C.; Caulton, K. G. *J. Am. Chem. Soc.*, **1981**, *103*, 695

49) Merola, J. S.; Bercaw, J. E. unpublished results

50) Nelson, G. O. *Organometallics*, **1983**, *2*, 1474

51) Green, M. L. H.; Wong, L-L *JCS Dalton*, **1987**, 411

52) For leading references see Dewar, M. J. S.; Ford, G. P *J. Am. Chem. Soc.*, **1978**, *101*, 783

53) As discussed for MCH_2OH and $MOCH_3$: See ref. 18

54) a) Crabtree, R. H.; Mihelcic, J. M.; Quirk, J. M. *J. Am. Chem. Soc.*, **1979**, *101*, 7738: b) Crabtree, R. H.; Mellea, M. F.; Mihelcic, J. M.; Quirk, J. M. *Ibid.*, **1982**, *104*, 107: c)

Crabtree, R. H.; Demou, P. C.; Eden, D.; Mihelcic, J. M.; Parnell, C. A.; Quirk, J. M.; Morris, G. E. *Ibid.*, **1982**, *104*, 6994

55) a) Baudry, D.; Ephritikhine, M.; Felkin, H. *JCS Chem. Commun.*, **1980**, 1243: b) Baudry, D.; Ephritikhine, M. Felkin, H.; Zakrzewski, J. *Ibid.*, **1982**, 1235

56) James, B. R. "Homogeneous Hydrogenation", Wiley, New York, 1973

57) a) Pez, G. P.; Grey, R. A.; Corsi, J. *J. Am. Chem. Soc.*, **1981**, *103*, 7528: b) Grey, R. A.; Pez, G. P.; Wallo, A. *Ibid.*, **1981**, *103*, 7536: c) Wilczynski, R.; Fordyce, W. A.; Halpern, J *Ibid.*, **1983**, *105*, 2066

58) Gilbert, T. M.; Bergman, R. G. *J. Am. Chem. Soc.*, **1985**, *107*, 3502

59) Bovey, F. A. "Nuclear Magnetic Resonance Spectroscopy", Academic Press, New York, 1969

60) See ref. 59, pg. 99

61) a) Kubas, G. J.; Ryan, R. R.; Swanson, B. I.; Vergamini, P. J.; Wasserman, J. J. *J. Am. Chem. Soc.*, **1984**, *106*, 451: b) Upmacis, R. K.; Gadd, G. E.; Poliakoff, M.; Simpson, M. B.; Turner, J. J.; Whyman, R.; Simpson, A. F. *JCS Chem. Commun.*, **1985**, 27: c) Church, S. P.; Grevels, F-W; Hermann, H.; Schaffner, K. *Ibid.,* **1985**, 30: d) Gadd, G. E.; Upmacis, R. K.; Poliakoff, M.; Turner, J. J. *J. Am. Chem. Soc.*, **1986**, *108*, 2547: e) Upmacis, R. K.; Poliakoff, M.; Turner, J. J. *Ibid.*, **1986**, *108*, 3645

62) a) Crabtree, R. H.; Lavin, M. *JCS Chem. Commun.*, **1985**, 794: b) Morris, R. H.; Sawyer, J. F.; Shiralian, M.; Zubkowski, J. D. *J. Am. Chem. Soc.*, **1985**, *107*, 5581: c) Crabtree, R. H.; Lavin, M.; Bonneviot, L. *Ibid.,* **1986**, *108*, 4032: d) Conroy-Lewis, F. M.; Simpson, S. J. *JCS Chem. Commun.*, **1986**, 506

63) Baird, G. J.; Davies, S. D.; Simpson, S. J.; Jones, R. H. *JCS Dalton Trans.*, **1985**, 1479

64) a) Crabtree, R. H.; Lavin, M. *JCS Chem. Commun.,* **1985**, 1661: b) Crabtree, R. H.; Hamilton, D. G. *J. Am. Chem. Soc.*, **1986**, *108*, 3124

65) Nowell, I. W.; Tabatabaian, K.; White, C. *JCS Chem. Commun.*, **1979**, 547

66) Davies, S. G.; Moon, S. D.; Simpson, S. J. *JCS Chem. Commun.*, **1983**, 1278

67) Labinger, J. A. in "Comprehensive Organometallic Chemistry", Wilkinson, G.; Stone, F. G. A.; Abel, E. W. eds., Pergamon, Oxford, 1982, 707

68) Kubas, G. J.; Ryan, R. R.; Wrobleski, D. A. *J. Am. Chem. Soc.*, **1986**, *108*, 1339

69) Drew, M. G. B. *Prog. Inorg. Chem.*, **1977**, *23*, 67

70) Brown, T.L.; Dickerhoff, D.W.; Bafus, D.A.; Morgan, G.L. *Rev. Sci. Instrum. 1962, 33*, 491

71) Marvich, R.H.; Brintzinger, H.H. *J. Am. Chem. Soc.* **1972**, *93*, 2046

72) Tilley, T. D.; Grubbs, R. H.; Bercaw, J. E. *Organometallics*, **1984**, *3*, 274

73) Fraenkel, G.; Dayagi, S.; Kobayashi, S. *J. Phys. Chem.,* **1968**, *72*, 953

74) Samson, S.; Goldish, E.; Dick, J. *J. Appl. Cryst.*, **1980**, *13*, 425

75) Duchamp, D. J. Presented at the Nation Meeting of the National Crystallographic Association, 1974; Paper no. B19, 29

76) Johnson, C. D. "ORTEP, a Fortran Thermal Ellipsoid Plot Program"; Report ORNL-3794, Oak Ridge National Laboratory, Oak Ridge, TN 1965

SYNTHESIS AND REACTIVITY OF HALIDE, HYDRIDE, AND ALKYL DERIVATIVES OF PENTAMETHYLCYCLOPENTADIENYL(BISPHOSPHINE)IRON(II) COMPLEXES

Abstract

The reaction of $[Fe(acac)_2]_x$ (acac = η^2-acetylacetonate) with LiCp* (Cp* = η^5-C_5Me_5) in the presence of PMe_3 or DMPE (DMPE = $Me_2PCH_2CH_2PMe_2$) yields Cp*LFe(acac) (L = PMe_3, η^1–DMPE). Cp*(PMe_3)Fe(acac) and Cp*(η^1–DMPE)Fe(acac) can be isolated or reacted *in situ* with $ClSiMe_3$ (in the presence of added PMe_3 for Cp*(PMe_3)Fe(acac)) to give Cp*L_2FeCl (L = PMe_3, L_2 = DMPE). Reaction of Cp*(PMe_3)Fe(acac) with Grignard reagents, RMgX (X = Cl, Br) in the presence of PMe_3 yields either Cp*$(PMe_3)_2$FeR (R = Me,Et) or Cp*$(PMe_3)_2$FeX (R = CMe_3, $CH_2C_6H_5$, C_3H_5), depending on the size of R. Cp*L_2FeX can be further reacted with RMgX to yield Cp*L_2FeR (R = H, Me, $CH_2C_6H_5$) or Cp*(PMe_3)Fe(η^3-C_3H_5). Routes to the cationic species [Cp*$(PMe_3)_2$FeL]PF_6 (L = PMe_3, CO) are described. Reaction of Cp*(PMe_3)Fe(acac) with EtMgX in the absence of PMe_3 yields Cp*(PMe_3)(C_2H_4)FeH. Treatment of this complex with dihydrogen yields a highly unstable Fe(IV) complex, Cp*(PMe_3)FeH_3. The reactivity of these complexes is discussed and proposed to involve a highly reactive, 16-electron unsaturated intermediate, Cp*(PMe_3)FeR (R = alkyl or hydride).

Introduction

We have been interested in the synthesis and reactivity of electron-rich, half sandwich complexes of the type $Cp^*(PR_3)_2RuX$.[1,2] These have proved to be precursors to a highly reactive, 16-electron species, $[Cp^*(PR_3)RuR]$ (R = alkyl, hydride), which is capable of activating C-H bonds both intra- and intermolecularly.[3] This is in large part due to stabilization by the electron-donating ligand set of the Ru(IV) intermediate that results from the oxidative addition of the C-H bond. We wished to extend these studies to the analogous iron complexes, $Cp^*(PMe_3)_2FeX$.

Although the synthesis and reactivity of $Cp(CO)_2FeX$ derivatives have been extensively investigated,[4] there are few synthetic routes to bisphosphine complexes. Attempts to effect disubstitution by thermolysis or photolysis have generally resulted in isolation of monosubstituted complexes, $Cp(CO)(L)FeX$ (L=PPh_3,[5] PMe_3), or cationic species such as $[CpFe(PMe_3)_3]Br$.[6] Disubstituted complexes have been generally prepared using chelating phosphines such as DPPE ($Ph_2PCH_2CH_2PPh_2$).[7] Tertiary phosphine complexes, $Cp(PMe_3)FeX$ (X =I, CN, Me[6]; X =$Si(NMe_2)_3$[8]) have been isolated in photochemical reactions, however, the reactions tend to be very sensitive to the conditions employed. In addition, the permethylcyclopentadienyl precursors, $Cp^*(CO)_2FeX$, for such reactions have only recently been reported.[9]

$Cp^*(PMe_3)_2FeH$ has been obtained from the reaction of $(\eta^6\text{–}C_6H_6)(PMe_3)_2Fe$ with Cp^*H,[10] and was reported to convert cleanly to $Cp^*(PMe_3)_2FeCl$, thus providing an entry to the $Cp^*(PMe_3)_2FeX$ system. However, this entry is limited by the necessity for the metal vapor synthesis of the precursor complex, $(\eta^6\text{–}C_6H_6)(PMe_3)_2Fe$.[11] The synthesis of $Cp^*Fe(acac)$ *via* treatment of $Fe(acac)_2$ with $LiCp^*$[12] and its reaction with MeMgI under CO to yield $Cp^*(CO)_2FeMe$ have recently been reported.[13] We have attempted to extend this synthetic route to the PMe_3 complexes, and now wish to report the facile synthesis of the

monophosphine acetylacetonate complexes **1** and **2**, and their utility in the synthesis of a wide variety of electron-rich iron complexes.

Results and Discussion

Preparation of base free, oligomeric $[Fe(acac)_2]_x$ is effected by sublimation of the commercially available product. Treatment of this material with LiCp* in the presence of one equivalent of phosphine, PMe_3 or DMPE, at -78°C in THF, yields Cp*LFe(acac) on warming to room temperature, eq 1.

$$[Fe(acac)_2] + LiCp^* + L \xrightarrow{THF} Cp^*LFe(acac) \quad (L = PMe_3,\ \eta^1\text{-DMPE}) \tag{1}$$

These complexes are most easily used *in situ,* but can also be isolated. $Cp^*(PMe_3)Fe(acac)$ is very soluble, but can be obtained as a dark red, crystalline solid in 71% yield from petroleum ether at low temperature. This complex exhibits a paramagnetic ^1H NMR spectrum, *i.e.*, with very broad peaks exhibiting temperature dependent shifts. Treatment with carbon monoxide yields the known, diamagnetic complex, Cp*(CO)Fe(acac),[10] on warming.

Treatment of $Cp^*(PMe_3)Fe(acac)$ or $Cp^*(\eta^1\text{-DMPE})Fe(acac)$ with $ClSiMe_3$ (and an additional equivalent of PMe_3 in the case of $Cp^*(PMe_3)Fe(acac)$) in THF at −78°C affords Cp^*L_2FeCl on warming to room temperature, eq. 2.

$$Cp^*LFe(acac) + ClSiMe_3 \xrightarrow{THF} Cp^*L_2FeCl + (acac)SiMe_3 \quad (L = PMe_3,\ L_2 = DMPE) \tag{2}$$

$Cp^*(PMe_3)_2FeCl$ is moderately soluble and can be most easily isolated as a dark blue crystalline compound in 58% yield by toluene extraction, reduction of solvent, and addition of petroleum ether. See Table 1 for spectral data. Cp*(DMPE)FeCl is quite insoluble but can be isolated as a slate blue powder in 20% yield by a toluene extraction followed by

recrystallization from diethyl ether. The yield for this reaction is lowered significantly by the formation of highly insoluble oligomeric products.

Treatment of $Cp^*(PMe_3)Fe(acac)$ with MeMgCl in the presence of PMe_3 yields the methyl complex, $Cp^*(PMe_3)_2FeMe$, on warming to room temperature, eq. 3.

$$Cp^*(PMe_3)Fe(acac) + MeMgCl \xrightarrow{THF} Cp^*(PMe_3)_2FeMe \qquad (3)$$

This complex is very soluble, but can be isolated as a dark red crystalline complex from petroleum ether at low temperature in 55% yield based on $[Fe(acac)_2]_x$. This compound hydrogenates cleanly to yield $Cp^*(PMe_3)_2FeH$ quantitatively by ^1H NMR. The hydride is less soluble and can be isolated as an orange crystalline complex from petroleum ether at low temperature. Hydrogenation of the crude product from the preparation of $Cp^*(PMe_3)_2FeMe$ affords $Cp^*(PMe_3)_2FeH$ in 74% yield based on $[Fe(acac)_2]_x$.

Treatment of $Cp^*(PMe_3)Fe(acac)$ with one equivalent of Me_3CMgCl or $C_6H_5CH_2MgCl$ in the presence of PMe_3 yields $Cp^*(PMe_3)_2FeCl$ as the isolated product. Treatment with one equivalent of C_3H_5MgBr affords a low yield, 39%, of violet $Cp^*(PMe_3)_2FeBr$; presumably by disproportionation, eq. 4.

$$Cp^*(PMe_3)Fe(acac) + RMgX + PMe_3 \xrightarrow[(R = CMe_3,\ CH_2C_6H_5,\ C_3H_5)]{THF} Cp^*(PMe_3)_2FeX \qquad (4)$$

Treatment of $Cp^*(PMe_3)Fe(acac)$ with one equivalent of EtMgX in the absence of PMe_3 yields $Cp^*(PMe_3)(C_2H_4)FeH$ quantitatively by ^1H NMR, eq. 5.

$$Cp^*(PMe_3)Fe(acac) + EtMgX \xrightarrow{THF} Cp^*(PMe_3)(C_2H_4)FeH \qquad (5)$$

TABLE 1

^1H AND $^{31}P\{^1H\}$ NMR DATA

Compound	^1H[a] C_5Me_5	^1H[a] PMe_3[c]/DMPE[d]	^1H[a] Other Assignments	^{31}P[b]
$Cp^*(PMe_3)_2FeCl$	1.43	1.26(7.3)		21.9
$Cp^*(DMPE)FeCl$	1.58	1.00(9.9) 1.54(7.6)		70.6
$Cp^*(PMe_3)_2FeMe$	1.57	1.05(7.0)	CH_3 -0.10(*t*, 7.6)	34.7
$Cp^*(PMe_3)_2FeH$	1.85	1.20(7.2)	Fe*H* -17.50(*t*, 75.1)	32.6
$Cp^*(PMe_3)_2FeBr$	1.48	1.30(7.3)		20.7
$Cp^*(PMe_3)Fe(\eta^3\text{-}C_3H_5)$	1.56	0.84(*d*, 6.6)	$\eta^3\text{-}C_3H_5$[e] 3.03(*m*),1.55 (*d*, 6.0), -0.5 (*q*, 10.2 of *t*, 1.2)	32.8
$Cp^*(PMe_3)_2FeCH_2C_6H_5$	1.48	1.05(7.1)	CH_2 1.93(*t*, 5.9) C_6H_5 7.25, 7.09, 6.99 (*m*)	28.7
$Cp^*(DMPE)FeMe$	1.67	1.07(*m*)	CH_3 -1.09(*t*, 6.9)	80.5
$Cp^*(DMPE)FeH$	1.95	1.29(8.2) 1.13(6.9)	Fe*H* -18.19(*t*, 71.5)	74.0
$[Cp^*(PMe_3)_2Fe(PMe_3)]PF_6$[f]	1.62	1.44(broad singlet)	PF_6 -144.5 (pentuplet $J_{P\text{-}F}$ = 710.4)	19.2
$[Cp^*(PMe_3)_2Fe(CO)]PF_6$[f]	1.80	1.50(9.6)	PF_6 -144.6 (pentuplet $J_{P\text{-}F}$ = 710.4)	22.0
$Cp^*(PMe_3)FeH_3$	1.90	1.1(*d*, 8.4)	Fe*H* -12.38(*d*,42.9)	38.7

a) Shifts in ppm referenced to $SiMe_4$ in C_6D_6, unless noted otherwise. b) Shifts in ppm referenced to 85% H_3PO_4 at 36.4 MHz in C_6D_6. All resonances are singlets. c) Number in parentheses is the seperation in Hz between the outer lines of the filled in doublet, $^2J_{P\text{-}H} + {}^4J_{P\text{-}H}$, unless noted otherwise. d) Number in parentheses is distance between outer lines in filled in doublet for each set of unique DMPE methyl protons. DMPE backbone methylene groups broad and obscured by other spectral features. e) Spectra obtained at -20°C in THF-d_8. f) Spectra obtained in THF-d_8.

This complex can be obtained as an off-white, crystalline solid, with some difficulty due to its high solubility, in 45.9% yield. A different preparation and spectral data for this fluxional complex have been reported previously.[8]

Reaction of Cp^*L_2FeCl with RMgX occurs cleanly to yield the alkyl or hydride (*via* β-H abstraction) derivatives, eq. 6. Reaction of $Cp^*(PMe_3)_2FeCl$ with C_3H_5MgBr is accompanied by phosphine loss to give the η^3-allyl complex, $Cp^*(PMe_3)Fe(\eta^3\text{-}C_3H_5)$.

$$Cp^*L_2FeCl + RMgX \xrightarrow{THF} Cp^*L_2FeR \quad (R = Me, H, CH_2C_6H_5, CH_2SiMe_3) \tag{6}$$

The allyl complex, $Cp^*(PMe_3)Fe(\eta^3\text{-}C_3H_5)$, can be isolated as an orange crystalline complex in 76% yield. The benzyl complex, $Cp^*(PMe_3)_2FeCH_2C_6H_5$, can be isolated as a dark red crystalline complex at 0°C from petroleum ether in low yield, 25%. Formation of this complex is accompanied by that of bibenzyl, which crystallizes from petroleum ether at -78°C in about 20% isolated yield. The trimethylsilylmethyl complex can be obtained at low temperature as well-formed very dark red crystals in *ca.* 53% yield. This complex has proved difficult to characterize. It is very unstable, decomposing in solution rapidly. It is also unstable in the solid state (at -40°C, the crystal faces dull and the edges degrade in *ca.* 12 hours).

$Cp^*(DMPE)FeMe$ can be obtained as red-orange crystals in 56% yield. This complex is extremely stable towards hydrogenation to yield the hydride. Heating $Cp^*(DMPE)FeMe$ under 3 atmospheres of hydrogen at 140°C for 6 hours does not yield hydride; some decomposition is observed to occur on further heating. Treatment with Me_3CMgCl yields the hydride complex cleanly.[14] $Cp^*(DMPE)FeH$ can be isolated as yellow-orange crystals in 52% yield. This complex is quite soluble. This is in contrast to the the behavior observed for the PMe_3 complexes, where the hydride derivative is less soluble than the methyl derivative.

Treatment of $Cp^*(PMe_3)_2FeCl$ with KPF_6 in methanol under one atmosphere of ethylene yields 57% of the light orange complex, $[Cp^*(PMe_3)_2Fe(PMe_3)]PF_6$ on extraction with CH_2Cl_2 and addition of Et_2O; presumably by disproportionation of the starting material. $[Cp^*(PMe_3)_2Fe(PMe_3)]PF_6$ can be prepared directly by treatment with KPF_6 in the presence of PMe_3. Treatment in the presence of CO affords $[Cp^*(PMe_3)_2Fe(CO)]PF_6$ on workup as a yellow powder in 83% yield. Reaction of $Cp^*(PMe_3)_2FeCl$ and $Cp^*(PMe_3)_2FeH$ with $HBF_4{\cdot}Et_2O$ does not occur cleanly, but reaction of Cp*(DMPE)FeH with $HBF_4{\cdot}Et_2O$ affords $[Cp^*(DMPE)FeH_2]BF_4$ as a white analytically pure precipitate in 81% yield. This complex is extremely unstable in solution.

Reaction of $Cp^*(PMe_3)_2FeMe$ with H_2 yields the hydride, $Cp^*(PMe_3)_2FeH$, cleanly at 80°C in less than one hour. It is observed that heating $Cp^*(PMe_3)_2FeH$ in C_6D_6 does not give the deuterophenyl complex, $Cp^*(PMe_3)_2FeC_6D_5$, but that the hydride signal disappears on extended heating and the proteo solvent peak increases. Catalytic H-D exchange can be achieved by heating the hydride under 3 atm D_2 in C_6D_6; this process is very slow, only 6-7 turnovers being observed after one week at 80°C. Heating the methyl and benzyl complexes in C_6D_6 leads to decomposition. This contrasts to the behavior of the analogous ruthenium alkyls, which thermolyze cleanly in C_6D_6 to give $Cp^*(PR_3)_2RuC_6D_5$.[3]

It has been observed that heating $Cp^*(PMe_3)_2RuH$ under dihydrogen yields $Cp^*(PMe_3)RuH_3$ with concomitant phosphine loss, eq. 7.[15]

$$Cp^*(PMe_3)_2RuH + H_2 \rightleftharpoons Cp^*(PMe_3)RuH_3 + PMe_3 \qquad (7)$$

Heating $Cp^*(PMe_3)_2FeH$ under 3 atm. H_2 in C_6H_6 at 80°C yields no observable $Cp^*(PMe_3)FeH_3$ by ^1H NMR (< 5%). However, treatment of $Cp^*(PMe_3)(C_2H_4)FeH$ with 3 atm. H_2 at room temperature affords clean conversion to a complex with an ^1H NMR spectrum (THF–d_8) characteristic of $Cp^*(PMe_3)FeH_3$, eq. 8. The spectral features are as follows: Cp*,

15 protons at 1.90 ppm relative to TMS; PMe_3, 9 protons at 1.10 ppm ($^2J_{P-H}$ = 8.4 Hz); H, 3 protons at -12.4 ppm ($^2J_{P-H}$ = 42.9 Hz).

$$Cp^*(PMe_3)(C_2H_4)FeH + 2H_2 \longrightarrow Cp^*(PMe_3)FeH_3 + C_2H_6 \quad (8)$$

When $Cp^*(PMe_3)FeH_3$ is generated in C_6D_6, deuterium is observed to wash into the hydride positions. The partially deuterated complexes, $Cp^*(PMe_3)FeH_2D$ and $Cp^*(PMe_3)FeHD_2$, are observed as a discrete species by ^1H NMR ($^2J_{H-D}$ = 4.80 Hz for $Cp^*(PMe_3)FeH_2D$) and ^{31}P NMR. Removal of H_2 causes rapid decomposition. The disproportionation product, $Cp^*(PMe_3)_2FeH$, is observed by ^1H NMR and infrared (ν(Fe-H) = 1780 cm^{-1}), no starting material is observed (ν(Fe-H) = 1860 cm^{-1}).

Attempts to grow crystals under H_2 yielded only decomposition products. An infrared spectrum of $Cp^*(PMe_3)FeH_3$ can be obtained by generating the trihydride in pentane, quickly blowing off the solvent with H_2, and running the infrared spectrum of the resulting oil (ν(FeH) = 1905 cm^{-1} vs polystyrene). The decomposition product, $Cp^*(PMe_3)_2FeH$, is observed as a minor product An infrared spectrum in solution can be obtained by generation of $Cp^*(PMe_3)FeH_3$ in tetrahydrofuran, and subsequent cannulation under H_2 into a CsCl liquid infrared cell. The decomposition product $Cp^*(PMe_3)_2FeH$ is observed as the major product.

$Cp^*(PMe_3)FeH_3$ is a highly fluxional and unstable molecule whose structure is probably that of a 4-legged piano stool. It can be directly compared to the structurally characterized Fe(IV) complex, $Cp(CO)Fe(SiCl_3)_2H$, also a 4-legged piano stool.[16] It joins tetrakis(1–norbornyl)iron[17] and $(PEtPh_2)_3FeH_4$[18] as one of the scarce neutral, organometallic Fe(IV) complexes that have been prepared.

The H-D coupling constant of 4.89 Hz observed on monodeuteration of $Cp^*(PMe_3)FeH_3$ can be extrapolated to an H-H coupling constant of 30.08 Hz. This coupling constant is larger than that usually expected for a H-H coupling constant in a transition metal polyhydride,[19] but still much smaller than those observed for a growing number of transition metal

dihydrogen complexes (~200 Hz).[20] For example, the recently reported complex, $[Cp(PPh_3)(CN^tBu)Ru(\eta^2\text{-}H_2)]PF_6$,[20f] exhibits an H-D coupling constant of 28.6 Hz. The Fe(IV) complex, $FeH_4(PEtPh_2)_3$, has recently been proposed to be a dihydrogen adduct based on T_1s data and a reinterpretation of the published infrared data.[20i]

It has been noted that the well-characterized transition metal dihydrogen complexes have been octahedral, d^6, and electron deficient.[20d-g] It has also been pointed out that these complexes have ligands trans to the η^2-H_2 moiety which exert a strong sigma trans effect.[20d,g] Hoffmann and coworkers have proposed a model for dihydrogen activation on transition metal centers that involves interaction of the filled sigma orbital of dihydrogen with an empty orbital on an octahedral metal center, and interaction of a filled orbital on the metal center with the sigma antibonding orbital on the dihydrogen.[21] This interaction is analogous to that long accepted for the synergistic binding of ethylene to transition metal centers.[22] This description,[20g] coupled to that of the orbital basis of the trans effect,[23] appears to offer a good conceptual basis for the difference in binding of η^2-H_2 *versus* terminal metal hydrides.[24]

In the pseudo-octahedral geometry that would exist at the metal center in $Cp^*(PMe_3)FeH_3$ if an η^2–H_2 was present, the ligand trans to the hydrides would be Cp* (assumed to occupy three sites in the octahedron). This is a much weaker trans ligand, one negative charge spread over five carbons, than CO, H, or R^- (the trans ligands in the well characterized dihydrogen adducts). The ligand set, Cp* and PMe_3, is electron donating, and the complex is neutral. These factors serve to increase the electron density at the metal center, thereby increasing the amount of density available for backbonding, and thus favoring the dihydride structure. Such is the case for the complexes $Cp^*(PMe_3)RuH_3$[25] and $Cp(PPh_3)RuH_3$.[26]

In the cationic complex, $[Cp(PPh_3)(CN^tBu)Ru(\eta^2\text{-}H_2)]PF_6$, the ligand set is less electron-donating (Cp and PPh_3), or is electron withdrawing (CN^tBu, analogous to CO). The electron deficiency of this metal center outweighs the sigma trans effect of the Cp and favors a true

dihydrogen adduct. In the fluxional complex $FeH_4(PEtPh_2)_3$, there is a strong probability that the trans ligand is predominantly a hydride, and that the complex is formally analogous to the characterized dihydrogen adduct, *trans*-$[Fe(\eta^2\text{-}H_2)(H)(DPPE)_2]BF_4$.[20f] In this case, the trans ligand and high oxidation state favor a dihydrogen bonding mode.

One criterion proposed for identification η^2-H_2 adducts has been the observation of unusually short T_1s. T_1s measurements on $Cp^*(PMe_3)FeH_3$ prepared from analytically pure $Cp^*(PMe_3)(C_2H_4)FeH$ samples have not proved reproducible. As T_1s measurements are very sensitive to even trace amounts of paramagnetic impurities,[27] such a result is not unexpected. T_1s measurements for the Fe(IV) complex, $FeH_4(PEt_2Ph)_3$, have been reported.[28] However, this complex is isolable as a crystalline solid, unlike $Cp^*(PMe_3)FeH_3$.

Another criterion has been the observation of a peak in the infrared spectrum attributable to bound dihydrogen.[29] Such a peak was not observed in the spectra obtained for $Cp^*(PMe_3)FeH_3$. This peak has often proved weak and difficult to see,[30] so its absence does not rule out a dihydrogen adduct. In addition, if a dihydrogen adduct were present as a minor component in a mixture of trihydride and dihydrogen hydride, it would be expected that the peak would not be observed.

One mechanism by which an intermediate sized coupling constant could be produced is *via* a fluxional process such as that shown below, Scheme 1. A simple weighted average (using "normal" values of ^1J = 200 Hz and ^2J = 10 Hz) would then predict about 10% of the dihydrogen hydride complex. A variable temperature study was undertaken of $Cp^*(PMe_3)FeH_3$ (400 MHz, to -80°C) in order to freeze out such an equilibrium, but the complex remained fluxional at all temperatures examined.

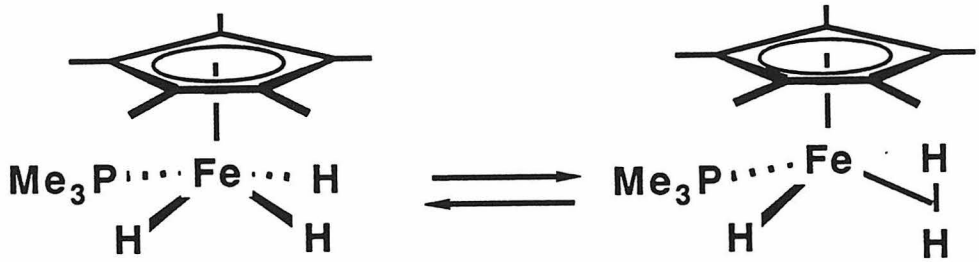

Scheme 1

A similar process has been proposed for the scrambling of a terminal hydride site with a η^2-H_2 site in an iridium complex, $[IrH(H_2)(PPh_3)_2(C_{13}H_8N)]^+$.[20d] An equilibrium mixture of an η^2-H_2 adduct and the corresponding dihydride has recently been reported for the complex $W(CO)_3(PR_3)_2H_2$, in this case *ca.* 15% dihydride can be directly observed.[20g,l]

It is proposed that an equilibrium with fast exchange offers the simplest explanation for the observed coupling constant in $Cp^*(PMe_3)FeH_3$. If such a process is occurring, then this complex represents a system where the amount of dihydrogen complex in equilibrium has been lowered to *ca.* 10%. The iron and tungsten systems are then complimentary, and represent intermediates between dihydride and dihydrogen adducts. The η^2–H_2 and terminal hydride in *trans*-$[Fe(\eta^2\text{-}H_2)(H)(DPPE)_2]BF_4$ have also been shown to exchange, however, the mechanism for this rearrangement is not clear.[20f]

The reactions of these iron complexes can be most easily explained by invoking a ligand loss mechanism to generate a highly reactive, $Cp^*(PMe_3)FeX$, species as shown in Scheme 2.

$$Cp^*(PMe_3)_2FeR \rightleftharpoons [Cp^*(PMe_3)FeR] + PMe_3$$

$$[Cp^*(PMe_3)FeR] + L \rightleftharpoons [Cp^*(PMe_3)(L)FeR]$$

or

$$[Cp^*(PMe_3)FeR] + H_2 \rightleftharpoons [Cp^*(PMe_3)FeH_2R]$$

$$[Cp^*(PMe_3)FeR] + R'\text{-}H \rightleftharpoons [Cp^*(PMe_3)FeRR'H]$$

$$[Cp^*(PMe_3)FeH_2R] \rightleftharpoons [Cp^*(PMe_3)FeH] + RH$$

Scheme 2

$$[Cp^*(PMe_3)FeH] + H_2 \rightleftharpoons Cp^*(PMe_3)FeH_3$$

or

$$[Cp^*(PMe_3)FeH] + L \rightleftharpoons Cp^*(PMe_3)(L)FeH$$

This scheme rationalizes the decrease in rate on replacement of the two PMe_3 ligands with DMPE, catalytic H-D exchange of the hydrides with deuterated solvent, ability to generate the unsaturated species using an easily lost ligand such as C_2H_4, and fast trapping by ligands such as CO (or PMe_3) to give $Cp^*(PMe_3)(L)FeX$. It is analogous to that proposed for the $Cp^*(PMe_3)_2RuX$ system,[31] but incorporates the observation that thermolysis of alkyls in the presence of arenes does not give the iron aryl and alkane.

In summary, a convenient one-pot synthesis of Cp^*L_2FeCl has been developed. The intermediate complex, Cp*LFe(acac), can be used *in situ* or isolated. The reactivity of this complex with Grignard reagents has been outlined. The reactions of the complexes, Cp^*L_2FeX, with hydrogen have been investigated and a mechanism for the reactivity observed proposed. Evidence for the novel Fe(IV) complex, $Cp^*(PMe_3)FeH_3$, has been presented. The nature of the hydrogen bonding mode in this complex has been discussed in some detail, and a fluxional process involving a dihydrogen hydride and trihydride proposed. The reaction chemistry of these iron complexes is proposed to occur *via* coordinatively unsaturated and highly reactive $Cp^*(PMe_3)FeX$ species.

Experimental Section

General Considerations: All syntheses and chemical manipulations were carried out by standard high vacuum and Schlenk techniques. Hydrogen, nitrogen, and argon were purified by passing the streams through MnO on vermiculite followed by activated 4 Å sieves.[32] Benzene, pentane, THF, diethyl ether and toluene were purified by distillation from purple sodium/benzophenone ketyl solutions under argon or by vacuum transfer from the same drying and degassing medium or from "titanocene".[33] Benzene, toluene and pentane

required the addition of tetraglyme (Aldrich) to effect dissolution of the sodium. Methylene chloride was vacuum transferred from calcium hydride. Methanol was dried by stirring over NaOMe and vacuum transferred. Deuterated solvents were purified and maintained in the same manner as the protonic isotopomers. $HBF_4 \cdot Et_2O$ was degassed and used as supplied from Aldrich. Hydrogen, carbon monoxide, and ethylene (freeze-pump-thawed three times) were used as obtained from Matheson. Grignard reagents were used as received from Aldrich. $[Fe(acac)_2]_x$ was obtained commercially (Sharpe Chemicals Company) and sublimed prior to use. The solid was heated at 100°C under vacuum to remove all base and H_2O, then sublimed at 160°C through glass wool plugs.

IR spectra were recorded as nujol mulls on KBr plates on a Beckman IR 4230 spectrophotometer. Routine ^1H and ^{31}P spectra for characterization were obtained in benzene-d_6 or THF-d_8 with Me_4Si or H_3PO_4 as standard references, on Jeol Model FX-90Q or Jeol GX-400 spectrometers. T_1s measurements were obtained using standard programs and data analysis packages on the Jeol GX-400.

Satisfactory elemental analysis on complexes reported were obtained from the California Institute of Technology analytical service.

Preparation of Cp*(PMe$_3$)Fe(acac): To a mixture of $[Fe(acac)_2]_x$ (5g, 19.7 mmol) and LiCp* (2.795g, 19.7 mmol) was added 50 mls THF and 2.2 mls PMe_3 (21.7 mmol) at -78°C. The solution was allowed to warm to room temperature and stirred for 10 min. The volatiles were removed under vacuum and the residue thoroughly dried. Extracted residue with petroleum ether until the residue appeared pink. Reduced the volume of the filtrate to *ca.* 20 mls and cooled slowly. Filtered dark red crystals on a cold frit and dried under vacuum. Yield 5.091g, 70.7%. Anal. Calcd.: C 59.02; H 8.53. Found; C 59.3; H 8.45.

Preparation of Cp*(PMe$_3$)$_2$FeCl: To a mixture of $[Fe(acac)_2]_x$ (3.5g, 13.8 mmol) and LiCp* (1.957, 13.8 mmol) was added 50 ml THF and PMe_3 (3.0 mls, 29.5 mmol) at -78°C. The

solution was warmed to room temperature with stirring, then cooled again to -78°C and $ClSiMe_3$ (3.48 mls, 27.6 mmol) added. The solution was warmed to room temperature and stirred 0.5 h. The volatiles were removed under vacuum and the residue thoroughly dried. The residue was extracted with toluene until almost white. The filtrate was pulled down to an oil and petroleum ether added. The dark blue crystals were filtered on a cold frit and dried under vacuum. Yield 3.028 g, 58%. Anal. Calcd.: C 50.75; H 8.72. Found: C 51.00; H 8.65.

Preparation of Cp*(DMPE)FeCl: To a mixture of $[Fe(acac)_2]_x$ (3 g, 11.8 mmol) and LiCp* (1.677 g, 11.8 mmol) was added 50 mls THF and 1.17 mls DMPE (11.9 mmols) at -78°C. The solution was allowed to warm to *ca.* 0°C, then cooled to -78°C again and $ClSiMe_3$ (3.13 mls, 24.8 mmol) added. The solution was warmed to room temperature and allowed to stir 0.5 h. The volatiles were removed under vacuum and the residue thoroughly dried. Extracted residue with 10 ml petroleum ether to remove soluble products. Extracted with toluene and removed volatiles from supernatant to give blue-grey residue. Extracted this residue with Et_2O and cooled filtrate slowly to give light blue crystals. Filtered on cold frit and dried under vacuum. Yield 887 mgs, 20%. Anal. Calcd.: C 51.02; H 8.30. Found: C 51.14; 8.14.

Preparation of Cp*$(PMe_3)_2FeCH_3$: To a mixture of $[Fe(acac)_2]_x$ (1.583, 6.2 mmol) and LiCp* (885 mgs, 6.2 mmol) was added 10 ml THF and 1.3 ml PMe_3 (12.8 mmol) at -78°C. The mixture was allowed to warm to room temperature with stirring then cooled to -78° MeMgCl (2.4 mls, 2.9 M in THF, 6.96 mmol) added. The solution was warmed to room temperature with stirring. Pulled of the volatiles and dried thoroughly under vacuum. Extracted the residue with petroleum ether, reduced the volume of the filtrate to *ca.* 5 ml. Cooled to -78°C for 12 h, filtered dark red crystals on a cold frit and dried under vacuum. Yield 1.218 g, 54.6% Anal. Calcd.: C 56.98; H 10.00. Found: C 57.06; H 9.72.

Preparation of Cp*$(PMe_3)_2FeH$: To a mixture of $[Fe(acac)_2]_x$ (1.5g, 5.9 mmol) and LiCp* (839 mg, 5.9 mmol) was added 15 ml THF and 1.2 ml PMe_3 (11.8 mmol) at -78°C. The solution was allowed to warm to room temperature with stirring, cooled again to -78°C,

MeMgCl was added (2.2 ml, 2.9 M in THF, 6.5 mmol), and the solution allowed to warm to room temperature with stirring. The volatiles were removed under vacuum and the residue thoroughly dried. The residue was extracted with C_6H_6, the filtrate transferred to a glass bomb and heated at 80°C for 1 h under 3 atm H_2. The volatiles were removed under vacuum and the residue thoroughly dried. The residue was extracted with petroleum ether, the filtrate reduced in volume to *ca.* 5 ml, and crystals were grown at -78°C. The light orange crystals were filtered on a cold frit and dried under vacuum. Yield 1.5 g, 74%. Infrared (Nujol Mull) 1780 cm^{-1} (s). Anal. Calcd.: C 55.84; H 9.60. Found: C 55.74; H 9.45.

Preparation of $Cp^*(PMe_3)_2FeBr$: To a mixture of $[Fe(acac)_2]_x$ (500 mg, 2.0 mmol) and LiCp* (280 mg, 2.0) was added 10 ml THF and PMe_3 (0.2 ml, 2.0 mmol) at -78°C. The solution was allowed to warm to room temperature with stirring, cooled again to -78°C, and C_3H_5MgBr (2.95 ml, 1 M in Et_2O, 2.95 mmol) added. The solution was warmed to room temperature and stirred for 15 min. The volatiles were removed under vacuum and the residue thoroughly dried. Extracted with petroleum ether, reduced the volume of the filtrate to *ca.* 2-3 ml, and grew crystals at -78°C. Filtered the violet crystals on a cold frit and dried under vacuum. Yield 290 mg, 39%. Anal. Calcd.: C 45.42; H 7.86. Found: C 45.81; H 7.79.

Preparation of $Cp^*(PMe_3)(C_2H_4)FeH$: To a mixture of $[Fe(acac)_2]_x$ (1 g, 3.9 mmol) and LiCp* (559 mg, 3.9 mmol) was added 10 ml THF and exactly one equivalent PMe_3 (0.4 ml, 3.9 mmol) at -78°C. The solution was warmed to room temperature, cooled again to -78°C, and EtMgCl (1.98 ml, 2 M in THF, 4.0 mmol) added. The solution was allowed to warm to room temperature, the volatiles removed under vacuum and thoroughly dried, and the residue extracted with petroleum ether. The filtrate was reduced to an oil, frozen, and then broken up by vigorous stirring under petroleum ether at -78°C. The resultant yellow powder was isolated on a cold frit, dried under vacuum, and recrystallized from petroleum ether to give off-white crystals. Yield 535 mg, 45.9%. Infrared (Nujol Mull) 1860 cm^{-1} (m). All NMR data identical to previously published results.[10]

Preparation of $Cp^*(PMe_3)Fe(\eta^3\text{-}C_3H_5)$: To a solution of $Cp^*(PMe_3)_2FeCl$ (496 mg, 1.3 mmol) in 15 ml THF was added C_3H_5MgBr (1.74 ml, 1 M in Et_2O, 1.74 mmol) at -78°C, and the solution warmed to room temperature and stirred 15 min. The volatiles were removed under vacuum and the residue dried thoroughly. The residue was extracted with petroleum ether, the filtrate reduce to *ca.* 2-3 ml, and crystals grown at -78°C. The orange crystals were isolated on a cold frit and dried under vacuum. Yield 305 mg, 76%. Anal. Calcd.: C 62.35; H 9.48. Found: C 62.09; H 9.26.

Preparation of $Cp^*(PMe_3)_2FeCH_2C_6H_5$: To a mixture of $[Fe(acac)_2]_x$ (775 mg, 3.1 mmol) and LiCp* (433 mg, 3.1 mmol) was added 40 ml THF and PMe_3 (0.62 ml, 6.1 mmol) at -78°C. The solution was warmed to room temperature, cooled to -78°C again, and $C_6H_5CH_2MgCl$ (1.6 ml, 2 M in THF, 3.2 mmol) was added. The solution was warmed to room temperature, the volatiles removed under vacuum, and the residue extracted with petroleum ether. The product was identified as $Cp^*(PMe_3)_2FeCl$ by ^1H NMR. The product was dissolved in 10 ml THF and another equivalent of Grignard reagent added at -78°C. The solution was warmed, the volatiles removed, the residue extracted, and crystals were grown at -78°C. The crystals proved to contain bibenzyl by ^1H NMR. The product was recrystallized slowly from petroleum ether; dark red crystals coming out at 0°C, followed by white crystals at -78°C. The red crystals were isolated and dried under vacuum. Yield 332 mg, 25%. Anal. Calcd.: C 63.59; H 9.22. Found: C 63.94; H 9.31.

Preparation of $Cp^*(DMPE)FeCH_3$: To a solution Cp*(DMPE)FeCl (200 mg, 0.6 mmol) in 10 ml THF was added MeMgCl (0.2 ml, 2.9 M in THF, 0.6 mmol) at -78°C. The solution was allowed to warm to room temperature, the volatiles removed under vacuum, and the residue thoroughly dried. The residue was extracted with petroleum ether, the volume of the filtrate reduced to *ca.* 5 ml, and crystals grown at -78°C. The orange crystals were filtered on a cold frit and dried under vacuum. Yield 105 mg, 55.6%. Anal. Calcd.: C 57.31; H 9.62. Found: C 57.53; H 9.57.

Preparation of Cp*(DMPE)FeH: To a solution of Cp*(DMPE)Fe (200 mg, 0.6 mmol) in 10 ml THF was added Me_3CMgCl (0.3 ml, 2 M in Et_2O, 0.6 mmol) at -78°C. The solution was allowed to warm to room temperature, the volatiles removed under vacuum, and the residue thoroughly dried. Extracted the residue with petroleum ether, reduced the filtrate volume to *ca.* 5 mls, and grew crystals at -78°C. Filtered the yellow crystals on a cold frit and dried under vacuum. Yield 94 mgs, 52%. Infrared (Nujol Mull) 1815 cm^{-1} (m). Anal. Calcd.: C 56.15; H 9.43. Found: C 56.04; H 9.33.

Preparation of $[Cp^*(PMe_3)_2Fe(PMe_3)]PF_6$: To a solution of $Cp^*(PMe_3)_2FeCl$ (108 mg, 0.29 mmol) and KPF_6 (53 mg, 0.29 mmol) in 10 ml methanol at -78°C was added two equivalents of PMe_3 (0.05 ml). The solution was warmed to room temperature and stirred 15 minutes. The volatiles were removed under vacuum and the residue extracted with CH_2Cl_2. The filtrate was reduced to an oil and Et_2O added. The resultant red-orange precipitate was filtered at low temperature and dried. Yield 100 mgs, 62%. Anal. Calcd.: C 40.44%; H 7.50%. Found: C 40.34; H 7.11.

Preparation of $[Cp^*(PMe_3)_2Fe(CO)]PF_6$: A solution of $Cp^*(PMe_3)_2FeCl$ (123 mg, 0.33 mmol) and KPF_6 (70 mg, 0.38 mmol) in 10 ml methanol at -78°C was allowed to warm to room temperature under 1 atm. CO, and stir for 0.5 h. The volatiles were removed under vacuum and the residue extracted with CH_2Cl_2. The filtrate was reduced to an oil and Et_2O added. The resultant yellow precipitate was filtered at low temperature and dried. Yield 129 mg, 77%. Infrared (Nujol Mull) 1935 cm^{-1} (s). Anal. Calcd.: C 39.56%; H 6.44%. Found: C 39.13; H 6.36.

Preparation of $Cp^*(PMe_3)FeH_3$: In a typical preparation, 15 mg $Cp^*(PMe_3)(C_2H_4)FeH$ was dissolved in 0.3 mls C_6D_6, C_6H_6, or tetrahydrofuran and sealed in an NMR tube under 3 atmospheres of H_2. The solution was agitated at room temperature and monitored by ^1H NMR; the reaction was complete in *ca.* 1.5 h. In C_6D_6, deuterium could then be observed to exchange into the hydride positions. Complete exchange, all positions of the complex

occurred in *ca.* 24 h. at room temperature. The complex was generated in pentane, the solvent blown off with H_2 at room temperature, and an infrared spectrum obtained of the resultant oil, ν(FeH) 1905 cm^{-1} (s). A solution infrared spectrum in tetrahydrofuran was obtained by generation of the trihydride in tetrahydrofuran, and subsequent cannulation into a CsCl liquid cell under H_2.

References

1) Tilley, T. D.; Grubbs, R. H; Bercaw, J. E. *Organometallics*, **1984**, *3*, 274

2) Bryndza, H. E.; Fong, L. K.; Paciello, R. A.; Tam, W.; Bercaw, J. E. *J. Am. Chem. Soc.* submitted for publication

3) a) Togni, Tilley, Paciello, Bercaw, Grubbs manuscript in preparation: b) Merola, J.; Bercaw; J. E. unpublished results

4) See for example: Pearson, A. J. in "Comprehensive Organometallic Chemistry" Wilkinson, G.; Stone, F. G. A.; Abel, E. W. ed., Pergamon, 1982, vol. 8, pg. 959-968

5) a) Treichel, P. M.; Shubkin, R. L.; Barnett, K. W.; Reichard, D. *Inorg. Chem.*, **1966**, *4*, 1177: b) Brown, D. A.; Lyons, H. J.; Manning, A. R.; Rowley, J. M. *Inorg. Chim. Acta*, **1969**, *3*, 346: c) Haines, R. J.; Du Preez, A. L.; Marais, I. L *J. Organomet. Chem.*,**1971**, *28*, 405: d) Cullen, W. R.; Sams, J. R.; Thompson, J. A. *Inorg. Chem.*, **1971**, *10*, 843: e) Treichel, P. M.; Komar, D. A. *J. Organomet. Chem.*, **1981**, *206*, 77

6) Treichel, P. M.; Komar, D. A. *J. Organomet. Chem.*, **1981**, *206*, 77

7) a) King, R. B.; Houk, L. W.; Pannell, K. H. *Inorg. Chem.* **1969**, *8*, 1042: b) Mays, M. J.; Sears, P. L. *J. Chem. Soc. Dalton* **1973**, 1873: c) Abbott, S.; Davies, S. G.; Warner, P. *J. Organomet. Chem.*, **1983**, *246*, C65: d) Baird, G. J.; Davies, S. G. *Ibid.,* **1984**, *262,* 215

8) Thum, G.; Malisch, W. *J. Organomet. Chem.*, **1984**, *264*, C5

9) a) Catheline, D.; Astruc, D. *Organometallics*, **1984**, *3*, 1094: b) Guerchais, V.; Astruc, D. *J. Chem. Soc.,Chem. Commun.*, **1985**, 835

10) Green, M. L. H.; Wong, L.-L. *J. Chem. Soc.,Chem. Commun.*, **1984**, 1442

11) Ittel, S. D.; Tolman, C. A. *Organometallics*, **1982**, *1*, 1432

12) This complex has been found to have a piperidine coordinated to the metal center under the conditions described. E. Bunel personal communication.

13) Bunel, E. E.; Valle, L.; Manriquez, J. M. *Organometallics*, **1985**, *4*, 1680

14) This process may not occur *via* a β-H elimination process, a concerted process has been proposed in an analogous system, Cp(Prophos)RuCl. Morandini, F.; Consiglio, G.; Lucchini, V. *Organometallics*, **1985**, *4*, 1202

15) Paciello and Bercaw unpublished results

16) a) Jetz, W.; Graham, W. A. G. *Inorg. Chem.*, **1971**, *10*, 1159; b) Manojlovic-Muir, L.; Muir, K. W.; Ibers, J. A. *Ibid.*, **1970**, *9*, 447

17) Bower, B. K.; Tennent, H. G. *J. Am. Chem. Soc.*, **1974**, *94*, 2512

18) Aresta, M.; Gioannoccaro, P.; Rossi, M.; Sacco, A. *Inorg. Chim. Acta.*, **1971**, *51*, 115

19) Moore, D. S.; Robinson, S. D. *Chem. Soc. Rev.*, **1983**, *12*, 415

20) a) Kubas, G. J.; Ryan, R. R.; Swanson, B. I.; Vergami, P. J.; Wasserman, H. J. *J. Am. Chem. Soc.*, **1984**, *106*, 451: b) Upmacis, R. K.; Gadd, G. E.; Poliakoff, M.; Simpson, M. B.; Turner, J. J.; Whyman, R.; Simpson, A. F. *J. Chem. Soc.,Chem. Commun.*, **1985**, 27: c) Church, S. P.; Grevels, F.-W.; Hermann, H.; Schaffner, K. *Ibid.*, **1985**, 30: d) Crabtree, R. H.; Lavin, M. *Ibid.*, **1985**, 794: e) Crabtree, R. H.; Lavin, M. *Ibid.*, **1985**, 1661: f) Morris, R. H.; Sawyer, J. F.; Shiralian, M.; Zubkowski, J. D. *J. Am. Chem. Soc.*, **1985**, *107*, 5581: f) Conroy-Lewis, F.; Simpson, S. J. *J. Chem. Soc.,Chem. Commun.*, **1986**, 506: g) Kubas, G. J.; Ryan, R. R.; Wrobleski, D. A. *J. Am. Chem. Soc.*, **1986**, *108*, 1339: h) Ozin, G. A.; Prieto-Garcia, J.; *J. Am. Chem. Soc.*, **1986**, *108*, 3099: i) Crabtree, R. H.; Hamilton, D. G. *J. Am. Chem. Soc.*, **1986**, *108*, 3124: j) Upmacis, R.; Poliakoff, M.; Turner, J. *J. Am. Chem. Soc.*, **1986**, *108*, 3645: k) Sweany, R. L. *J. Am. Chem. Soc.*, **1986**, *108*, 6986: l) Kubas, G. J.; Unkefer, C. J.; Swanson, B. I.; Fukushima, E. *J. Am. Chem. Soc.*, **1986**, *108*, 7000

21) Saillard, J.-Y.; Hoffmann, R. *J. Am. Chem. Soc.*, **1984**, *106*, 2006

22) See for example Cotton, F. A.; Wilkinson, G. "Advanced Inorganic Chemistry, Fourth Edition", Wiley and Sons, 1980, pg. 96

23) Langford, C. H.; Gray, H. B. "Ligand Substitution Processes", Benjamin, 1966, pg. 25

24) Crabtree, R. H.; Lavin, M.; Bonneviot, L. *J. Am. Chem. Soc.*, **1986**, *108*, 4032

25) See Chapt. 1 this thesis

26) Baird, G. J.; Davies, S. D.; Simpson, S. J.; Jones, R. H. *JCS Dalton Trans.*, **1985**, 1479

27) Becker, E. D. "High Resolution NMR" Academic Press, New York, 1980

28) Crabtree, R. H.; Hamilton, D. G. *J. Am. Chem. Soc.*, **1986**, *108*, 3124

29) a) Kubas, G. J.; Ryan, R. R.; Swanson, B. I.; Vergamini, P. J.; Wasserman, J. J. *J. Am. Chem. Soc.*, **1984**, *106*, 451: b) Upmacis, R. K.; Gadd, G. E.; Poliakoff, M.; Simpson, M. B.; Turner, J. J.; Whyman, R.; Simpson, A. F. *JCS Chem. Commun.*, **1985**, 27: c) Church, S. P.; Grevels, F-W; Hermann, H.; Schaffner, K. *Ibid.,* **1985**, 30: d) Gadd, G. E.; Upmacis, R. K.; Poliakoff, M.; Turner, J. J. *J. Am. Chem. Soc.*, **1986**, *108*, 2547: e) Upmacis, R. K.; Poliakoff, M.; Turner, J. J. *Ibid.*, **1986**, *108*, 3645

30) a) Crabtree, R. H.; Lavin, M. *JCS Chem. Commun.*, **1985**, 794: b) Morris, R. H.; Sawyer, J. F.; Shiralian, M.; Zubkowski, J. D. *J. Am. Chem. Soc.*, **1985**, *107*, 5581: c) Crabtree, R. H.; Lavin, M.; Bonneviot, L. *Ibid.,* **1986**, *108*, 4032: d) Conroy-Lewis, F. M.; Simpson, S. J. *JCS Chem. Commun.*, **1986**, 506

31) See 3a, and Chapt. 1 this thesis

32) Brown, T.L.; Dickerhoff, D.W.; Bafus, D.A.; Morgan, G.L. *Rev. Sci. Instrum. 1962, 33*, 491

33) Marvich, R.H.; Brintzinger, H.H. *J. Am. Chem. Soc.* **1972**, *93*, 2046

RELATIVE METAL-HYDROGEN, -OXYGEN, -NITROGEN, AND -CARBON BOND STRENGTHS FOR ORGANORUTHENIUM COMPOUNDS; EQUILIBRIUM STUDIES OF THE $Cp^*(PMe_3)_2RuX$ SYSTEM.

Abstract

A series of ruthenium compounds, $Cp^*(PMe_3)_2RuX$ ($Cp^* = \eta^5\text{-}C_5Me_5$), has been prepared. The equilibria: $\mathbf{L_nM\text{-}X + H\text{-}Y \rightleftharpoons L_nM\text{-}Y + H\text{-}X}$ ($L_nM = Cp^*(PMe_3)_2Ru$; X,Y = hydride, alkoxide, hydroxide, amide, alkyl, alkynyl, hydrosulfide, cyanide), have been examined. The equilibrium constants allow for the determination of relative M-X, M-Y bond dissociation energies (BDEs) for this series of compounds. A lower limit of the Ru-N bond strength has been estimated by analysis of the kinetics of the thermolysis of $Cp^*(PMe_3)_2RuNPh_2$. A linear correlation of L_nM-X to H-X BDEs has been found for a number of dissimilar metal centers. The generality to other systems and predictive value of this correlation are discussed.

Introduction

Despite the widespread use of organometallic catalysts to effect homogeneous organic transformations, little is known about the thermochemistry of individual steps comprising catalytic cycles. Recent advances have led to values for some metal-hydrogen and metal-carbon bond strengths,[1] but the factors governing the reactivity of transition metal-heteroatom bonds (M-X, X = OH, OR, NR_2, PR_2, SiR_3, and SH) have been left relatively unexplored.

Early transition metal-oxygen and -nitrogen bonds are quite robust, presumably due to ligand-to-metal π-donation of an oxygen or nitrogen lone electron pair to an empty orbital of the electrophilic metal center.[2] In contrast, there has been a common perception that late transition metal-nitrogen and -oxygen linkages are intrinsically weak due to the mismatch of hard ligand base with soft metal acid,[3] thus explaining the relative scarcity of such complexes in the literature. Only recently has the reaction chemistry of late transition metal alkoxides and amides been examined.[4]

Recent examples of the types of reaction chemistry available to late metal-oxygen and -nitrogen bonds include CO[5] and olefin[6] insertions, β-hydride elimination[7] and "σ-bond metathesis" reactions;[8] the last provide a means of determining relative metal-X sigma bond strengths for a series of complexes. In this chapter, we report L_nM-X bond strengths obtained from measurements of the equilibrium constants for a series of reactions involving $Cp^*(PMe_3)_2RuX$ complexes.

Results

1. Synthesis. Our initial efforts were directed toward the synthesis of well-defined, monomeric hydroxide, amide and alkoxide derivatives of group VIII metals. Syntheses of

some of the $Cp^*(PMe_3)_2RuX$ complexes utilized in our studies have been published previously.[9] Syntheses of new $Cp^*(PMe_3)_2RuX$ derivatives are described below.

$Cp^*(PMe_3)_2RuOH$ (1) is prepared by treating a diethyl ether solution of $Cp^*(PMe_3)_2RuR$ (**2**, R = CH_3; **3**, R = CH_2SiMe_3) with 1.05 equivalents of triflic acid, followed by reaction of the resultant cation with an aqueous THF solution of KOH (eq 1).[10] Extended reflux of $Cp^*(PMe_3)_2RuCl$ with KOH in THF/H_2O fails to yield the hydroxide complex **1**. The hydroxide compound, $Cp^*(PMe_3)_2RuOH$ (**1**), is best isolated after solvent removal and subsequent freeze-drying in benzene to give a material suitable for recrystallization.

$$\underset{\mathbf{2}}{Cp^*(PMe_3)_2RuCH_3} \xrightarrow[Et_2O]{HSO_3CF_3} [Cp^*(PMe_3)_2Ru(CH_3)H]^+SO_3CF_3^- \xrightarrow[Et_2O]{-\,CH_4}$$

$$[Cp^*(PMe_3)_2Ru(Et_2O)]^+SO_3CF_3^- \xrightarrow[THF]{KOH,H_2O} \underset{\mathbf{1}}{Cp^*(PMe_3)_2RuOH} + KSO_3CF_3 \qquad (1)$$

$Cp^*(PMe_3)_2RuOH$ crystallizes from anhydrous petroleum ether solutions as stable orange-red crystals, which decompose on exposure to air. The anhydrous complex is monomeric in solution (MW = 389; ebulliometry in C_6H_6), and a weak O-H stretch is observed at 3687 cm^{-1} in CH_2Cl_2 solution.[11] The NMR spectrum (benzene-d_6) for **1** exhibits a triplet at -5.57 ppm ($^3J_{P-H}$ = 3.66 Hz), assigned to the hydroxide proton. Compound **1** is less pentane soluble when even small amounts of water of hydration are present, and it can be readily isolated as a yellow crystalline solid from benzene/pentane mixtures in this hydrated form.

Treatment of **1** with CO or ethylene (THF solution, 25°C) leads to multiple products in either case. Traces of hydride were observed upon heating (35°C) **1** with ethylene, while $Cp^*(PMe_3)Ru(CO)H$, $Cp^*(PMe_3)_2RuH$, and $Cp^*(PMe_3)_2RuCO_2H$ were observed on carbonylation.

The cationic Ru(IV) hydrido methyl complex intermediate in the synthesis of **1** subsequently has been isolated as the tetrafluoroborate salt (**4**) (eq 2). Cation **4** precipitates from

$$\underset{\mathbf{2}}{Cp^*(PMe_3)_2RuCH_3} + HBF_4 \xrightarrow{Et_2O} \underset{\mathbf{4}}{[Cp^*(PMe_3)_2Ru(CH_3)H]^+BF_4^-} \qquad (2)$$

diethyl ether as it forms, and can be isolated in high yield as a relatively insoluble off-white powder. ^1H Nuclear Magnetic Resonance (NMR) spectra obtained in acetone-d_6 (in which the compound decomposes in 1-2 h) show a triplet for the methyl group at 0.13 ppm ($^3J_{P-H}$ = 9.5 Hz) and an upfield triplet for the hydride at -10.0 ppm ($^2J_{P-H}$ = 41.8 Hz). The compound can be stored indefinitely under an inert atmosphere at -20°C in the solid state, but discolors slowly at room temperature.

All attempts to isolate the corresponding ruthenium methoxide complex, $Cp^*(PMe_3)_2RuOMe$, by treating the cation with NaOMe under a wide variety of conditions (eq 3) have resulted instead in

$$[Cp^*(PMe_3)_2Ru(Et_2O)]^+SO_3CF_3^- + NaOMe \longrightarrow Cp^*(PMe_3)_2RuH \qquad (3)$$

isolation of $Cp^*(PMe_3)_2RuH$ from the product mixture. Refluxing $Cp^*(PMe_3)_2RuCl$ and sodium methoxide in methanol yields various ratios of $Cp^*(PMe_3)_2RuH$ and $Cp^*(PMe_3)_2RuCO_2CH_3$ as the sole organometallic products. Treatment of hydroxide **1** with methanol in THF-d_8 at 0°C leads to an unisolable intermediate species, which may be the methoxide, that ultimately gives $Cp^*(PMe_3)_2RuH$.

The diphenylamide compound, $Cp^*(PMe_3)_2RuNPh_2$ (**5**), is prepared by metathesis of $Cp^*(PMe_3)_2RuCl$ with $LiNPh_2$ in THF at room temperature (eq 4). Treatment of **5** with carbon monoxide results

$$Cp^*(PMe_3)_2RuCl + LiNPh_2 \longrightarrow \underset{\mathbf{5}}{Cp^*(PMe_3)_2RuNPh_2} \qquad (4)$$

in phosphine loss and formation of $Cp^*(PMe_3)(CO)RuNPh_2$, with no indication of products arising from insertion of CO into the Ru-NPh_2 bond. Reaction with ^{13}CO leads to the expected carbonyl band shift to lower frequency (ν(CO) = 1928 cm^{-1}, $\nu(^{13}CO)$ = 1885 cm^{-1}); the region from 1500-2000 cm^{-1} exhibits no other bands.

Attempts to prepare other ruthenium amides *via* metathesis with alkali metal amides have failed. Treatment of $Cp^*(PMe_3)_2RuCl$ with $LiNH(CMe_3)$ affords $Cp^*(PMe_3)Ru(n^2\text{-}PMe_2CH_2)$, presumably by loss of *tert*-butyl amine from initially formed $[Cp^*(PMe_3)_2RuNH(CMe_3)]$ (eq 5). Reactions with other primary amide salts leads to intractable product mixtures.

$$Cp^*(PMe_3)_2RuCl \xrightarrow{Li^+NH(CMe_3)^-} Cp^*(PMe_3)Ru(\eta^2\text{-}CH_2PMe_2) \qquad (5)$$

The most general synthetic route to other complexes, $Cp^*(PMe_3)_2RuSH$, $Cp^*(PMe_3)_2RuCN$, $Cp^*(PMe_3)_2RuCH_2COCH_3$, $Cp^*(PMe_3)_2RuC{\equiv}CPh$, and $Cp^*(PMe_3)_2RuNHPh$, is *via* treatment of a THF solution of $Cp^*(PMe_3)_2RuOH$ with an excess of H_2S, HCN, acetone, $HC{\equiv}CPh$, or H_2NPh, respectively (eq 6). Removal of solvent and

$$\underset{\mathbf{1}}{Cp^*(PMe_3)_2RuOH{\cdot}nH_2O} + HX \longrightarrow \begin{array}{l} Cp^*(PMe_3)_2RuX + (n+1)H_2O \\ \quad \mathbf{6}, X = SH; \\ \quad \mathbf{7}, X = CN; \\ \quad \mathbf{8}, X = CH_2COCH_3; \\ \quad \mathbf{9}, X = CCPh; \\ \quad \mathbf{10}, X = NHPh \end{array} \qquad (6)$$

other volatile components, extraction into hydrocarbon solvent, concentration, and crystallization at low temperature yields analytically pure samples of each of the above compounds (See Table 1 for spectral data).

2. Exchange Equilibria. It is observed that reaction of $Cp^*(PMe_3)_2RuOH$ with stoichiometric amounts of diphenylamine produces some $Cp^*(PMe_3)_2RuNPh_2$ and water. ^1H

TABLE 1. ^{1}H and $^{31}P\{^{1}H\}$ NMR Data for $Cp^*(PMe_3)_2RuX$ Complexes

Compound	^{1}H[a] C_5Me_5[b]	T_1[c]	PMe_3[d]	T_1[c]	Other Assignments[j]		^{31}P[e]	T_1[c]
$Cp^*(PMe_3)_2RuOH$	1.69(1.34)	3.8	1.34(7.81)	2.78	RuOH	-5.57(t, $^{3}J_{P-H}$ = 3.66 Hz)	3.10	10.94
$[Cp^*(PMe_3)_2Ru(Me)H]BF_4$[f]	1.85(g)	h	1.51(10.21)	h	Ru-CH_3 Ru-H	-0.13(t, $^{3}J_{P-H}$ = 9.52) -10.00(t, $^{2}J_{P-H}$ = 41.75)	10.49	h
$Cp^*(PMe_3)_2RuNPh_2$	1.66(1.59)	1.43	1.29(7.77)	1.14	$RuNPh_2$	7.1(m), 6.9(m), 6.6(m), 6.3(m)	0.51	5.43
$Cp^*(PMe_3)_2RuSH$	1.69(1.44)	4.67	1.35(8.10)	3.02	RuSH	-4.54(t, $^{3}J_{P-H}$ = 8.42) T_1 = 15.13	5.85	14.30
$Cp^*(PMe_3)_2RuCN$	1.82(1.47)	4.27	1.43(7.83)	2.64			7.33	12.30
$Cp^*(PMe_3)_2RuCH_2(CO)CH_3$	1.69(1.41)	5.90	1.54(7.83)	3.20	Ru*CH_2* *CH_3*	1.38(t, $^{3}J_{P-H}$ = 0.49) T_1 = 3.2 1.80(s) T_1 = 4.0	6.30	11.30
$Cp^*(PMe_3)_2RuCCPh$	1.82(1.19)	3.01	1.42(8.74)	1.67	RuCCPh	7.02(m), 6.96(m), 6.8(m)	8.74	8.1
$Cp^*(PMe_3)_2RuNHPh$	1.69(1.52)	2.34	1.37(7.95)	1.52	RuN*H*Ph RuNH*Ph*	g 6.51(m), 6.05(m), 5.6(m)	5.51	7.2
$Cp^*(PMe_3)_2Ru\text{-}Mo(CO)_3Cp$	1.35(g)	3.00	1.09(7.92)	2.52	C_5H_5	5.32(s); T_1 = 21.08	0.29	10.00
$Cp^*(PMe_3)_2Ru\text{-}W(CO)_3Cp$	1.38(1.30)	2.81	1.11(8.05)	1.80	C_5H_5	5.22(s); T_1 = 22.07	1.32	11.95
$Cp^*(PMe_3)(PHPh_2)RuSH$	1.60(1.80)	h	1.08(8.40)[i]	h	P*H*Ph_2	6.95(d, $^{1}J_{P-H}$ = 345)	3.16	h

					PH*Ph*$_2$	g	41.36 h ($^2J_{P-P}$ = 46.4)
					RuSH	-3.50 (dd, $^3J_{P-H}$ = 7.5, 9.6)	
Cp*(PMe$_3$)Ru(n^2-CH$_2$PMe$_2$)	1.92(1.59)	h	1.15(7.21)[i]	h	P(*CH*$_3$)$_2$ P(*CH*$_3$) P*CH*$_2$ P*CH*$_2$	1.29(d, 9.76) 1.05(d, 9.52) -0.20(ddd, $^2J_{P-H}$ = 13.0, $^4J_{P-H}$ = 1.35, $^2J_{H-H}$= 7.60) 0.53(ddd, $^2J_{P-H}$ = 4.89, $^4J_{P-H}$ = 0.75)	-2.3 h (d, $^2J_{P-P}$ = 37) 39.5 h
Cp*(PMe$_3$)$_2$RuSi(OEt)$_3$	1.69(1.50)	h	1.42(8.28)[i]	h	O*CH*$_2$CH$_3$ OCH$_2$*CH*$_3$	3.76(q, 6.99) 1.13(t, 6.98)	2.82 7.2

a) Shifts in ppm referenced to SiMe$_4$ in THF-*d*$_8$ at 300 MHz and 30°C, unless noted otherwise. b) Number in parentheses is $^4J_{P-H}$ in Hz. c) Value in seconds. d) Number in parentheses is distance between outer lines of the filled in doublet, $^2J_{P-H}$ + $^4J_{P-H}$, in Hz. e) Shift in ppm, referenced to 85% H$_3$PO$_4$ at 121 MHz at 30°C. f) Acetone-*d*$_6$, 30°C. g) Not resolved. h) Not obtained. i) Doublet. j) J values in Hz. T$_1$s values in seconds.

and ^{31}P NMR observations show an equilibrium amount of hydroxide and amine remain (eq 7).

$$\underset{\mathbf{1}}{Cp^*(PMe_3)_2RuOH} + HNPh_2 \underset{}{\overset{K_{eq}}{\rightleftharpoons}} \underset{\mathbf{5}}{Cp^*(PMe_3)_2RuNPh_2} + H_2O \qquad (7)$$

The equilibrium constant, measured by NMR in THF-d_8 solution, is invariant to widely different starting concentrations and conditions (concentration ranges between 0.078 and 0.0065 M for $Cp^*(PMe_3)_2RuOH$ and $Cp^*(PMe_3)_2RuNPh_2$, and between 0.80 and 0.02 M for diphenylamine and water).[12] The equilibrium constant is found to be 0.0046 (varying in a nonsystematic manner between 0.0027 and 0.009), corresponding to a free energy of equilibrium of 3.2 $\pm$ 0.6 kcal·mol^{-1}. The same equilibrium is established starting with $Cp^*(PMe_3)_2RuNPh_2$ and H_2O. Measurements in benzene-d_6 show the equilibrium constant is not especially solvent dependent (K_{eq} = 0.000369; ΔG = 4.7 kcal • mol^{-1})[13].

Variable temperature NMR measurements of the equilibrium constant for eq 7 from 20 °C to 65 °C in THF-d_8 show ΔH = 1.2 kcal·mol^{-1} and ΔS = -6 eu (Figure 1). Thus, even in this case, where a sterically uncongested hydroxide ligand is converted to a sterically demanding diphenylamido ligand on ruthenium, the entropy contribution to the equilibrium free energy amounts to only -1.8 kcal·mol^{-1} at 25 °C. These observations suggest that it will be the general case that entropy contributions to the equilibria observed will be negligible.[14]

The thermoneutral character of this equilibrium is quite significant. If we assume the only changes represented in the equilibrium correspond to making H-N and Ru-O bonds at the expense of H-O and Ru-N bonds, the near-unity value of K_{eq} requires the Ru-O bond in $Cp^*(PMe_3)_2RuOH$ be stronger than the Ru-N bond in $Cp^*(PMe_3)_2RuNPh_2$ by the same amount as the H-O bond in water is stronger than the H-N bond in diphenylamine, with a small correction for the equilibrium enthalpy value of 1.2 kcal·mol^{-1}. Moreover, since the equilibrium

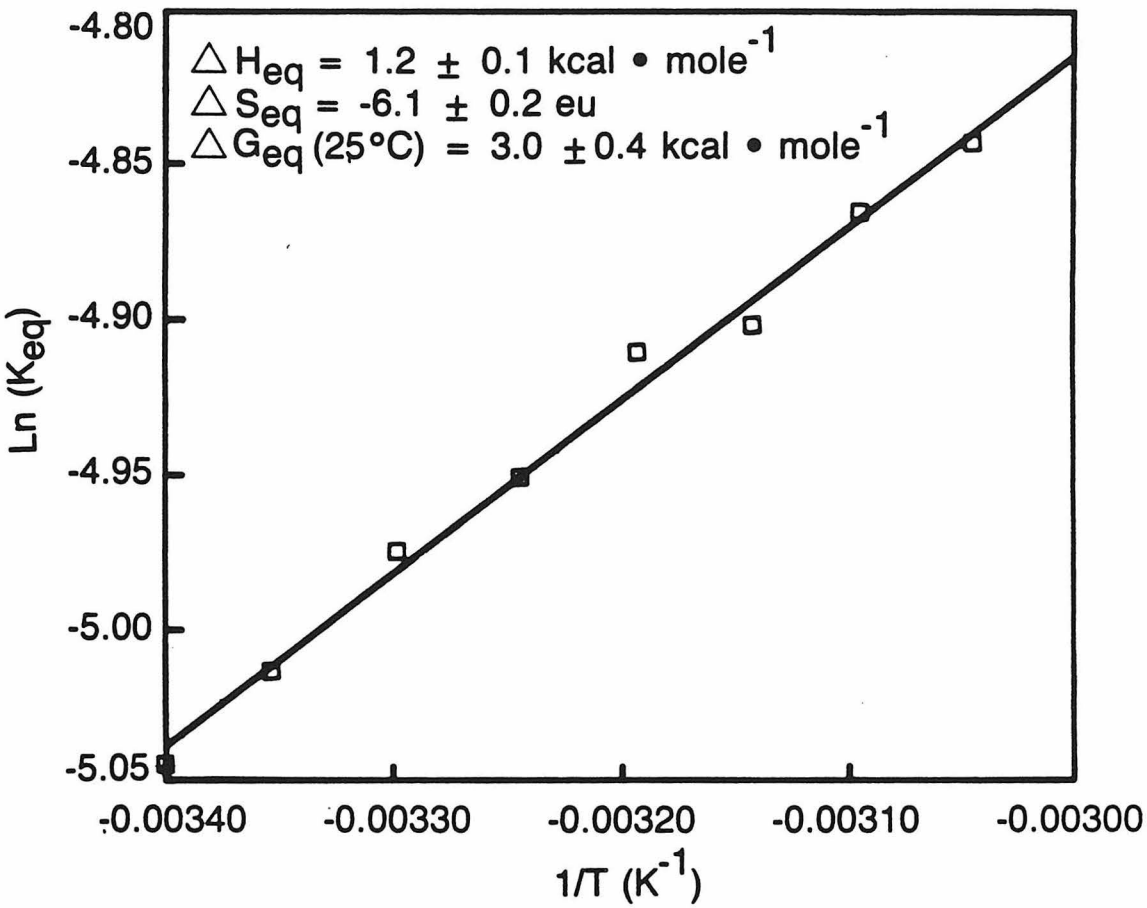

Figure 1. $Ln(K_{eq})$ *vs* -1/T plot for the equilibrium:

$Cp^*(PMe_3)_2RuOH + HNPh_2 \rightleftharpoons Cp^*(PMe_3)_2RuNPh_2 + HOH$

between 20 and 55°C in THF-d_8. $[Cp^*(PMe_3)_2RuX]_{total}$ = 0.05 M;

$[HNPh_2] + [H_2O]$ = 0.25 M. Correlation coefficient = 0.990.

constant is not solvent dependent, gas phase bond dissociation energies of 119 and *ca.* 85 kcal·mol^{-1},[15] respectively, for the H-O and H-N bonds in water and diphenylamine may be used to estimate that the Ru-O bond in $Cp^*(PMe_3)_2RuOH$ is about 35 kcal·mol^{-1} stronger than the Ru-N bond in $Cp^*(PMe_3)_2RuNPh_2$. This functional group approach to solution phase bond dissociation energies has been exploited very effectively by Benson and others[16] in organic systems.

Nearly thermoneutral equilibrations were found on combining $Cp^*(PMe_3)_2RuOH$ with acetone, phenyl acetylene, or aniline as shown in eq 8-10.

$$\underset{\mathbf{1}}{Cp^*(PMe_3)_2RuOH} + CH_3COCH_3 \rightleftharpoons \underset{\mathbf{8}}{Cp^*(PMe_3)_2RuCH_2COCH_3} + H_2O \qquad (8)$$

$$\underset{\mathbf{1}}{Cp^*(PMe_3)_2RuOH} + HCCPh \rightleftharpoons \underset{\mathbf{9}}{Cp^*(PMe_3)_2RuCCPh} + H_2O \qquad (9)$$

$$\underset{\mathbf{1}}{Cp^*(PMe_3)_2RuOH} + H_2NPh \rightleftharpoons \underset{\mathbf{10}}{Cp^*(PMe_3)_2RuNHPh} + H_2O \qquad (10)$$

Reaction of $Cp^*(PMe_3)_2RuOH$ or $Cp^*(PMe_3)_2RuNPh_2$ with 4 atm H_2 gives a mixture of $Cp^*(PMe_3)_2RuH$ (**11**) and $Cp^*(PMe_3)RuH_3$[17]; however, $Cp^*(PMe_3)_2RuH$ can be equilibrated with a large excess of H_2O (at very low H_2 pressures) as shown in eq. 11. Spiking the

$$\underset{\mathbf{11}}{Cp^*(PMe_3)_2RuH} + H_2O \rightleftharpoons \underset{\mathbf{1}}{Cp^*(PMe_3)_2RuOH} + H_2 \qquad (11)$$

equilibrium mixture with a small amount of pure $Cp^*(PMe_3)_2RuOH$ confirmed the presence of this constituent. Dynamic range problems limit the precision of this reaction free energy; however, the magnitude of the equilibrium constant for eq 11 does, nevertheless, establish a Ru-H bond strength relative to Ru-OH to within 4 kcal·mol^{-1}.

Irreversible reactions between $Cp^*(PMe_3)_2RuOH$ and H_2S, HCN and $Cp(CO)_3MH$ (M = Mo, W) also take place (eq 12-14). Addition of

$$\underset{\mathbf{1}}{Cp^*(PMe_3)_2RuOH} + H_2S \longrightarrow \underset{\mathbf{6}}{Cp^*(PMe_3)_2RuSH} + HOH \qquad (12)$$

$$\underset{\mathbf{1}}{Cp^*(PMe_3)_2RuOH} + HCN \longrightarrow \underset{\mathbf{7}}{Cp^*(PMe_3)_2RuCN} + HOH \qquad (13)$$

$$\underset{\mathbf{1}}{Cp^*(PMe_3)_2RuOH} + Cp(CO)_3MH \longrightarrow \underset{(\mathbf{12},\ M = Mo;\ \mathbf{13},\ M = W)}{Cp^*(PMe_3)_2RuM(CO)_3Cp} \qquad (14)$$

$Cp^*(PMe_3)_2RuSH$ and $Cp^*(PMe_3)_2RuCN$ to 50/50 solutions of THF-d_8/H_2O failed to generate detectable amounts of $Cp^*(PMe_3)_2RuOH$, even at elevated temperatures. Addition of water to THF-d_8 solutions of $Cp^*(PMe_3)_2RuM(CO)_3Cp$ resulted in the formation of $Cp^*(PMe_3)_2RuH$ and products derived from the decomposition of $[CpM(CO)_3]$.

While addition of water to $Cp^*(PMe_3)_2RuSH$ failed to generate detectable amounts of the hydroxide complex **1**, addition of $HSi(OEt)_3$ establishes the equilibrium shown in eq 15. The

$$\underset{\mathbf{6}}{Cp^*(PMe_3)_2RuSH} + HSi(OEt)_3 \rightleftharpoons \underset{\mathbf{14}}{Cp^*(PMe_3)_2RuSi(OEt)_3} + H_2S \qquad (15)$$

equilibrium constant of 0.75 appears to signal that second row main group substituents will be in nearly thermoneutral equilibrium with each other, although such Ru-X linkages are apparently substantially stronger than analogous bonds to comparable first row substituents. An attempt to equilibrate $Cp^*(PMe_3)_2RuSH$ and Ph_2PH led instead to phosphine substitution ($Cp^*(PMe_3)(PHPh_2)RuSH + PMe_3$), contrary to what might be expected on the basis of the relative phosphine cone angles[18].

Equilibrium measurements of the reversible reaction of $Cp^*(PMe_3)_2RuNPh_2$ with (DPPE)MePt(OH) show only a small energetic preference for $Cp^*(PMe_3)_2RuOH$ and (DPPE)$MePtNPh_2$ (eq 16).

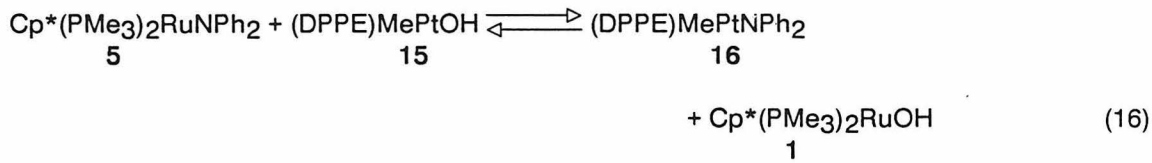

(16)

The equilibrium constant for the reaction in eq 16 was found to be 470, which translates to a free energy of equilibrium of -3.6 kcal·mol^{-1}, within experimental error of the -3.4 $\pm$ 0.8 kcal·mol^{-1} value predicted by summing the free energies for the relevant equilibria listed in Table 2. The internally consistent nature of these equilibria further demonstrates their very small solvent dependence, since the equilibrium constants are apparently unaffected when substantial amounts of protic "co-solvents" (such as methanol, water and diphenyl amine) are present, *vis-a-vis* absent (eq 16). Furthermore, this result suggests that the *combination* of ruthenium's preference for oxygen and the relief of steric crowding inherent on going from $Cp^*(PMe_3)_2RuNPh_2$ to $Cp^*(PMe_3)_2RuOH$ are small (3.6 kcal·mol^{-1}), even in the relatively congested $Cp^*(PMe_3)_2RuX$ system. The results of all such equilibrium measurements are summarized in Table 2.

3. Thermolysis of $Cp^*(PMe_3)_2RuNPh_2$. Current estimates of Ru-C bond strengths of 35-45 kcal/mole[1], combined with the series of relative bond strengths shown in Table 2, indicate that the $Cp^*(PMe_3)_2Ru\text{-}NPh_2$ bond dissociation energy should fall in the range 15-25 kcal·mol^{-1}, thus suggesting that $Ru\text{-}NPh_2$ bond homolysis should occur at kinetically significant rates at easily attainable temperatures. The following observations show the Ru-N bond strength in $Cp^*(PMe_3)_2RuNPh_2$ is greater than 17 kcal·mol^{-1} and *suggest* it may be weaker than 23 kcal·mol^{-1} (although the evidence for the latter is rather inconclusive):

(i) Thermolysis of $Cp^*(PMe_3)_2RuNPh_2$ does indeed occur readily at 30-80 °C in benzene-d_6, accompanied by generation of tetraphenyl hydrazine and its C-N bonded isomeric dimers (eq 17). Loss of **5** is between first and second order (Figure 2) as might be expected from a mechanism such as that outlined in eq. 18.

Table 2. $Cp^*(PMe_3)_2Ru\text{-}X + H\text{-}Y \underset{THF\text{-}d_8}{\overset{K_{eq}}{\rightleftharpoons}} Cp^*(PMe_3)_2Ru\text{-}Y + H\text{-}X$

X	K_{eq}	ΔG_{eq} (kcal • mol^{-1})	rel D(Ru-X)$_{soln}$ (kcal • mol^{-1})
OH	1	0	0
C≡CPh	8.9	-1.3 ± 0.2	14.3
CH_2COCH_3	2.3	-0.5 ± 0.2	-20.2
NHPh	4.2	-0.9 ± 0.2	-30.1
NPh_2	0.0046	3.2 ± 0.6[a]	-37.2
SH	> 8 X 10^6	< -9.4	> -18.5
CN	> 8 X 10^6	< -9.4	> 14.2
H	2.12 X 10^4	-5.9 ± 0.8	-8.9

$Cp^*(PMe_3)_2RuSH + HSi(OEt)_3 \rightleftharpoons Cp^*(PMe_3)_2RuSi(OEt)_3 + H_2S$

$K_{eq} = 0.75$ $\Delta G_{eq} = 0.2 \pm 0.2$ kcal • mol^{-1}

[a] $\Delta H_{eq} = 1.2$ kcal • mol^{-1}

$$\underset{\mathbf{5}}{Cp^*(PMe_3)_2RuNPh_2} \xrightarrow{30°\text{-}80°C} N_2Ph_4 \text{ (+ isomers) + ...} \tag{17}$$

$$\underset{\mathbf{5}}{Cp^*(PMe_3)_2RuNPh_2} \underset{k_{-1}}{\overset{k_1}{\rightleftharpoons}} \{Cp^*(PMe_3)_2Ru\cdot\ \cdot NPh_2\} \xrightarrow{k_2} N_2Ph_4 \tag{18}$$

The moderately slow rate of decomposition of **5** under these conditions requires the Ru-N bond strength be at least 17 kcal·mol^{-1}[19].

(ii) Thermolysis of **5** in the presence of the good hydrogen atom donor 9,10-dihydroanthracene (DHA) at 65°C in benzene-d_6 results in clean conversion of $Cp^*(PMe_3)_2RuNPh_2$ to $Cp^*(PMe_3)_2RuH$, diphenylamine, and anthracene (eq 19) in a process which is first

$$\underset{\mathbf{5}}{Cp^*(PMe_3)_2RuNPh_2} + C_{14}H_{12} \longrightarrow \underset{\mathbf{11}}{Cp^*(PMe_3)_2RuH} + HNPh_2 + C_{14}H_{10} \tag{19}$$

order in **5** (Figure 3) and first order in DHA over the range: [DHA] = 0.00 M - to 1.09 M (Figure 4).[20] These observations are consistent with pre-equilibrium bond homolysis followed by competition between cage recombination[21] and hydrogen atom abstraction,[22] as shown in eq 20.

$$\underset{\mathbf{5}}{Cp^*(PMe_3)_2RuNPh_2} \underset{k_{-1}}{\overset{k_1}{\rightleftharpoons}} \{Cp^*(PMe_3)_2Ru\cdot\ \cdot NPh_2\}$$

$$k_{esc} \qquad k_{recomb}$$

$$\{Cp^*(PMe_3)_2Ru\cdot\} + \{NPh_2\cdot\}$$

$$k_2[DHA]$$

$$\underset{\mathbf{11}}{Cp^*(PMe_3)_2RuH} + NHPh_2 + C_{14}H_{10} \tag{20}$$

(iii) Addition of 4 equivalents of free PMe_3 to a solution of $Cp^*(PMe_3)_2RuNPh_2$ containing 0.8 M DHA slightly *accelerated*, rather than slowed the rate of reaction 19. This result suggests

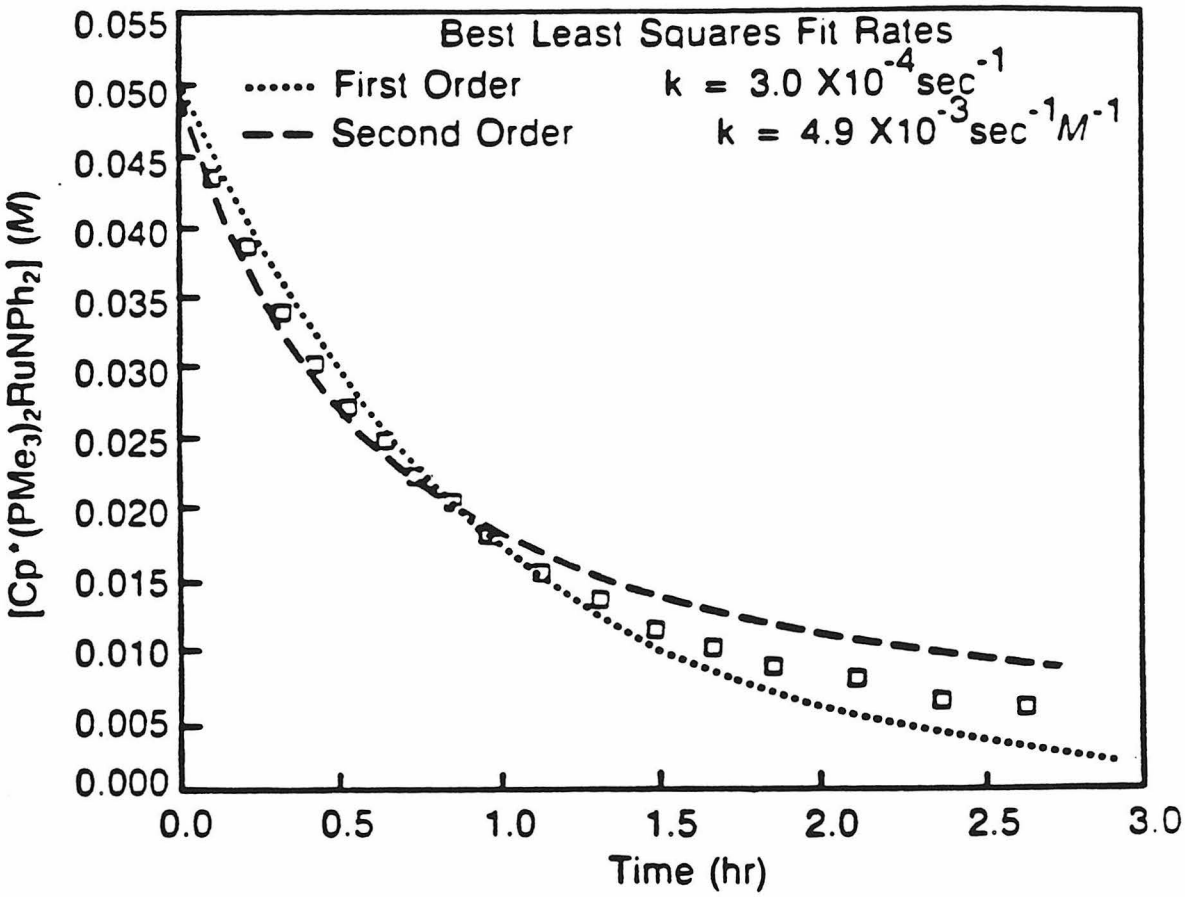

Figure 2. Thermolysis of $Cp^*(PMe_3)_2RuNPh_2$ at 80 °C in C_6D_6 in the absence of 9,10-dihydroanthracene. Data plotted as concentration (M) against time (hr) with best least squares fits of the first and second order mechanisms as determined by iterative version of HAVECHEM software; see ref. 42. Initial $[Cp^*(PMe_3)_2RuNPh_2]_0$ = 0.051 M. The reaction is apparently between first and second order under these conditions, with the first order line seemingly more appropriate at early times (high $[Cp^*(PMe_3)_2RuNPh_2]$) and the second order fit perhaps describing the data better when $[Cp^*(PMe_3)_2RuNPh_2]$ low.

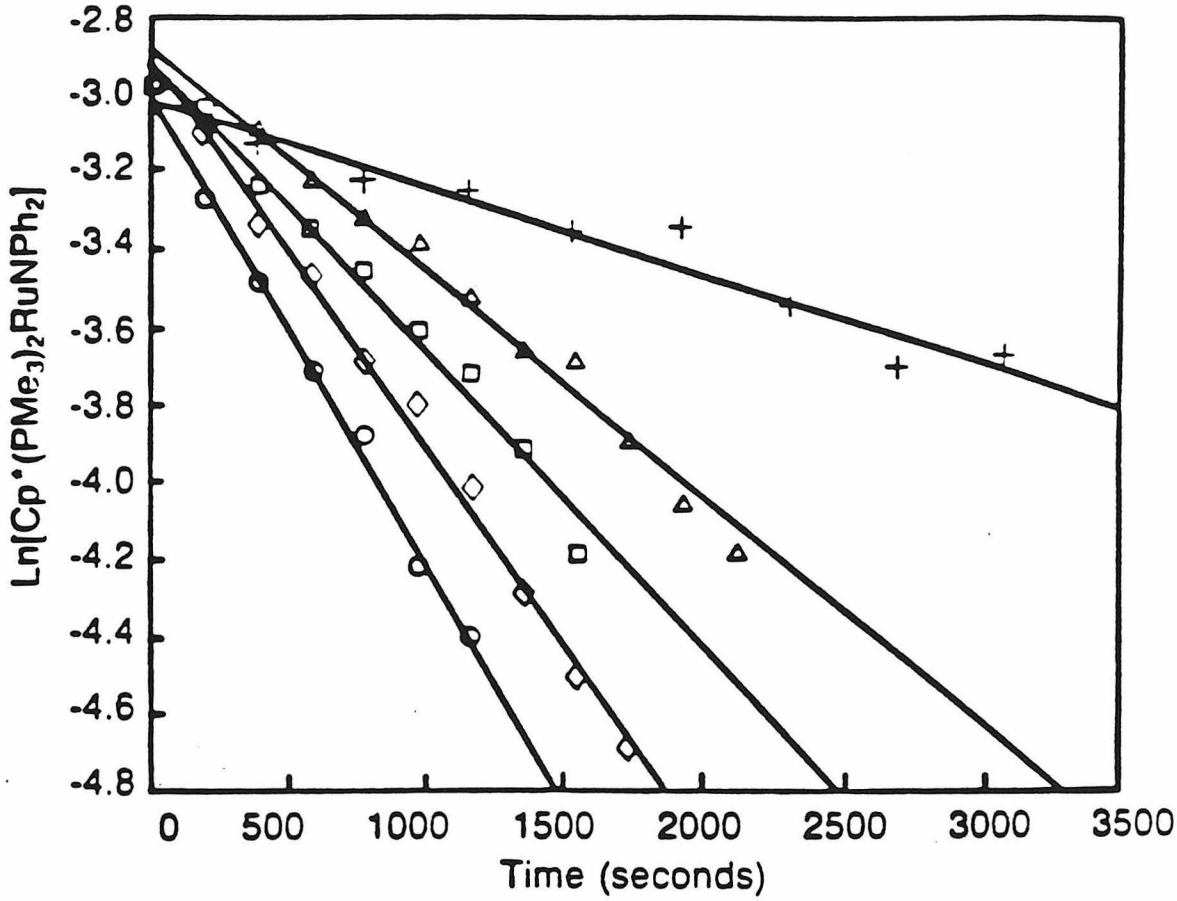

Figure 3. Thermolysis kinetics for $Cp^*(PMe_3)_2RuNPh_2$ at 65°C in C_6D_6 in the presence of 9,10-dihydroanthracence (DHA). Data plotted as $Ln[Cp^*(PMe_3)_2RuNPh_2]$ against time (sec) for $[Cp^*(PMe_3)_2RuNPh_2]_0$ = 0.051; [DHA] = 0.00-1.09 M. A first order thermolysis rate $Cp^*(PMe_3)_2RuNPh_2$ in the absence of DHA was estimated from initial data although it is clear that under these conditions a first order process cannot fully explain the data in Fig. 2. The initial first order rate thus obtained does fall very close to that predicted by a fit of the k_{obs} *vs* [DHA] data listed below (and shown in Fig. 4).

Symbol	[DHA] M	k_{obs} X 10^4 (sec^{-1})	Correlation coeff.
+	0.00	2.29 ± 0.19	0.953
△	0.42	5.81 ± 0.24	0.983
□	0.59	7.59 ± 0.39	0.990
◇	0.85	10.06 ± 0.28	0.994
o	1.09	12.33 ± 0.39	0.995

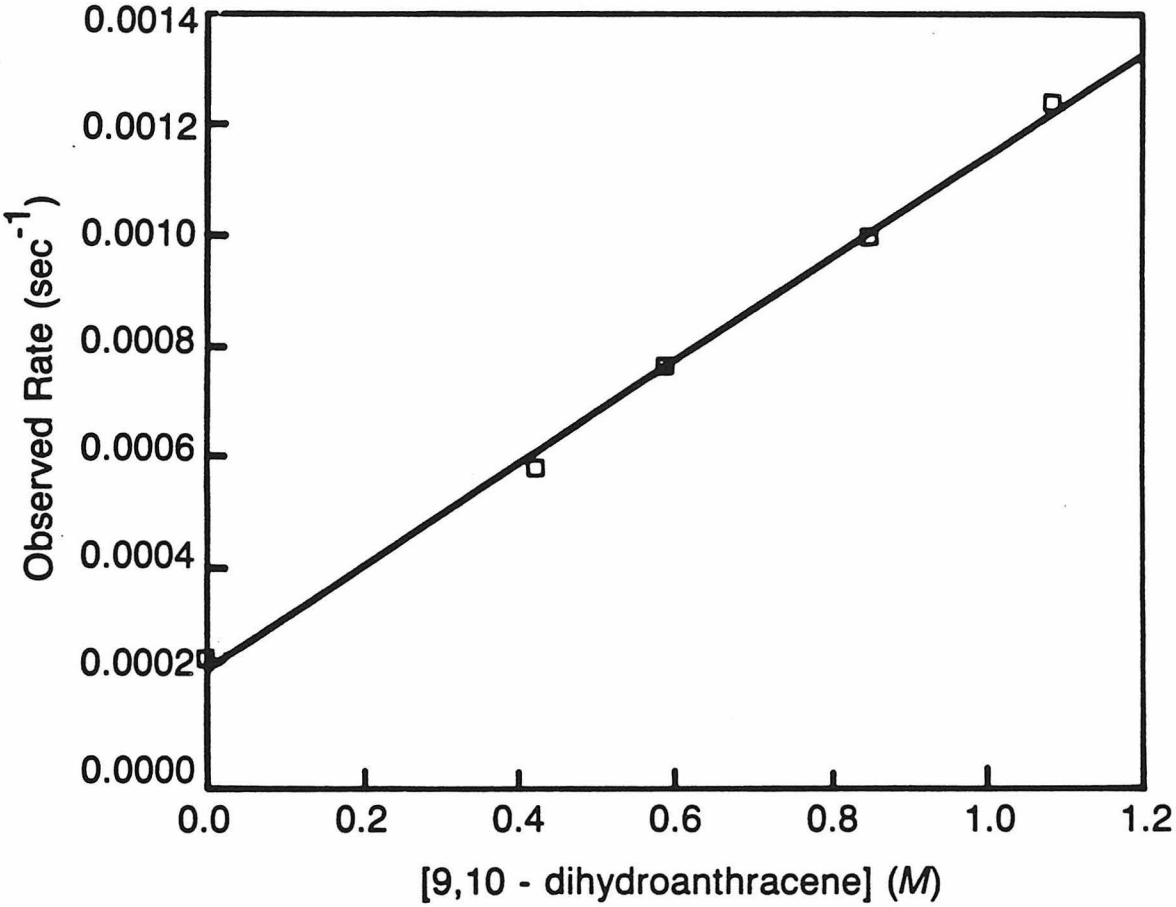

Figure 4. Order in [DHA]: thermolysis kinetics for $Cp^*(PMe_3)_2RuNPh_2$ at 65 °C in C_6D_6 plotted as k_{obs} *vs* [DHA]. Starting conditions: [DHA] 0.00-1.09 M; $[Cp^*(PMe_3)_2RuNPh_2]_0$ = 0.051; data listed in Fig. 3. Nonweighted linear least squares shows the following: k_{obs} = (9.27 ± 0.20) X 10^{-4}[DHA] + (2.14 ± 0.01) X 10^{-4} (in s^{-1}); correlation coefficient = 0.999

mechanisms involving prior phosphine dissociation from **5** are probably not involved in formation of $Cp^*(PMe_3)_2RuH$. Moreover, ^{31}P CIDNP enhanced emission signals are observed during these experiments, indicating at least some component of radical pathways. No further evidence of radical intermediates has been obtained; thermolyses conducted in ESR probes failed to reveal any detectable concentrations of paramagnetic species.[23]

Thus, failure to efficiently trap or unambiguously detect and quantify the radicals proposed in eqs 17 and 19 has thwarted our attempts to confidently place an upper limit on the Ru-N bond strength for $Cp^*(PMe_3)_2RuNPh_2$. If bond homolysis is a primary step as shown in reaction 20, the pseudo-first order rate constant of 3×10^{-3} s^{-1} for trapping less than 10% of the diphenyl aminyl radicals produced when **5** is thermolyzed in the presence of 1.09 M DHA, indicates a k_1 larger than 10^{-2} s^{-1}; which, in turn, places an upper limit of 23 kcal·mol^{-1} for the Ru–N bond strength for **5**.[24] Whereas this estimate does appear reasonable in view of the modest stability of **5**, even in the absence of DHA (*i.e.* eq 17), it should be reemphasized that the possibility that DHA reacts principally *via* an associative or pre-equilibrium dissociative (*i.e.* non-radical) pathway cannot be excluded by our data.[25] Thus, *no definite conclusions regarding the absolute magnitudes of Ru-X BDEs may be reached on the basis of the kinetics of the thermolyses of* $Cp^*(PMe_3)_2RuNPh_2$. These thermolysis experiments do place a *lower limit* on the Ru-N BDE for $Cp^*(PMe_3)_2RuNPh_2$, and hence, lower limits on all of the $Cp^*(PMe_3)_2Ru$-X complexes listed in Table 2.

Discussion

The equilibration studies described herein have also been carried out on a series of platinum complexes, (DPPE)MePtX,[26] as part of a collaborative project between CIT and DuPont Central Research. The discussion of results in this chapter will include the platinum data, see Table 3, as they are necessary to the completeness of the argument. However, only the synthesis of the ruthenium complexes and their equilibrations are part of this thesis.

Table 3. $(DPPE)(Me)PtOMe + H\text{-}Y \underset{THF\text{-}d_8}{\overset{K_{eq}}{\rightleftharpoons}} (DPPE)(Me)Pt\text{-}Y + HOMe$

X	K_{eq}	ΔG_{eq} (kcal • mol^{-1})	rel $D(Pt\text{-}X)_{soln}$ (kcal • mol^{-1})
OCH_3	1	0	-15.3
OH	3.2	-0.7 ± 0.2	0
NPh_2	1.5	-0.5 ± 0.2	-34.5
NMePh	0.80	0.1 ± 0.2	-32.3
CH_2COCH_3	27	-2.1 ± 0.2	-19.3
SH	> 8 X 10^6	< -9.4	> -18.5
CN	> 8 X 10^6	< -8.4	> 14.2

$(DPPE)(Me)PtOH + Cp^*(PMe_3)_2RuNPh_2 \rightleftharpoons (DPPE)(Me)PtNPh_2 + Cp^*(PMe_3)_2RuOH$

$K_{eq} = 470$ $\Delta G_{eq} = -3.6$ kcal • mol^{-1}

The nearly thermoneutral character of the equilibria represented by equation 21 appears to be general for a number of σ-bonded ligands. This observation naturally implies that

$$L_nM\text{-}X + H\text{-}Y \xrightleftharpoons{K_{eq}} L_nM\text{-}Y + H\text{-}X \qquad (21)$$

(L_nM = (DPPE)MePt, Cp*$(PMe_3)_2$Ru)

the difference in H-X and H-Y BDEs is the same as the difference in L_nM-X and L_nM-Y BDEs, assuming that the functional group approach so successfully applied to organic systems by Benson[18] is equally valid for these ruthenium and platinum systems. Alternatively, one may take the observation that $K_{eq} \approx 1$ to indicate that heterolytic dissociation of basic ligands from these metal centers ($L_nM\text{–}X \longrightarrow [L_nM^+] + X^-$) parallels the K_a values of the corresponding organic acids ($H\text{–}X \longrightarrow H^+ + X^-$). The very small solvent dependence of the equilibrium constants allows quantitative estimates of relative bond strengths in these L_nM-X systems from the appropriate gas phase H-X bond dissociation energies.[17] This common assumption that functional groups are solvated equivalently in different complexes has proven to be valid for both organic[27] and organometallic[28] systems.

An effective method of graphically illustrating the data from Tables 2 and 3 is shown in Figure 5. For this plot of relative D(H-X) vs relative D(L_nM-X), the L_nM-OH bond dissociation energies for (DPPE)MePtOH and Cp*$(PMe_3)_2$RuOH are arbitrarily assigned a relative value of zero, and a line with a slope of one is drawn through this point. Two important conclusions can be drawn from the remarkably good correlation of relative H-X and L_nM-X bond strengths which is readily apparent: (i) the close linear fit for the bond dissociation energies of {Cp*$(PMe_3)_2$Ru·} and {(DPPE)MePt·} with first row {X·} substituents (except for the metal cyanides, *vide infra*) indicates that other relative L_nM-X (X = first row element) bond strengths should be predictable, even for complexes we have not yet examined, by simple extrapolation from the H-X bond strength of the organic analog. (ii) the one-to-one correlation between L_nM-X BDEs and H-X BDEs may well be generally valid for a range of organometallic

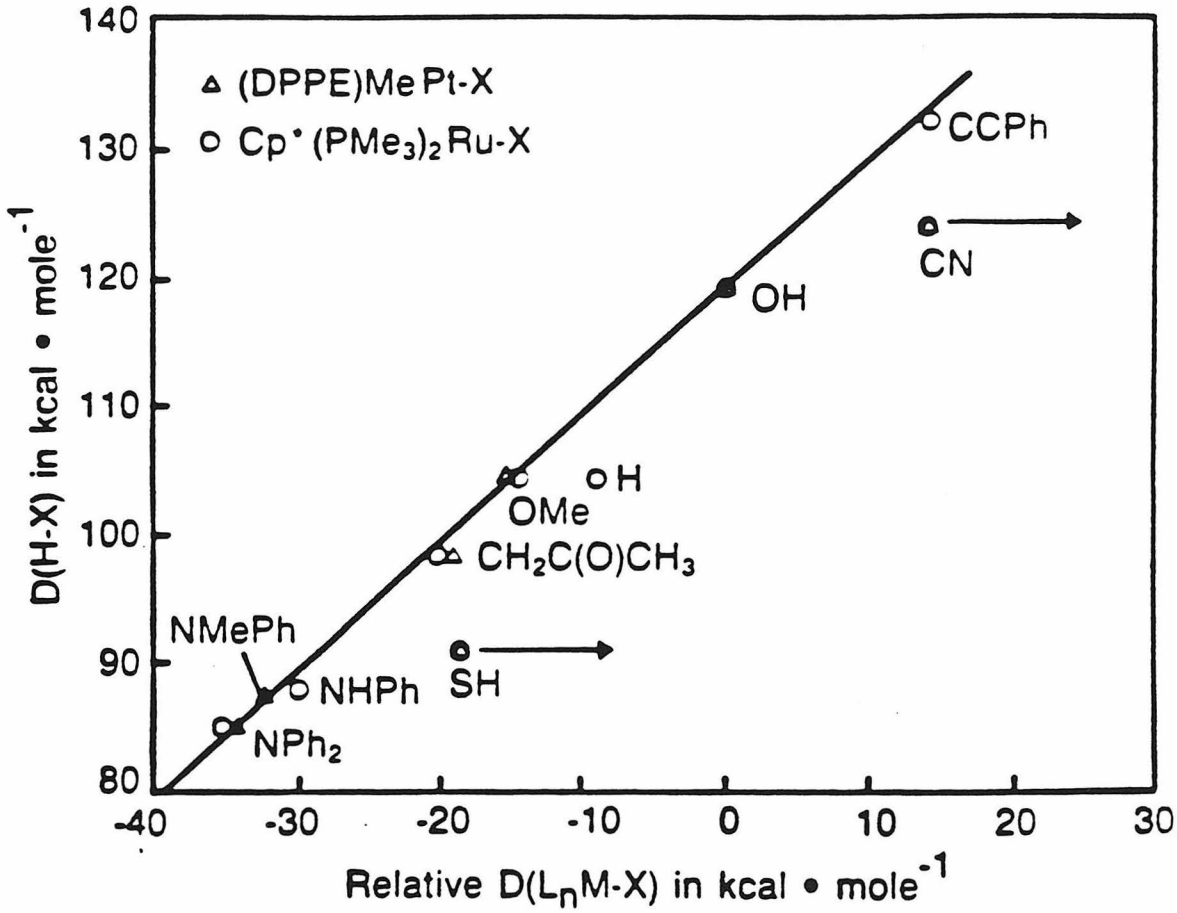

Figure 5. H-X *vs* relative L_nM-X bond dissociation energies (BDEs) in kcal•mol^{-1}. Data plotted from Tables 2 and 3 for both $Cp^*(PMe_3)_2RuX$ (o) and (DPPE)(Me)PtX (Δ) systems with L_nM–OH arbitrarily assigned a relative BDE of 0.0 kcal•mol^{-1}. A line with arbitrary slope has been drawn through the hydroxide "point". Data depicted for L_nM-CN and L_nM-SH are *minimum* L_nM–X bond strengths (against absolute H-X bond strengths) which, as indicated by the arrows, may be much stronger that the 9 kcal•mol^{-1} deviation detectible by our experimental methods.

compounds, in the absence of L_nM-X multiple bonding (*vide infra*). That the data fit so well on the line drawn for Figure 5 is quite persuasive in this regard, since the same close correlation holds both for square planar, 16-electron, third-row (d^8) platinum complexes and for "three-legged-piano-stool", 18-electron, second-row (d^6) ruthenium complexes.

While examples of comparable σ-bond strength measurements for series of organometallic complexes are rare in the literature, thermochemical data on two other organometallic systems lend support to the generality of this H-X vs relative M-X bond strength correlation. Bergman and coworkers[29] have shown that the reaction between $Cp^*(PMe_3)(H)Ir$-*cyclo*-C_6H_{11} and various alkanes does not proceed to completion to generate the corresponding alkyls and cyclohexane (eq 22) suggesting a one-to-one correspondence for Ir–C_6H_{11}, Ir-R (R = *cyclo*-C_5H_9, *neo*-C_5H_9, *n*-C_5H_9, $CH_2CH(CH_3)CH(CH_3)_2$), and

$$Cp^*(PMe_3)(H)Ir\text{-}cyclo\text{-}C_6H_{11} + HR \rightleftharpoons Cp^*(PMe_3)(H)IrR + cyclo\text{-}C_6H_{12} \quad (22)$$

H-*cyclo*-C_6H_{11} and H-R BDEs. Furthermore, if the (solution phase) thorium-carbon bond dissociation energies, obtained by reaction calorimetry by Bruno, Marks, and Morss[30], are evaluated in this same manner, once again, a one-to-one correlation between $Cp^*_2(OCMe_3)Th$-R and H–R BDEs is evident (Figure 6). On the other hand, for those compounds with alkoxide or amide ligands, significant deviations from the one-to-one correlation are noted. For example, the $Cp^*_2(OCMe_3)Th$-OR and $Cp^*_2(OCMe_3)Th$-NR_2 BDEs are greater than would be predicted[34] for a single sigma Th-OR or Th-NR_2 bond (*i.e.* by comparison to the corresponding H-OR or H-NR_2 BDE). Indeed, such deviations are entirely expected, since the coordinatively unsaturated, Lewis acidic thorium center of these $Cp^*_2Th^{IV}X_2$ complexes is a powerful π-acceptor of oxygen or nitrogen lone electron pairs, increasing the Th-OR or Th–NR_2 bond order. An estimate of the thermodynamic importance of such multiple bonds can be made from the magnitude of such deviations form the 1:1 correlation expected.

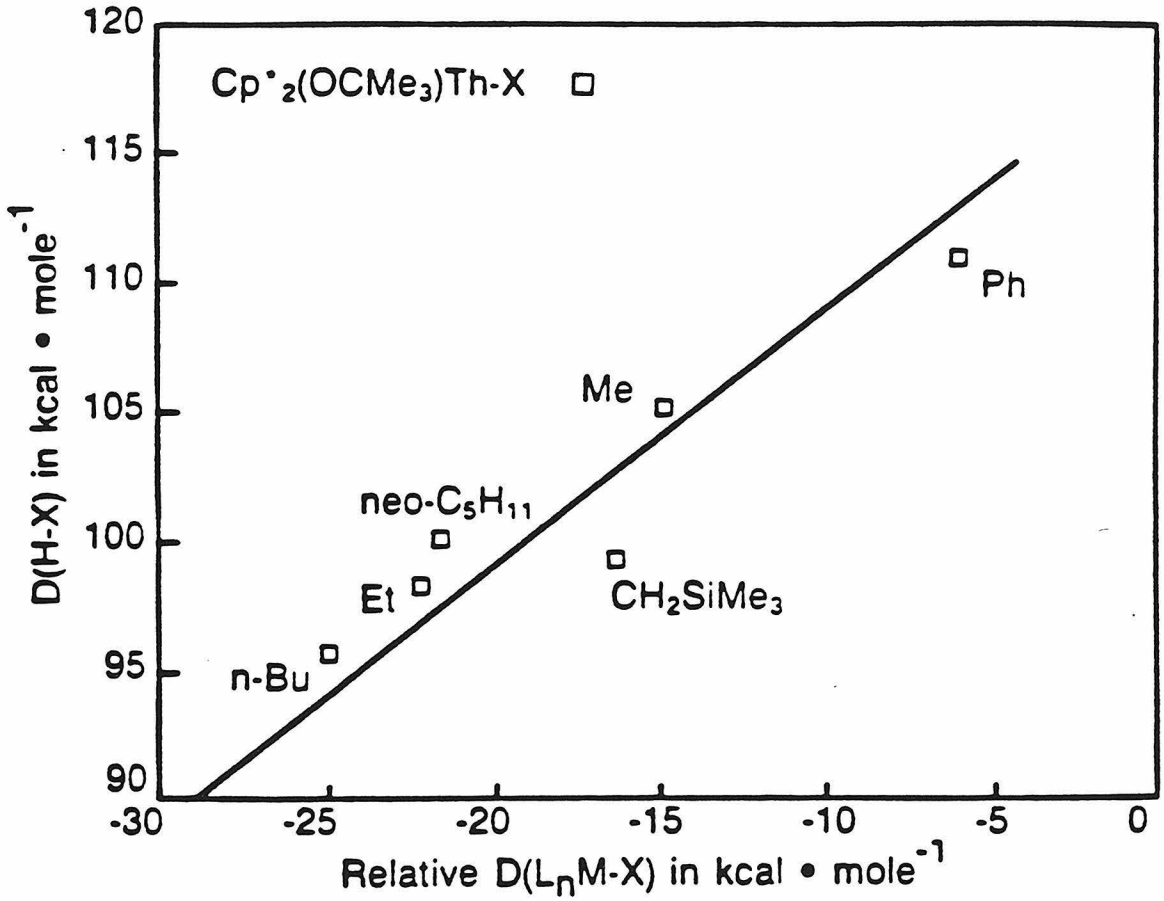

Figure 6. H-X *vs* relative $Cp^*_2(OCMe_3)Th$-C bond strengths in kcal•mol^{-1}. Data taken from solution phase values reported in ref. 30 and placed on the same arbitrary scale as Figure 5 by assigning a relative Th-CH_3 bond strength of -14.9 kcal•mol^{-1}. The line is the same one depicted on Figure 5 (slope = 1.00; intercept = 119 kcal•mol^{-1}) with the maximum deviation of these data, noted for $Cp^*_2(OCMe_3)ThCH_2SiMe_3$, of about 2.5 kcal•mol^{-1}. This is well within the uncertainty of the Th-X and H-X bond strengths, noting that the calorimetric methods used to determine these numbers must be corrected for the heats of vaporization of gaseous products of the alcoholysis reactions; see ref. 16.

Returning to the platinum and ruthenium systems, three types of compounds exhibit anomalously large L_nM-X BDEs: L_nM-CN, L_nM-SH, and Cp*$(PMe_3)_2$Ru-H (Tables 2 and 3; Figure 5). The cyanide ligand is a moderate π-acceptor, and considering the extremely electron-rich character of Cp*$(PMe_3)_2$Ru(II), considerable ruthenium-to-cyanide back donation is anticipated, which reconciles the higher than one bond order observed. The low energy of the ν(CN) (2058 cm^{-1} for **7**; *cf.* ν(CN) = 2240 - 2260 cm^{-1} for organic nitriles[32]) is indeed indicative of substantial Ru=C=N character for Cp*$(PMe_3)_2$RuCN (**7**). While the platinum center in (DPPE)MePtCN is not as electron rich as the ruthenium case, similar, though reduced, M=C multiple bonding is indicated for this complex by ν(CN) at 2128 cm^{-1}.

Overlap between ruthenium or platinum sigma orbitals and the 3s/3p orbitals of the second row main group elements may be significantly better than overlap between these orbitals and the 2s/2p orbitals of the first row elements. Such arguments, akin to those used to account for the preferences of "hard" and "soft" acids and bases, may be offered to explain the larger than expected L_nM-SH BDEs for **6** and (DPPE)MePtSH. In this regard, it is significant that, although Cp*$(PMe_3)_2$RuSH is unreactive towards a variety of first-row H-X compounds, a nearly thermoneutral equilibrium is established between Cp*$(PMe_3)_2$RuSH, $(EtO)_3SiH$, Cp*$(PMe_3)_2$RuSi$(OEt)_3$, and H_2S (eq. 15). This observation suggests a second "parallel" H-X vs relative L_nM-X bond strength correlation may hold for second row main group substituents. Because of the experimental limitations of our equilibrium measurements, we cannot quantify the energetic displacement between the L_nM-X and L_nM-Y (X = first row substituent; Y = second row substituent) relationships. We do, however, know the line for second row elements must lie at least 9 kcal·$mole^{-1}$ to the "right" of the established correlation for first row substituents.

Although the value of the Ru-H BDE for Cp*$(PMe_3)_2$RuH (**11**) is rather imprecise due to the small value of the equilibrium constant for eq 11,[33] its deviation (7 kcal·mol^{-1}) from the linear correlation in Figure 5 clearly exceeds the conservative estimate of the uncertainty in

the BDE of $\pm$ 2 kcal·mol^{-1}. Moreover, Thompson and Bercaw[34] have found that Cp^*_2ScH reacts with benzene to establish an equilibrium mixture of Cp^*_2ScH, $Cp^*_2ScC_6H_5$, C_6H_6, and H_2, from which the thermodynamic parameters ΔH^o = 6.7(3) kcal·mol^{-1} and ΔS^o = –1.5(1) e.u. were obtained for eq 23.

$$Cp^*_2ScH + C_6H_6 \rightleftharpoons Cp^*_2ScC_6H_5 + H_2 \qquad (23)$$

Assuming the one-to-one correlation between L_nM-X and H-X BDEs, the Sc-H BDE is 6.7 (or *ca* 7.5(4) in the gas phase) kcal·mol^{-1} stronger than expected,[35] *i.e.*, again, one finds that there is an increased stability associated with the L_nM–H bonds, amounting to approximately 7 kcal·mol^{-1} for the systems considered here. Even the *average* of the two Th–H BDEs in $[Cp^*_2ThH_2]_2$ (which include bridging hydride ligands which must bond to two thorium centers more strongly than a terminal hydride bonds to a single thorium) obtained by reaction calorimetry[33] deviates approximately 15 kcal·mol^{-1}, again to the right, of the linear correlation in Figure 6. The common assumption, based on the reported BDE difference between $(CO)_5Mn$–H and $(CO)_5Mn$-CH_3, has been that "metal-carbon" bonds in organotransition metal compounds are approximately 25 kcal·mol^{-1} weaker than metal-hydrogen bonds.[36] Our data, and that of others cited herein, appear to indicate that (i) the difference in L_nM-H and L_nM-CH_3 BDEs is likely to be substantially smaller, and (ii) one must be cautious to correct the L_nM-R (R = alkyl, alkenyl, aryl, alkynyl, etc.) bond dissociation energy for the stability of {R·} when discussing the relative strengths of metal-carbon and metal-hydrogen bonds. As the data of Figures 5 and 6 demonstrate, metal-carbon bond strengths may be expected to vary over a range as large as 40 kcal·mol^{-1} (R = CH_2Ph to CCR'). An appropriate one-to-one comparison would be between L_nM-H and L_nM-CH_3, since the bond dissociation energies of H-H and H-CH_3 are 104 and 105 kcal·mol^{-1}, respectively.

Although the bond strength information presented here, as summarized for the $Cp^*(PMe_3)_2Ru$-X, (DPPE)MePt-X, $Cp^*_2(OCMe_3)Th$-X, Cp^*_2Sc-X and $Cp^*(PMe_3)(H)Ir$-X systems (X = singly-bonded first-row main group substituent) in Figure 7, is somewhat limited,

we note some interesting trends. The metal-oxygen bonds examined for late metals are not, despite conventional perceptions, particularly weak. The L_nM-OH bond is stronger than L_nM-H and L_nM–(sp^3)C bonds (as in the carbon-bound metal enolates **8** and **14**), but weaker than L_nM-(sp)C bonds (as in the phenylacetylide complex **9**). Interestingly, L_nM-O bond strengths are consistently stronger than the L_nM-N bond strengths measured, suggesting that L_nM-N bonds may be weaker than L_nM-O bonds for both early and late metal systems.[37] Thus, the higher reactivity associated with (DPPE)MePt-OR (R = H, CH_3) bonds (*vis a vis* (DPPE)(OMe)Pt-Me bonds) is kinetic rather than thermodynamic in origin.[38] Interestingly, the enhanced stability of transition metal bonds to second row main group substituents, observed in both platinum and ruthenium systems, may explain the efficiency of silicon and sulfur compounds as poisons for catalysts meant for the transformation of first row main group substrates. Perhaps most importantly, the excellent correlation of H–X and M–X bond strengths is seen for widely disparate types of organometallic complexes and ligand environments. The same correlation appears general for first, second, and third row transition metal complexes as well as for trans-uranium elements. Both 16- and 18-electron complexes are included in Figure 7, and the trend fits the data for early metal complexes, as well as late metal derivatives. Finally, the observations concerning the metal-X single bonds holds for carbon, oxygen, nitrogen, and hydrogen, suggesting this correlation may be general for many types of organometallic systems.

Since the trends in M-X BDEs correlate so well with H-X BDEs, we may estimate the thermodynamics for individual steps in proposed catalytic cycles and for simple processes such as olefin or carbon monoxide insertion into L_nM-OR or L_nM-NR_2 bonds by evaluating the thermodynamics of the corresponding processes for H-OR and H-NR_2 (eq 24-eq 27).[39]

$$L_nM\text{-}OH + CO \longrightarrow L_nM\text{-}COOH \qquad \Delta H^o \approx -6.8\ \text{kcal}\cdot\text{mol}^{-1}\text{, since}$$
$$H\text{-}OH + CO \longrightarrow H\text{-}COOH \qquad \Delta H^o = -6.8\ \text{kcal}\cdot\text{mol}^{-1} \qquad (24)$$

$$L_nM\text{-}NH_2 + CO \longrightarrow L_nM\text{-}CONH_2 \qquad \Delta H^o \approx -7.1\ \text{kcal}\cdot\text{mol}^{-1}\text{, since}$$
$$H\text{-}NH_2 + CO \longrightarrow H\text{-}CONH_2 \qquad \Delta H^o = -7.1\ \text{kcal}\cdot\text{mol}^{-1} \qquad (25)$$

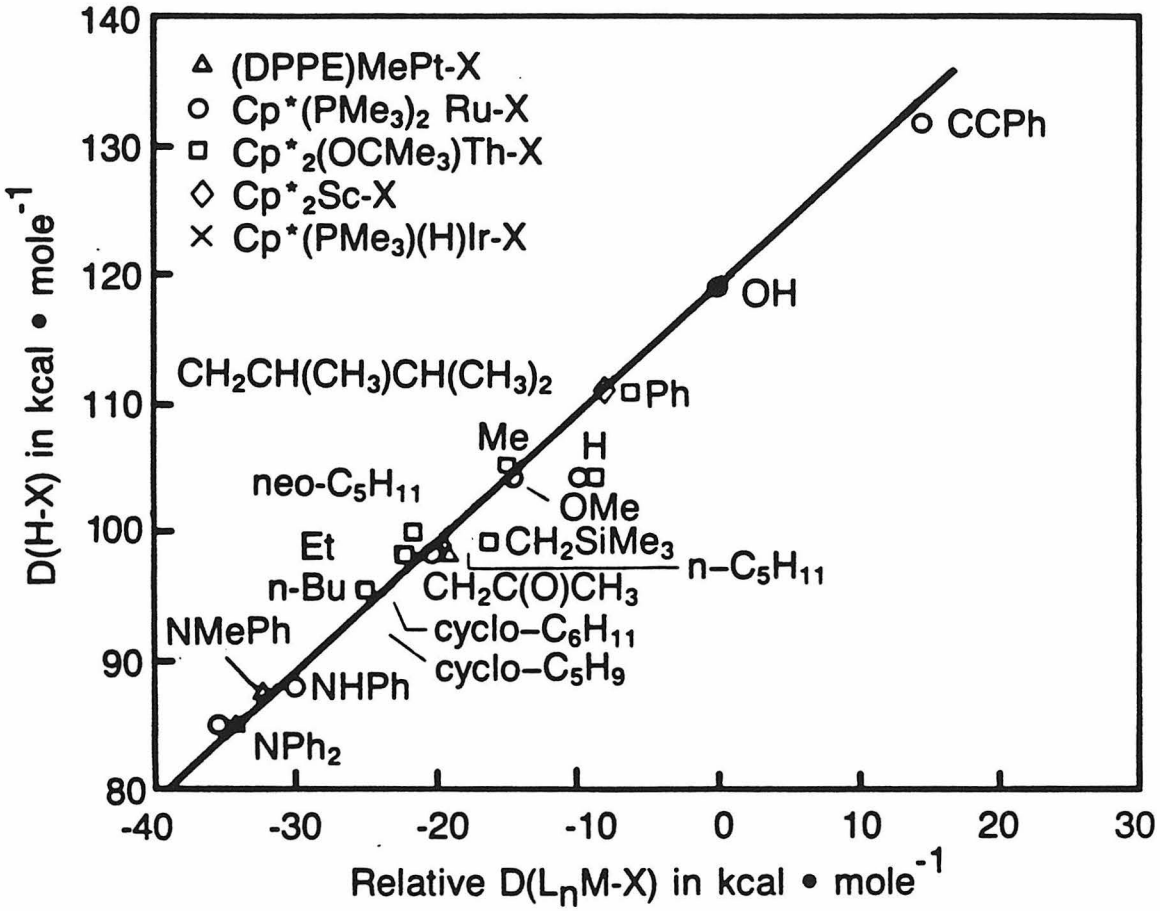

Figure 7. Cumulative plot of H-X *vs* relative L_nM-X bond strengths discussed in this chapter. Data for (DPPE)(Me)Pt-X (o), Cp^*_2Sc-X (◊), $Cp^*_2(OCMe_3)Th$-X (□), and $Cp^*(PMe_3)(H)IrX$ (x) depicted for X = first row main group substituents along with the arbitrary line (slope = 1.00, intercept = 119.0 kcal•mol^{-1}) described in Figure 5. Scale definitions for (DPPE)(Me)PtX, $Cp^*(PMe_3)_2RuX$, and $Cp^*_2(OCMe_3)ThX$ data as described in Figures 5 and 6. To put the Sc-X data on these axes, the Sc-C bond has been defined as -8.1 kcal•mol^{-1}; similarly, the Ir–C bond in $Cp^*(PMe_3)(H)Ir$-*cyclo*-C_6H_{11} has been assigned an arbitrary value of -21 kcal•mol^{-1}. Good 1:1 correlation of H-X and L_nM-X bond strengths is noted.

$$L_nM\text{-}OH + CH_2{=}CH_2 \longrightarrow L_nM\text{-}CH_2CH_2OH \qquad \Delta H^o \approx -10.6\ kcal{\cdot}mol^{-1}, \text{ since}$$
$$H\text{-}OH + CH_2{=}CH_2 \longrightarrow H\text{-}CH_2CH_2OH \qquad \Delta H^o = -10.6\ kcal{\cdot}mol^{-1} \tag{26}$$

$$L_nM\text{-}NH_2 + CH_2{=}CH_2 \longrightarrow L_nM\text{-}CH_2CH_2NH_2 \qquad \Delta H^o \approx -19.2\ kcal{\cdot}mol^{-1}, \text{ since}$$
$$H\text{-}NH_2 + CH_2{=}CH_2 \longrightarrow H\text{-}CH_2CH_2NH_2 \qquad \Delta H^o = -19.2\ kcal{\cdot}mol^{-1} \tag{27}$$

Our data also suggest that hydroxymethyl transition metal complexes, L_nMCH_2OH, should have approximately the same thermodynamic stability as the corresponding methoxy tautomer, L_nMOCH_3 (in the absence of oxygen-to-metal dative pi-bonding, as, for example, with early transition metal systems), since according to Figures 5 and 7 there is a one-to-one trade-off of L_nM-C, H-O, H-C and L_nM-O BDEs (eq 28). Both of these species have been

$$L_nM\text{-}CH_2OH \underset{}{\overset{K_{eq} \approx 1}{\rightleftharpoons}} L_nM\text{-}OCH_3 \tag{28}$$

proposed as key intermediates in numerous schemes for CO hydrogenation and alcohol homologation.[40] Hence, pathways which predominate *via* one of these two tautomers are likely to arise from a greater *kinetic* reactivity of that tautomer (assuming there is a facile interconversion of the two), since comparable concentrations of each should be present at equilibrium.

The relatively small difference between M-CH_3 and M-H bond strengths evident in some of the species discussed in this manuscript suggests that while metal alkyl hydride complexes may never become as commonplace as metal dihydrides, C-H bond activation may generally produce species which are (thermodynamically) only 5-15 $kcal{\cdot}mol^{-1}$ less stable than analogous dihydrides (eq 29). While most such species may not be isolable,

$$[L_nM] + H\text{–}H \rightleftharpoons L_nMH_2 \qquad \Delta H = 0\ kcal{\cdot}mol^{-1}$$
$$[L_nM] + H\text{-}CH_3 \rightleftharpoons L_nM(H)CH_3 \qquad \Delta H = +\ 5\text{-}15\ kcal{\cdot}mol^{-1} \tag{29}$$

they are, nevertheless, energetically accessible, and therefore viable, catalytic intermediates.

Our data show there are surprisingly small thermodynamic consequences to steric considerations even in the rather uncongested $Cp^*(PMe_3)_2RuX$ derivatives. We stress that even the several $kcal \cdot mol^{-1}$ uncertainties inherent in our H-X/L_nM-X correlation (Figures 5 and 7) can produce large changes in selectivities.

In summary, we note that the observed order in L_nM-X homolytic bond strengths: L_nM-(sp)C > L_nM-O > L_nM-H > L_nM-(sp^3)C > L_nM-N might not have been predicted prior to this work. The correlation of L_nM-X bond strengths with those of the parent H-X BDEs allows prediction of the thermodynamics accompanying many elementary processes of interest in organotransition metal chemistry.

Experimental Section

General Considerations: All syntheses and chemical manipulations were carried out in a Vacuum Atmospheres Model HE-453 drybox equipped with either nitrogen purge or oxygen/water scrubbing recirculation "Dri-Train" or by high vacuum and Schlenk techniques. Hydrogen, nitrogen, and argon were purified by passing the streams through MnO on vermiculite followed by activated 4 A sieves.[41] Benzene, pentane, THF, diethyl ether and toluene were purified by distillation from purple sodium/benzophenone ketyl solutions under argon or by vacuum transfer from the same drying and degassing medium or from "titanocene".[42] Benzene, toluene and pentane required the addition of tetraglyme (Aldrich) to effect dissolution of the sodium. Methylene chloride was degassed by sparging with argon and then distilled, under argon, from calcium hydride. Each two liters of pentane was first washed with 3X100 mL mixed H_2SO_4/HNO_3 (85/15% v/v), 1X100 mL distilled water, 2X100 mL satd. aq. $NaHCO_3$ solution, 2X100 mL distilled water and filtered through $MgSO_4$ before storage over activated (350°C, 4 hours) 4 Å molecular sieves. Drybox solvents were maintained over activated 4 Å molecular sieves. Distilled water was degassed by five freeze-pump-thaw cycles on a high vacuum line and methanol was first distilled from freshly prepared magnesium methoxide and degassed with five freeze-pump-thaw cycles. Deuterated solvents

were purified and maintained in the same manner as the protonic isotopomers. Diphenyl amine and 9,10-dihydroanthracene were recrystallized from pentane and vacuum dried. $LiNPh_2$ was prepared with n-Butyl lithium in pentane, the resultant white precipitate was thoroughly washed with pentane and vacuum dried. Triflic acid, $HBF_4 \cdot Et_2O$, KOH, phenyl acetylene, aniline, methyl aniline, and triethyoxysilane were degassed and used as supplied from Aldrich. Hydrogen, carbon monoxide, hydrogen sulfide and ethylene (freeze-pump-thawed three times) were used as obtained from Matheson. ^{13}CO (Monsanto-Mound) was used as received. HCN was purified by vacuum transfer after degassing by freeze-pump-thaw cycles. **CAUTION: HCN IS AN EXTREMELY TOXIC, HIGHLY VOLATILE LIQUID WHICH MAY SPONTANEOUSLY POLYMERIZE WHEN REMOVED FROM THE STABILIZER IT IS SUPPLIED WITH. EXTREME CAUTION MUST BE USED WHEN HANDLING THIS COMPOUND AND ONLY WELL VENTILATED HOOD AREAS ARE APPROPRIATE FOR ITS USE. STORAGE AS A SOLID BELOW -20C IN AN EFFICIENTLY VENTED FREEZER IS RECOMMENDED.**

IR spectra were recorded in 0.1 mm path length KBr solution cells on a Varian model 983G optical null spectrophotometer or in nujol mulls on KBr plates on a Beckman IR 4230 spectrophotometer. Routine ^1H and ^{31}P spectra for characterization were obtained in benzene-d_6, THF-d_8, or acetone-d_6, with Me_4Si or H_3PO_4 as standard references, on Jeol Model FX-90Q or Jeol GX-400 spectrometers. Physical NMR measurements were made using Wilmad #507-TR screw-capped NMR tubes in either GE Model NT-300, NT-360 or QE-300 NMR spectrometers operating in pulsed-FT mode at 300.06, 360.80 and 300.01 MHz proton frequencies, respectively. T_1s data were acquired using Nicolet (GE) spin-inversion/recovery pulse sequences and data analysis software. For equilibrations involving hydrogen a 16-bit external digitizer was used to extend maximum dynamic range. Nuclear Overhauser Enhancement (NOE) differences in ^{31}P nuclei were determined to be insignificant by integration of known-concentration solutions. Variable temperature measurements were conducted in NMR probes calibrated with a chromel-alumel thermocouple which was, in turn,

calibrated with water at 0°C and 100°C. Equilibria were evaluated by acquiring NMR spectra using 90 degree pulse lengths and at least five T_1s delay periods between pulses. Equilibrium constants were calculated by direct integration of multiple NMR spectra acquired over a period of, generally, days to weeks. A fit of the approach to equilibrium was calculated through the use of GIT software based on HAVECHEM programs.[43] Physical mass determinations were made using a Mettler model AE160 balance calibrated with external weights and operated in a drybox. Solution concentrations were determined by standard volumetric dilution techniques or sometimes by solvent height determinations in Wilmad 507-TR screw-capped NMR tubes which were calibrated by Hamilton microliter syringes. A least squares fit of these data shows: Volume (uL) = height (mm) * 14.00 + 5.55, which could be used directly to determine sample volumes. Addition of liquid components to equilibrium systems was generally measured by weight. Occasionally volume measurements were used (Hamilton uL syringe) instead.

Satisfactory elemental analysis on complexes reported were obtained from the Dornis and Kolbe Microanalytical Laboratory, the California Institute of Technology analytical service, Galbraith Microanalytical Laboratories, or Micro-Analysis Inc.. Solution molecular weights were obtained by isothermal distillation using the Singer method.[44]

$Cp^*(PMe_3)_2RuCl$ and $Cp^*(PMe_3)_2RuR$ (**2**, R = CH_3; **3**, R = $CH_2Si(CH_3)_3$; **11**, R = H) were prepared as previously reported.[9]

Preparation of $Cp^*(PMe_3)_2RuOH$ (1): To a solution of $Cp^*(PMe_3)_2RuCH_3$ (2g, 5 mmol) in 20 mL Et_2O at -40°C was added one equivalent of CF_3SO_3H (440 uL, 5 mmol). The solution was allowed to warm to room temperature and stir for 3 h. The solution turned orange on warming and a light colored precipitate formed. A mixture of *ca.* 1.5 equiv. KOH (400 mg, 7.1 mmol), *ca.* 3 mL H_2O (enough to completely dissolve the KOH), and 15 mL THF was prepared and added to the cation solution at -40°C. The combined solutions were warmed to room temperature and stirred for 3 h. All solids dissolved to yield a red-orange solution.

Volatiles were removed under vacuum and the residue was thoroughly dried. Extraction with *ca.* 50 mL benzene, filtration, and freeze-drying yielded a yellow powder consisting of $Cp^*(PMe_3)_2RuOH{\cdot}nH_2O$. This extraction and freeze-drying cycle was repeated while monitoring for the appearance of the ^1H NMR peak at –5.57 ppm (in THF-d_8), which is broadened by H_2O. The resultant powder was extracted with *ca.* 50 mL pentane, the solution filtered, reduced to *ca.* 10 mL, and cooled to -40 °C. Orange-red cubic crystals of anhydrous $Cp^*(PMe_3)_2RuOH$ were isolated on a cold frit and vacuum dried. 960 mg, 47.8%. The residue from the pentane extraction was recrystallized from THF to yield hydrated product, $Cp^*(PMe_3)_2RuOH{\cdot}nH_2O$, 633 mg. Combined yield 1.593 g, *ca.* 80%. IR(CH_2Cl_2) 3687 cm^{-1} (w). Anal. Calcd. for $C_{16}H_{34}P_2ORu$: C 47.40; H 8.28. Found : C 47.47; H 8.40. Molecular weight Calcd. 405. Found 389.

Preparation of $[Cp^*(PMe_3)_2Ru(H)Me]BF_4$ (4): To a solution of $Cp^*(PMe_3)_2RuCH_3$ (150 mg, 0.4 mmol) in 5 mL Et_2O at -78 °C was added *ca.* 1 equiv. $HBF_4{\cdot}Et_2O$ (70 μL). The solution was warmed to room temperature and stirred 15 min. A precipitate formed on warming, which was isolated and washed one time with Et_2O, yielding an analytically pure white powder. Yield 123 mg, 67%. IR(Nujol) 2115 cm^{-1} (m). Anal. Calcd. for $C_{17}H_{37}BF_4P_2Ru$: C 41.56; H 7.59. Found: C 40.92; 7.45.

Preparation of $Cp^*(PMe_3)_2RuNPh_2$ (5): 20 mL of THF were added at -78 °C to a mixture of $Cp^*(PMe_3)_2RuCl$ (1.5 g, 3.5 mmol) and $LiNPh_2$ (930 mg, 5.3 mmol). The solution was warmed to room temperature and stirred 12 h. Volatiles were removed under vacuum and the residue thoroughly dried. Extraction with *ca.* 30 mL benzene, filtration, and removal of volatiles yield a yellow orange powder. This powder was slurried in *ca.* 20 mL Et_2O, isolated on a cold frit, and washed three times with Et_2O. The resultant orange powder was recrystallized from THF. Yield 1.616g, 82%. Anal. Calcd. for $C_{28}H_{43}NP_2Ru$: C 60.43; H 7.73; N 2.52. Found: C 60.31; H 7.83; N 2.51.

Preparation $Cp^*(PMe_3)_2RuSH$ (6): To a solution of $Cp^*(PMe_3)_2RuOH$ (200 mg, 0.5 mmol) in 10 mL Et_2O at -78°C was introduced 1 atm of H_2S. The solution was warmed to room temperature and stirred for 15 min. A white precipitate formed on warming and dissolved on continued stirring. Volatiles were removed under vacuum and the residue extracted with *ca.* 10 mL petroleum ether. The solution was filtered, reduced to ca. 3 mL, and slowly cooled to -78°C. The resultant yellow crystals were isolated on a cold frit and dried under vacuum. Yield 145 mg, 69.4%. IR(Nujol) 2508 cm^{-1} (w). Anal. Calcd. for $C_{16}H_{34}SP_2Ru$: C 45.59; H 8.13. Found: C 45.93; H 7.92.

Preparation of $Cp^*(PMe_3)_2RuCN$ (7): To a solution of $Cp^*(PMe_3)_2OH$ (100 mg, 0.25 mmol) in 5 mL THF was added 30 uL liquid HCN in a cold syringe. The solution lightened immediately and was stirred for 15 minutes before the volatiles were removed under vacuum into a trap containing an aqueous bleach solution which was subsequently thawed in a well ventilated hood. The resulting oil was redissolved in 0.5 mL THF and pentane was added until the mixture became cloudy (ca 5 mL). The solution was cooled to -40°C and the resulting crystals collected on a cold frit and dried under vacuum. Yield = 57 mg (56%). IR(THF) 2058 cm^{-1} (s). Anal. Calcd. for $C_{17}H_{33}NP_2Ru$: C 49.26; H 8.03. Found: C 49.58; H 8.05.

Preparation of $Cp^*(PMe_3)_2RuCH_2C(O)CH_3$ (8): To a solution of $Cp^*(PMe_3)_2RuOH$ (228 mg, 0.56 mmol) in 10 mL THF was added 1.5 mL acetone (20 mmol) at -40°C. The solution was warmed to room temperature and stirred 12 h. Volatiles were removed under vacuum and the resultant residue extracted thoroughly with petroleum ether. The solution was filtered, reduced to *ca.* 10 mL, and cooled to -78°C. The orange yellow crystals were isolated on a cold frit and dried under vacuum. The supernatant was reduced to yield a second crop. Combined yield 191 mg, 76%. IR(CH_2Cl_2) 1601 cm^{-1} (s), 1771 cm^{-1} (m). Anal. Calcd. for $C_{19}H_{38}OP_2Ru$: C 51.22; H 8.60. Found: C 51.34; H 8.58.

Preparation of $Cp^*(PMe_3)_2RuCCPh$ (9): To a solution of $Cp^*(PMe_3)_2RuOH$ (423 mg, 1.04 mmol) in 10 mL THF was added HCCPh (1.14 mL, 10.4 mmol). The solution was stirred at

room temperature for 12 h. Volatiles were removed under vacuum and the residue slurried in petroleum ether (10 mL) and THF (*ca.* 2 mL, enough to dissolve the complex). The solution was filtered, reduced to *ca.* 6 mls and slowly cooled to -78°C. The supernatant was removed from the resultant orange crystals and concentrated to yield a second crop. Combined yield 387 mg, 75%. IR(Nujol) 2060 cm^{-1} (s), 2000 cm^{-1} (w). Anal. Calcd. for $C_{24}H_{38}P_2Ru$: C 58.88; H 7.82. Found: C 58.62; H 7.56.

Preparation of $Cp^*(PMe_3)_2RuNHPh$ (10): To a solution of $Cp^*(PMe_3)_2RuOH$ (473 mg, 1.17 mmol) in 10 mL THF was added H_2NPh (1.06 mL, 11.6 mmol). The solution was stirred at room temperature for 12 h. Volatiles were removed under vacuum and the resultant solid slurried in petroleum ether (10 mL) and THF (*ca.* 2 mL, enough to dissolve the complex). The solution was filtered, reduced in volume to *ca.* 6 mL, and slowly cooled to -78°C. The supernatant was removed from the crystals and reduced to yield a second crop. Combined yield 356 mg, 64%. IR(Nujol) 3320 cm^{-1} (w). Anal. Calcd. for $C_{22}H_{39}NP_2Ru$: C 54.98; H 8.18; N 2.91. Found: C 55.28; H 8.00; N 2.78.

Preparation of $Cp^*(PMe_3)_2Ru(n^2\text{-}PMe_2CH_2)$: 20 mL of THF were added to a mixture of $Cp^*(PMe_3)_2RuCl$ (1.0g, 2.4 mmol) and two equiv. LiNH(*tert*-Butyl) (412 mg, 5.0 mmol) at -78°C. The solution was warmed to room temperature and stirred for 12 h. Volatiles were removed under vacuum and the residue thoroughly dried. Extraction with petroleum ether (*ca.* 50 mL), filtration, and removal of volatiles under vacuum yielded a red oil. This oil was frozen then broken up by vigorous stirring under petroleum ether at -78°C to yield an analytically pure yellow powder which was isolated and dried on a cold frit. Yield 580 mg, 63%. Anal. Calcd. for $C_{16}H_{32}P_2Ru$: C 49.6l; H 8.32. Found: C 49.85; H 8.27.

Preparation of $Cp^*(PMe_3)_2RuM(CO)_3Cp$ (12, M = Mo; 13, M = W) Both complexes were prepared by the same method which follows. To a solution of 100 mg (0.25 mmoles) $Cp^*(PMe_3)_2RuOH$ in 5 mL THF was added $Cp(CO)_3MoH$ (59 mg, 0.25 mmoles). The resulting solution was stirred for three hours and filtered through a medium frit. The filtrate was

evaporated to dryness under vacuum and the resulting oil redissolved in minimal THF (*ca* 1 mL). This solution was layered with 10 mL pentane and carefully set in a drybox freezer to mix over the course of 72 hours. The resulting crystals were filtered and vacuum dried to give 130 mg (0.21 mmoles, 83%) of the heterobimetallic product. Anal. Calcd. for $C_{24}H_{38}O_3P_2MoRu$: C 46.23; H 6.14. Found: C 46.03; H 5.84. Similarly, using 83 mg (0.25 mmoles) $Cp(CO)_3WH$ led to isolation of 151 mg (0.21 mmoles, 83%) of product. Anal. Calcd. for $C_{24}H_{38}O_3P_2RuW$: C 39.96; H 5.31. Found: C 39.83; H 5.21.

Preparation of $Cp^*(PMe_3)_2RuSi(OEt)_3$ (14) In a 5 mm screw-capped NMR tube 17 mgs (0.040 mmoles) of $Cp^*(PMe_3)_2RuSH$ were dissolved in 600 uL THF-d_8 and treated with 26 mg (0.32 mmoles, 8 eq) $HSi(OEt)_3$. The tube was sealed and gently warmed (45°C) for five days during which time complete conversion of the starting material was noted. Addition of pentane (2 mL) to the tube followed by cooling for 48 hr at -40°C gave 9 mg (0.016 mmoles, 41%) of the desired silane. No evidence for the formation of any ruthenium(IV) $Cp^*(PMe_3)Ru(H)(Si(OEt)_3)_2$ was noted at any time during the thermolysis.

Reaction of $[Cp^*(PMe_3)_2Ru(Et_2O)]^+OTf^-$ with NaOMe: To a solution of $Cp^*(PMe_3)_2RuCH_2SiMe_3$ (250 mg, 0.53 mmol) in 10 mL Et_2O at -78°C was added 1 equiv. of CF_3SO_3H (47 μl, 0.53 mmol). The solution was warmed to room temperature, stirred for 1 h., and cooled to -78°C again. 1.1 equiv. of Na metal (13 mg, 0.57 mmol) were added to 3 mL MeOH; upon complete reaction, the solution was cooled to -78°C and added to the solution of ruthenium cation. The reaction appeared instantaneous, yielding a yellow solution; the mixture was allowed to stir for 15 min. Volatiles were removed under vacuum at the lowest possible temperature, *ca*. 5-10 ^{0}C, and the residue was dried thoroughly and extracted with 40 mL petroleum ether. Filtration, reduction in volume, and cooling to -78°C afforded yellow crystals which were isolated on a cold frit. The product was identified as $Cp^*(PMe_3)_2RuH$ by comparison to an authentic sample. Yield 205 mg, 82 %.

Carbonylation of $Cp^*(PMe_3)_2RuNPh_2$: A 20 mg sample of $Cp^*(PMe_3)_2RuNPh_2$ in 0.3 mL benzene-d_6 in an NMR tube was sealed under 1 atm. of CO at -196°C and allowed to warm to room temperature. The subsequent reaction was monitored by ^1H NMR; upon apparent completion, the tube was opened under an inert atmosphere and an infrared spectrum of the contents obtained (C_6D_6 vs C_6D_6); ν(CO)=1928 cm^{-1}. The experiment was repeated using ^{13}CO; $\nu(^{13}CO)$=1885 cm^{-1} (predicted 1858 cm^{-1}), no other bands were observed to shift from 1500-2000 cm^{-1}.

Reaction of $Cp^*(PMe_3)_2RuSH$ with $HPPh_2$: To a 15 mg sample of $Cp^*(PMe_3)_2RuSH$ in 0.3 mL benzene-d_6 was added *ca.* 5 equiv. of $HPPh_2$ (30 μl) and the tube heated at 80°C until apparent completion of reaction (2 h). A single product was observed by ^1H and ^{31}P NMR and assigned as $Cp^*(PMe_3)(HPPh_2)RuSH$.

Equilibrium Studies. In a typical experiment 17.0 mg (0.0266 mmol) (DPPE)MePtOMe was dissolved in approximately 600 uL THF-d_8 in a 5 mm Wilmad #507 TR screw-capped NMR tube. The tube was charged with 25.3 mg (0.236 mmol) methyl aniline and 9.8 mg (0.31 mmol) methanol before being tightly sealed. NMR spectra were acquired as previously described and an equilibrium constant was determined after 10 d at 25.4°C. Confirmation of this constant was obtained by fitting the time-dependent concentration data using the software described. The same equilibrium was established from (DPPE)MePtNMePh and methanol to confirm the reversible nature of the reaction and concentrations of starting materials ranging from 0.005 - 0.021 *M* Pt and 0.015 - 0.95 *M* organics were studied. Heating the solution at 45°C for 10 d followed by remeasuring the equilibrium constant confirmed the temperature independence of this equilibrium. Other more robust complexes were heated over a wider range. Absolute concentrations of individual reagents were determined from the quantities added and the height of solution in the NMR tube although only the ratios really mattered in the equilibrium calculations. Other equilibrium studies (as indicated on Table 2) were

conducted in similar fashion. Equilibration times ranged from minutes to weeks depending on the exact equilibrium involved.

$Cp^*(PMe_3)_2RuNPh_2$ Thermolysis: In a 5 mm Wilmad #507 TR screw-capped NMR tube a solution of 17.5 mg (0.032 mmol) $Cp^*(PMe_3)_2RuNPh_2$ in 600 mL C_6D_6 was heated at 80°C. The concentration of amide was determined by integration of the ^{31}P NMR spectra acquired, which is shown in figure 2. Another experiment conducted at 0.018 *M* amide concentration interestingly fit a second order decay much better than a first order process. A similar experiment was conducted at 30°C ([$Cp^*(PMe_3)_2RuNPh_2$] = 0.052 *M*) with the same results; an initial rate constant obtained by first order fit of the first few points was *ca* 10^{-7} sec^{-1} which is very slow on the timescale of the equilibria involving this complex.. Interestingly, the 0.018 *M* thermolysis fit a second order decay much better than the 0.052 *M* case. Organic thermolysis products were determined by capillary gas chromatography on a 25 m methylsilicone column in a Hewlett Packard model 3890 gas chromatograph using both N,P-thermionic and flame ionization detectors. An authentic sample of tetraphenyl hydrazine was thermolyzed in benzene-d_6 at 80°C and used to confirm the identity of the products obtained.

Amide thermolyis in the presence of 9,10-dihydroanthracene was carried out in benzene-d_6 at 65°C by the same techniques. Both amide and DHA were added to the NMR tubes and solvent added. Concentrations were determined by sample height. Concentration vs time data was acquired automatically using Nicolet KINET software and was analyzed using RS1 software operating on a VAX 11/780 system. Figure 3 shows the loss of amide plots obtained, while the rate dependence on dihydroanthracene is shown on Figure 4. Products were identified by spiking product solutions with authentic samples of $Cp^*(PMe_3)_2RuH$, $HNPh_2$ and anthracene. Both GC and NMR methods were used.

When trimethylphosphine was added to a solution of amide and 9,10-dihydroanthracene in benzene-d_6 ([$Cp^*(PMe_3)_2RuNPh_2$] = 0.052 M; [PMe_3] = 0.20 *M*; [9,10-DHA] = 0.80 *M*) thermolysis at 60°C demonstrated the loss of amide to be faster than in the absence of

phosphine. Only *ca.* 60% of the amide was converted to hydride in this case (the other products were not identified) and during the thermolysis ^{31}P CIDNP signals were noted.

References

1) For leading references see (a) Connor, J. A. *Top. Curr. Chem.* **1977**, *71*, 71 (b) Halpern, J. *Acc. Chem. Res.* **1982**, *15*, 238 (c) Pearson, R. G. *Chem. Rev.* **1985**, *85*, 41 (d) Halpern, J. *Inorg. Chim. Acta* **1985**, *100*, 41 (e) Martinho Simoes, J. A.; Beauchamp, J. L. *Chem. Rev.* **1985** *in press*

2) Connor, J. A. *Top. Curr. Chem.* **1977**, *71*, 71

3) (a) Pearson, R. G. *J. Am. Chem. Soc.* **1963**, *85*, 3533. (b) Pearson, R. G. *J. Chem. Educ.* **1968**, *45*, 643

4) (a) Cotton, F. A.; Wilkinson, G. "Advanced Inorganic Chemistry, 4th Edition", John Wiley and Sons, New York, **1980** (b) Mehrotra, R. C. *Adv. Inorg. Chem. Radiochem.* **1983**, *26*, 269 (c) Michelin, R. A.; Napoli, M.; Ros, R. *J. Organometal. Chem.* **1979**, *175*, 239 (d) Rees, W. M.; Atwood, J. D. *Organometallics* **1985**, *4*, 402 (e) Abel, E. W.; Farrow, G.; Towie, I. D. H. *J. Chem. Soc., Dalton Trans.* **1979**, 71 (f) Komiya, S.; Tane-ichi, S.; Yamamoto, A.; Yamamoto, T. *Bull. Chem. Soc. Jpn.* **1980**, *53*, 673 (g) Arnold, D. P.; Bennett, M. A. *J. Organometallic Chem.* **1980**, *199*, 119 (h) Yoshida, T.; Okano, T.; Otsuka, S. *J. Chem. Soc., Dalton Trans.* **1976**, 993 (i) Bennett, M. A.; Yoshida, T. *J. Am. Chem. Soc.* **1978**, *100*, 1750 (j) Bryndza, H. E.; Calabrese, J. C.;Wreford, S. S. *Organometallics* **1984**, *3*, 1603 (k) Bryndza, H. E.; Kretchmar, S. A.; Tulip, T. H. *J. Chem. Soc., Chem. Commun.* **1985**, 977 (l) Newman, L. J.; Bergman, R. G. *J. Am. Chem. Soc.* **1985**, *107*, 5314 (m) Coulson, D. R. *J. Am. Chem. Soc.* **1976**, *98*, 3111 (n) Bennett, M. A.; Robertson, G. B.; Whimp, P. O.; Yoshida, T. *J. Am. Chem. Soc.* **1973**, *95*, 3028 (o) Monaghan, P. K.; Puddephatt, R. J. *Organometallics* **1984**, *3*, 444 (p) Arnold, D. P.; Bennett, M. A. *Inorg. Chem.* **1984**, *23*, 2110 (q) Flynn, B. R.; Vaska, L. *J. Am. Chem. Soc.* **1973**, *95*, 5081 (r) Chaudret. B. N.; Cole-Hamilton, D. J.; Nohr, R. S.;

Wilkinson, G. *J. Chem. Soc., Dalton Trans.* **1977**, 1546 (s) Fryzuk, M. D.; MacNeil, P. A. *Organometallics* **1983**, *2*, 355 (t) Fryzuk, M. D.; MacNeil, P. A. *Organometallics* **1983**, *2*, 682 (u) Fryzuk, M. D.; MacNeil, P. A.; Rettig, S. J.; Secco, A. S.; Trotter, J. *Organometallics* **1982**, *1*, 918 (v) Lappert, M. F.; Power, P. P.; Sanger, A. R.; Srivastava, R. C. "Metal and Metalloid Amides", Ellis Horwood, **1980** (w) Beck, W.; Bauder, M. *Chem. Ber.* **1970**, *103*, 58 (x) Bryndza, H. E. *Organometallics* **1985**, *4*, 1686 (y) Bryndza, H. E. *Organometallics* **1985**, *4*, 406 (z) Bryndza, H. E.; Fultz, W. C.; Tam, W. *Organometallics* **1985**, *4*, 939.

5) (a) Bryndza, H. E. *Organometallics* **1985**, *4*, 1686 (b) Bryndza, H. E.; Kretchmar, S. A.; Tulip, T. H. *J. Chem. Soc., Chem. Commun.* **1985**, 977 (c) Michelin, R. A.; Napoli, M.; Ros, R. *J. Organometal. Chem.* **1979**, *175*, 239 (d) Deeming, A. J.; Shaw, B. L. *J. Chem. Soc. A* **1969**, 443 (e) Bennett, M. A.; Yoshida, T. *J. Am. Chem. Soc.* **1978**, *100*, 1750 (f) Appleton, T. G.; Bennett, M. A. *J. Organometal. Chem.* **1973**, *55*, C88.

6) (a) Bryndza, H. E.; Calabrese, J. C.; Wreford, S. S. *Organometallics* **1984**, *3*, 1603 (b) Bryndza, H. E. *Organometallics* **1985**, *4*, 406.

7) (a) Bryndza, H. E.; Calabrese, J. C.; Marsi, M.; Roe, D. C.; Tam, W.; Bercaw, J. E. *Submitted* **1986** (b) Bennett, M. A.; Arnold, D. P. *J. Organometal. Chem.* **1980**, *199*, C17 (c) Arnold, D. P.; Bennett, M. A. *Inorg. Chem.* **1984**, *23*, 2110 (d) Yoshida, T.; Okano, T.; Otsuka, S. *J. Chem. Soc., Dalton Trans.* **1976**, 993 (e) Monaghan, P. K.; Puddephatt, R. J. *Organometallics* **1984**, *3*, 444 (f) Michelin, R. A.; Napoli, M.; Ros, R. *J. Organometal. Chem.* **1979**, *175*, 239 (g) Bernard, K. A.; Rees, W. M.; Atwood, J. D. *Organometallics* **1986**, *5*, 390.

8) (a) Bryndza, H. E.; Fultz, W. C.; Tam, W. *Organometallics* **1985**, *4*, 939 (b) Appleton, T. G.; Bennett, M. A. *Inorg. Chem.* **1978**, *17*, 738.

9) Tilley, T.D.; Grubbs, R.H.; Bercaw, J.E. *Organometallics* **1984**, *3*, 274.

10) A cautionary note, the following observations have been made during the synthesis of $Cp^*(PMe_3)_2RuOH$: i) Treatment of $[Cp^*(PMe_3)_2Ru{\cdot}Et_2O]^+SO_3CF_3^-$ with KOH in the

absence of H_2O results in the formation of (η^4- $C_5Me_4CH_2$)Ru(PMe_3)$_3$, L.K. Fong and J.E. Bercaw *unpublished results*; ii) Treatment of Cp*(PMe_3)$_2$RuOH with base leads to formation of the dimer, (Cp*(PMe_3)$_2$Ru)O; iii) The following equilibrium has been observed in diethyl ether: 3 Cp*(PMe_3)$_2$RuOH $\rightleftharpoons$ (Cp*(PMe_3)$_2$Ru)O + Cp*(PMe_3)$_2$RuOH·H_2O.

11) Weak OH absorbances are characteristic of late metal hydroxides-see for example (a) Michelin, R. A.; Napoli, M.; Ros, R. *J. Organometallic Chem.* **1979**, *175*, 239 (b) Yoshida, T.; Okano, T.; Otsuka, S. *J. Chem. Soc., Dalton Trans.* **1976**, 993.

12) The equilibrium constant is also independent of the reaction vessel wall material; **e.g.** pyrex, silylated pyrex, sapphire or quartz. The authors wish to thank Professor Herb Kaesz for suggesting these experiments to us.

13) The nearly solvent independent nature of the equilibrium is further demonstrated by the fact that the [H_2O] (between 0.02 and 0.80 *M*), and hence the dielectric of the THF-d_8/H_2O solution, does not systematically change the measured K_{eq} for eq 7. Further evidence for the insensitivity of the equilibria measured to protic solvents comes from the study of eq 16 (*vide infra*) which gives results, in the absence of protic materials, which were predicted by equilibria involving those protic organic compounds.

14) Since $\Delta G_{eq} \sim 0$. and since no measureable temperature dependence of ΔG_{eq} was noted, this implies $\Delta H_{eq} \sim \Delta S_{eq} \sim 0$.

15) (a) McMillen, D. F.; Golden, D. M. *Ann. Rev. Phys. Chem.* **1982**, *33*, 493 (b) Stull, D. R.; Westrum, E. F.; Sinke, G. C. "The Chemical Thermodynamics of Organic Compounds" John Wiley and Sons, New York, **1969** (c) Benson, S. W. *Chem. Rev.* **1969**, *69*, 279. (d) Benson, S. W. "Thermochemical Kinetics, Second Edition", John Wiley and Sons, New York, **1976** (e) Sanderson, R. T. "Chemical Bonds and Bond Energies, Second Edition" Academic Press, New York, **1976**

16) Throughout this manuscript we use interchangeably "L_nM-X bond strengths", "bond dissociation energies (BDEs)" and "homolytic bond strengths" to mean relative *solution phase* D(M-X) values. By using gas phase D(H–X) values, we necessarily assume equivalent solvation of the functional groups on both sides of the equilibria and that the bonding of ancillary ligands (Cp*, phosphines, etc) to the metal does not appreciably change. Other studies have noted that the sublimation, dissolution and vaporization energies needed to convert such solution data to gas phase values make very small corrections to the relative bond strengths obtained when nongaseous reagents are involved (*vide infra*, reference 28). Moreover, the values and assumptions needed to correct solution phase BDEs to gas phase numbers commonly introduce errors as large as the corrections to be made. Thus, we prefer to use the solution values obtained; we suggest the gas phase values will be similar. The applicability of this approach is evident from the utility of the thermodynamic functional group additivity tables for organic systems in solution as well as the gas phase. See: (a) Benson, S. W. "Thermochemical Kinetics, Second Edition" John Wiley and Sons, Hew York, **1976** (b) Benson, S. W. "The Foundation of Chemical Kinetics" Robert E. Krieger Publishing Company, Malabar, Florida **1982.**

17) $Cp^*Ru(PMe_3)H_3$ is in equilibrium with $Cp^*Ru(PMe_3)_2H$ at high pressure of H_2, R. Paciello and J.E. Bercaw unpublished results.

18) Tolman, C. A. *Chem. Rev.* **1977**, *77*, 313

19) Since the rate of aminyl radical dimerization under these conditions is known to be 10^8 - 10^9 $sec^{-1}\cdot M^{-1}$ (reference 21) and the maximum rate of radical/radical recombination can be estimated as 10^9 $sec^{-1}\cdot M^{-1}$ from the fastest radical-radical combination rates known for diphenylaminyl radicals (reference 21), straightforward steady state approximations indicate the rate of bond homolysis must be slower than 10^2 sec^{-1}. Assuming a preexponential factor of 10^{12} (as found for diphenylaminyl

radical dimerizations in benzene at 60°C; reference 21), this corresponds to a Ru-NPh_2 BDE of 17 kcal/mole.

20) Since no evidence of "saturation kinetics" (*i.e.* a regime in which the rate becomes less than first order in [DHA]) is observed during thermolysis at 65°C, even in the presence of 1.09 M dihydroanthracene, the reaction mechanism represented by eq 19 is brought into question. It is well established that diphenylaminyl radicals abstract hydrogen atoms from dihydroanthracene rather inefficiently ($k_{H\ abstraction}$ = 10 $s^{-1}\cdot M^{-1}$ at 63°C, 2 M in benzene).[22] Therefore, the failure to observe saturation kinetics under these conditions was not entirely unexpected, given the 10^6 ratio of radical dimerization[21] to hydrogen abstraction[22] rates. Indeed, if eq 20 does accurately depict the mechanism, the observed pseudo-first order rate constant of 3 X 10^{-3} s^{-1} (65°C, [DHA] = 1.09 M) indicates that the DHA radical trapping efficiency is well below 10% of the free diphenylaminyl radicals present, the remainder being much more efficiently trapped by free {$Cp^*(PMe_3)_2Ru\cdot$} to regenerate **5**

21) Rates for diphenylaminyl radical dimerizations have been measured in benzene from 20 to 80°C. At 65°C the self-dimerization rate is 10^8 - 10^9 $sec^{-1}\cdot M^{-1}$ as found in (a) Shida, T.; Kira, A. *J. Phys. Chem.* **1969**, *73*, 4315 (b) Welzel, P. *Chem. Ber.* **1970**, *103*, 1318 (c) Welzel, P. *Chem. Ber.* **1971**, *104*, 808 (d) Marshall, J. H. *J. Phys. Chem.* **1974**, *78*, 2225 (e) Welzel, P; Gunther, L.; Eckhardt, G. *Chem. Ber.* **1974**, *107*, 3624 (f) Welzel, P.; Muther, I.; Volk, H. *Tetrahedron Lett.* **1977**, 745. Reports of pre-exponential factors for the N-N bond homolysis in tetraphenyl hydrazine range from Log(A) = 10.4 to Log(A) = 12.2 as found in references (a) and (d) and (g) Cain, C. K.; Wiselogle, F. Y. *J. Am. Chem. Soc.* **1940**, *62*, 1163 (h) Franzen, V. *Liebigs Ann. Chem.* **1957**, *604*, 251 (i) Zhivechkova, L. A.; Tanaseichuk, B. S.; Ermishov, A. Yu. *Zh. Org. Khim.* **1971**, *7*, 2379 (j) anaseichuk, B. S.; Zhivechkova, L. A.; Ermishov, A. Yu. *Zh. Org. Khim.* **1972**, *8*, 758.

22) Rates of hydrogen atom abstraction for a variety of diarylaminyl radicals and hydrogen atom sources can be found in (a) Bridger, R. F. *J. Am. Chem. Soc.* **1972**, *94*, 3124 (b) Meskina, M. Ya.; Karpukhina, G. V.; Maizus, A. K. *Izv. Akad. Nauk SSSR, Ser. Khim.* **1974**, 1755 (c) Bridger, R. F. private communication to K. U. Ingold as reported in "Landold-Bornstein; Numerical Data and Functional Relationships in Science and Technology, New Series (editor in chief K.-H. Hellwege), Volume 13 (Radical Reaction Rates in Liquids; editor H. Fisher), subvolume c (Radicals Centered on N, S, P and other Heteroatoms; compiled by K. U. Ingold)" Springer-Verlag, Berlin **1983**. The rates of hydrogen atom abstraction from 2.0 *M* 9,10-dihydroanthracene in benzene at 63°C by phenyl-1-napthylaminyl radicals is between 5 and 10 $sec^{-1} \cdot M^{-1}$.

23) As is often the case, radical lifetimes and relaxation times leading to the observation of CIDNP often precludes obtaining ESR evidence of these same radical intermediates. For a discussion of this phenomenon see Lepley, A. R.; Closs, G. L. "Chemically Induced Magnetic Polarization" John Wiley and Sons, New York **1973**

24) Again (ref 20) assuming a homolysis Log(A) of 12, a homolysis rate of 10^{-2} sec^{-1} corresponds to a bond dissociation energy of 23 $kcal \cdot mol^{-1}$.

25) Current efforts are directed at evaluating the viability of these alternative mechanisms, including those which involve $(\eta^6\text{–}C_5Me_4CH_2)(PMe_3)_2Ru$ and $Cp^*(PMe_3)Ru(\eta^2\text{–}CH_2PMe_2)$ intermediates. Some component of the loss of **5** in these thermolysis experiments can be inhibited by the presence of high concentrations of diphenylamine, suggesting that a tetramethylfulvene decomposition route may account for part of the loss of **5**. Moreover, the thermolysis of the isolable complex, $(\eta^4\text{–}C_5Me_4CH_2)(PMe_3)_2Ru(PMe_3)$, in the presence of DHA leads to the formation of $Cp^*(PMe_3)_2RuH$. Thermolysis of the benzyl derivative, $Cp^*(PMe_3)_2RuCH_2Ph$, does not occur by a free radical mechanism at temperatures comparable to those necessary for $Cp^*(PMe_3)_2RuNPh_2$. Much higher temperatures are observed to lead to loss of toluene and formation of the phenyl complex.

26) The ramifications of the thermoneutral character observed for these equilibrations was has been previously reported: Bryndza, H. E.; Fultz, W. C.; Tam, W. *Organometallics*, **1985**, 4, 939

27) Many examples are illustrated in Benson, S. W. "Thermochemical Kinetics, Second Edition" John Wiley and Sons, New York **1976**.

28) (a) Janowicz, A. H.; Periana, R. A.; Buchanan, J. M.; Kovac, C. A.; Stryker, J. M.; Wax, M. J.; Bergman, R. G. *Pure & Appl. Chem.* **1984**, *56*, 13 (b) Jones, W. D.; Feher, F. J. *J. Am. Chem. Soc.* **1985**, *107*, 620 (c) Bergman, R. G. *Science* **1984**, *223*, 902 (d) Jones, W. D.; Feher, F. J. *J. Am. Chem. Soc.* **1984**, *106*, 1650 (e) Bruno, J. W.; Marks, T. J.; Morss, L. R. *J. Am. Chem. Soc.* **1983**, *105*, 6824 (f) Wax, M. J.; Stryker, J. M.; Buchanan, J. M.; Kovac, C. A.; Bergman, R. G. *J. Am. Chem. Soc.* **1984**, *106*, 1121 (g) Bryndza, H. E.; Fultz, W. C.; Tam, W. *Organometallics* **1985**, *4*, 939.

29) Buchanan, J. M.; Stryker, J. M.; Bergman, R. G. *J. Am. Chem. Soc.*, **1986**, *108*, 1537

30) Bruno, J. W.; Marks, T. J.; Morss, L. R. *J. Am. Chem. Soc.* **1983**, *105*, 6824.

34) While the data for the alkoxides and amides was obtained on complexes having slightly different spectator ligand environments than the $Cp^*_2(OCMe_3)ThX$ data plotted in Figure 6, the deviations of more than 20 $kcal{\cdot}mol^{-1}$ (from the values expected based on the H-X vs Th-X plot) are large with respect to deviations seen in Th-X bonds on changing spectator ligands. For example, in the series $Cp^*_2(Et)ThEt$, $Cp^*_2(OCMe_3)ThEt$, $Cp^*_2(Cl)ThEt$ the solution phase Th-C bond strengths range over only 4.1 $kcal{\cdot}mole^{-1}$ (73.5, 76.3, 72.2 $kcal{\cdot}mol^{-1}$ respectively).

32) Pasto, D. J.; Johnson, C. R. "Laboratory Text for Organic Chemistry" Prentice-Hall, Englewood Cliffs, New Jersey, **1979**

33) The fact that most of the dihydrogen is in the gas phase above the solution also contributes to the error in translating the Ru-H BDE for **11** to relative gas phase values, because the enthalpy of dissolution of dihydrogen in THF, which is likely to differ substantially from the enthalpies of condensation and dissolution of the other organics

used in this study, must be incorporated into the calculation. Although this quantity has not yet been measured to our knowledge, it is unlikely that it exceeds the $\pm$ 2 kcal·mol^{-1} uncertainty in the measurement of the equilibrium constant for eq 11.

34) (a) Thompson, M. E. Thesis, California Institute of Technology **1985** (b) Thompson, M. E.; Bulls, A. R.; Burger, B. J.; Nolan, M. C.; Santarsiero, B. D.; Schaefer, W. P.; Bercaw, J. E., *J. Amer. Chem. Soc.*, **1987**, *109*, 203

35) Assuming a C-H BDE of 111 kcal·mol^{-1} for benzene, H-H BDE of 104 kcal·mol^{-1} and $\Delta H_{sol'n}$= 0.9 kcal • mol^{-1} for H_2 in benzene.

36) The M-CH_3 *vs* M-H bond strength difference of 14 kcal • mol^{-1} quoted by Connor (*Organometallics*, **1982**, *1*, 1166) has been discussed in the more recent reviews cited in ref. 3 which take into account other experimental data, as well. We feel the cited value of 25 kcal • mol^{-1} more accurately reflects the perceptions of these reviews, which have been widely adopted as state-of-the-art information.

37) Bercaw, J. E.; Davies, D. L.; Wolczanski, P. T. *Organometallics*, **1986**, *5*, 443

38) (a) Bryndza, H. E. *Organometallics* **1985**, *4*, 1686 (b) Bryndza, H. E. *Organometallics* **1985**, *4*, 406 (c) Bryndza, H. E.; Calabrese, J. C.; Wreford, S. S. *Organometallics* **1984**, *3*, 1603.

39) Standard state used: 298.15°K, 0.1 mPa, HCO_2H(g), H_2O(g), CO(g), $HCONH_2$(g), NH_3(g), CH_3CH_2OH(g), C_2H_4(g), $CH_3CH_2NH_2$(g). S^o values unavailable for $CH_3CH_2NH_2$. Values obtained from *Journal of Physical and Chemical Reference Data*, **1982**, *11*, supplement 2

40) (a) Collman, J. P.; Hegedus, L. S. "Principles and Applications of Organotransition Metal Chemistry" University Science Books, Mill Valley CA, **1980** (b) Parshall, G. W. "Homogeneous Catalysis" John Wiley and Sons, New York, **1980**

41) Brown, T.L.; Dickerhoff, D.W.; Bafus, D.A.; Morgan, G.L. *Rev. Sci. Instrum. 1962, 33*, 491

42) Marvich, R.H.; Brintzinger, H.H. *J. Am. Chem. Soc.* **1972**, *93*, 2046

43) An iterative least squares version of HAVECHEM (as reported in R. N. Stabler and J. Chesnick *Int. J. Chem. Kinetics* **1978**, *10*, 461) has been developed at DuPont by Dr. F. J. Weigert.

44) (a) Singer, J.A. *Justus Liebigs Ann. Chem.* **1930**, *478*, 246. (b) Clark, E.P. *Ind. Eng. Chem., Anal. Ed. 1941*, *13*, 820

KINETICS AND MECHANISM OF PHOSPHINE EXCHANGE FOR RUTHENIUM(II) COMPLEXES IN THE SERIES $Cp^*(PMe_3)_2RuX$. ANCILLARY LIGAND EFFECTS ON THE RELATIVE TRANSITION STATE ENERGIES FOR DATIVE LIGAND DISSOCIATION

Abstract

Dissociative trimethylphosphine exchange kinetics have been studied for the complexes $Cp^*(PMe_3)_2RuX$ ($Cp^* = \eta^5$–C_5Me_5, X = NPh_2, NHPh, OH, SPh, OPh, SH, Cl, Br, CH_2SiMe_3, CH_2COCH_3, I, Ph, CH_2Ph, CH_3, C≡CPh, H). Activation parameters for phosphine dissociation have been obtained for all these complexes which, in turn, makes it possible to evaluate both the steric and electronic contributions of ancillary 'X' ligands to phosphine ligand dynamics. Activation enthalpies for phosphine dissociation, which approximate Ru-P bond strengths, show a marked dependence on X ligand steric requirements which suggests the functional group additivity approach to organometallic thermochemistry may have limited applicability. The presence of lone electron pairs on X results in dramatic accelerations of phosphine dissociation in complexes which are about the same size.

Introduction

An appreciation of the strength of transition metal-to-ligand bonds (M–L and M–X bond dissociation energies (BDEs) for L_nMX_m; L = datively bonded ligand, X = covalently bonded ligand) is of unquestioned importance to an understanding of the reaction patterns and mechanisms involving organotransition metal and coordination compounds. To this end, we have recently reported an interesting one-to-one correlation between the relative L_nM–X bond dissociation energies for organoruthenium and organoplatinum compounds of the types (η^5–C_5Me_5)(PMe_3)$_2$Ru–X and ($Ph_2PCH_2CH_2PPh_2$)(CH_3)Pt–X (X = NPh_2, NHPh, OH, SPh, OPh, SH, Cl, Br, CH_2SiMe_3, CH_2COCH_3, I, Ph, CH_2Ph, CH_3, C≡CPh, H) and the corresponding H–X BDEs.[1]

We have previously shown that the phosphine ligands of the organoruthenium complexes, Cp*(PMe_3)$_2$RuR (R = alkyl, hydride), are thermally labile, and have observed intra- and intermolecular C–H bond activations upon thermolysis of these compounds.[2] We have also observed that these phosphine ligands are photochemically labile, and have observed similar C–H bond activations upon irradiation of these complexes.[3] A mechanism involving phosphine dissociation, formation of very reactive, coordinatively unsaturated complex, [Cp*(PMe_3)RuR], and subsequent trapping by **L** or insertion of C–H bonds has been proposed for the thermal reactions.[2] Moreover, the electronic structure proposed for the complexes of the type Cp*L_2MX (M = Ru, Fe; L = PMe_3, PEt_3, CO; X = hydride, halide, alkyl, aryl) is indicative of an excited state which is antibonding with respect to Ru–L, confirming that the reactive species [Cp*(PMe_3)RuR] is also accessible upon broadband photochemical excitation.[4] Phosphine loss appears to dominate the chemistry of these Cp*(PMe_3)$_2$RuX complexes, yet it is still not clear what factors govern this "simple" dissociation process.

The kinetics and mechanisms for phosphine dissociation from organometallic complexes have been studied for a number of systems.[5] Generally, these have involved equilibria of the type shown in eq. 1

$$\mathbf{L_nM} \underset{k_{-1}}{\overset{k_1}{\rightleftharpoons}} \mathbf{L_{n-1}M} + \mathbf{L} \qquad (1)$$

The effects of varying the steric bulk of **L** on the rates of dissociation (k_1) and the position of the equilibrium (k_1/k_{-1}) have been examined. Attainment of equilibrium in these cases permits an estimate of the absolute **M–L** BDE.[6] There have also been numerous studies of the effects of *cis* and *trans* labilizing, σ-bonded ligands on **M–L** bond strengths for "classical" coordination complexes.[7] However, there have been no studies where ligand loss from organometallic complexes has been investigated in a systematic way as the ancillary ligand, X, is varied. Hence, we undertook a study of the rates of trimethylphosphine dissociation for the series of complexes, $Cp^*(PMe_3)_2RuX$, in hopes of defining the factors governing phosphine loss and, assuming a small and/or constant barrier for re-coordination of PMe_3, the values of the Ru–P dative bond strengths.

An assumption inherent to the evaluation of the equilibrium bond strength measurements reported for $Cp^*(PMe_3)_2RuX$ and (DPPE)(Me)PtX, see eq. 2, as well as virtually every other solution phase thermochemical investigation into organotransition metal chemistry,[8] has been the principle of functional group thermochemical additivity.

$$Cp^*(PMe_3)_2Ru\text{-}X + H\text{-}Y \rightleftharpoons Cp^*(PMe_3)_2Ru\text{-}Y + H\text{-}X \qquad (2)$$

Functional group additivity has been successfully applied to numerous organic systems.[9] The availability of dative bond dissociation enthalpies for a representative series of L_nM–X would allow a test of the validity of this fundamental assumption for organometallic systems.

We report herein activation parameters for ligand dissociation in the complexes $Cp^*(PMe_3)(X)Ru–PMe_3$, and an interpretation of the trends with varying X.

Results

The complexes $Cp^*(PMe_3)_2RuX$ (X = NPh_2, NHPh, OH, SPh, OPh, SH, Cl, Br, CH_2SiMe_3, CH_2COCH_3, I, Ph, CH_2Ph, CH_3, C≡CPh, H) were prepared as previously reported.[10]

There are certain limitations to the traditional kinetic treatment for a system undergoing reversible loss of **L** according to Scheme 1.

$$Cp^*(PMe_3)_2Ru\text{-}X \underset{k_{-1}}{\overset{k_1}{\rightleftharpoons}} Cp^*(PMe_3)Ru\text{-}X + PMe_3$$

$$Cp^*(PMe_3)Ru\text{-}X + {}^*PMe_3 \underset{k_1}{\overset{k_{-1}}{\rightleftharpoons}} Cp^*(PMe_3)({}^*PMe_3)Ru\text{-}X$$

(Scheme 1)

$$Cp^*(PMe_3)({}^*PMe_3)Ru\text{-}X \underset{k_{-1}}{\overset{k_1}{\rightleftharpoons}} Cp^*({}^*PMe_3)Ru\text{-}X + PMe_3$$

$$Cp^*({}^*PMe_3)Ru\text{-}X + {}^*PMe_3 \underset{k_1}{\overset{k_{-1}}{\rightleftharpoons}} Cp^*({}^*PMe_3)_2Ru\text{-}X$$

The method of initial rates for approach to equilibrium or use of a large excess of **L** to achieve pseudo first order kinetics assume that the trapping rate, k_{-1}, is very much faster than the dissociation rate, k_1, and is irreversible. These are approximate methods used to simplify the kinetic treatment of the approach of the entire system to equilibrium. Experimentally, use of ^1H NMR and a labelled phosphine such as $P(CD_3)_3$ does not allow quantification of the concentrations of all components in the system.[11] Such considerations suggest the use of ^{31}P NMR as the proper analytical technique, and multi-parameter fitting of a suitable kinetic model to the resultant data as a method of extracting the dissociation rate constant of interest.

Initial efforts to examine ligand exchange processes in $Cp^*(PMe_3)_2RuSPh$ *via* ^{31}P NMR utilized $(^{13}CH_3)PMe_2$ as the labelled phosphine, see Scheme 1. We observed that the $^1J_{(C\text{-}P)}$

(of *ca.* 13 Hz) in ruthenium complexes which contain $(^{13}CH_3)PMe_2$ is too small to reliably resolve and integrate the metal-bound labelled and unlabelled ligand signals. However, signals corresponding to the free phosphines in solution are amenable to quantification, and this allowed some preliminary observations. Pseudo first-order reaction conditions, in which 10 equivalents of added $(^{13}CH_3)PMe_2$ were used, showed PMe_3 exchange rates only incrementally slower than those in a similar experiment utilizing 20 equivalents of added phosphine. This exhibition of the anticipated saturation kinetics strongly suggests that ligand exchange in these ruthenium complexes procedes *via* a dissociative pathway. In addition, the amount of free phosphine in solution could be monitored against an internal standard as a function of temperature, and it was observed that significant amounts were in the gas phase (*ca.* 20% after two half-lives at 100°C).

Ligand exchange reactions were then studied by the addition of $P(CD_3)_3$ to unlabelled $Cp^*(PMe_3)_2RuX$ complexes. A large isotopic shift was observed in the ^{31}P NMR for perdeutero- and perproteo-phosphine (*ca.* 0.9 ppm at 100°C), and the spectral features for Ru-PMe_3 and Ru-$P(CD_3)_3$ were well separated, see Figure 1. However, large differences were observed in the ^{31}P NOE enhancements for labelled *vs* unlabelled phosphines when conventional "1 pulse" Fourier transform techniques were used; a factor of *ca.* 2.5 was noted for the intensity of PMe_3 *vs* $P(CD_3)_3$. In addition, long spin-lattice relaxation values (T_1's) of 5-15 seconds have been observed for the ^{31}P signals of $Cp^*(PMe_3)_2RuX$ complexes, so long delays between acquisition pulses must be used to obtain spectra where integrals accurately reflect concentrations of individual species in solution.[1]

These observations led to the final experimental design. Metal-bound labelled and unlabelled phosphine, and free labelled and unlabelled phosphine were measured versus time at a given temperature by ^{31}P NMR. Quantitative results were obtained by using an NOE suppressed kinetics pulse sequence,[12] and by using 60 second (*ca.* 5 T_1) pulse delays. Measurement of the initial weight of $Cp^*(PMe_3)_2RuX$ (no more than 5% loss of metal

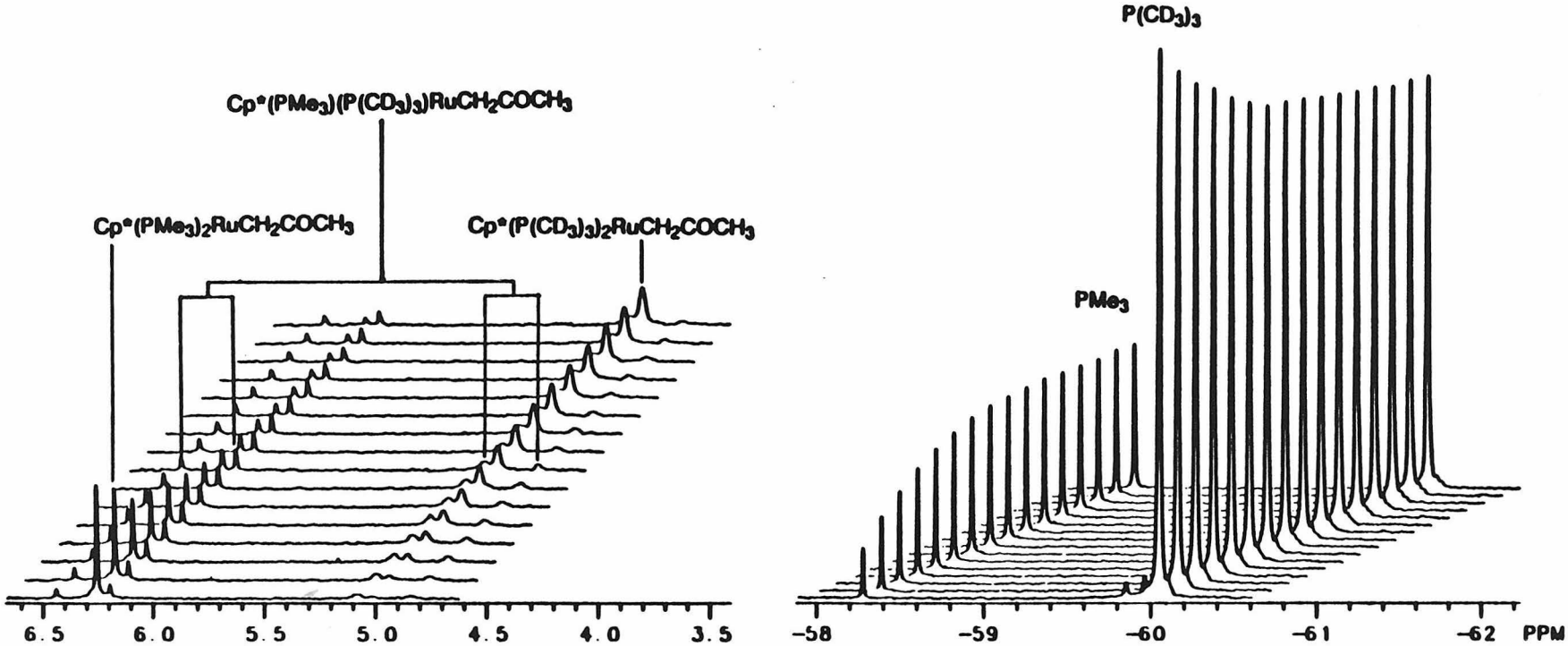

Figure 1. ^{31}P spectrum (shifts in ppm, referenced to 85% H_3PO_4, 121 MHz) of the approach to equilibrium of $Cp^*(PMe_3)_2RuCH_2COCH_3 + P(CD_3)_3$ at 78°C: $[Cp^*(PMe_3)_2RuCH_2COCH_3] = 0.048$ M; $[P(CD_3)_3] = 0.680$ M; $k_1 = 3.91 \times 10^{-5}$ sec^{-1}

complex was ever observed) and of the initial weight of $P(CD_3)_3$ allowed calculation of the amount of each phosphine migrating to the gas phase ($PMe_{3(g)}$ and $P(CD_3)_{3(g)}$) as a function of time.

The acquired data were numerically integrated by an iterative process to the following kinetic model, see Scheme 2, which incorporates dissociative ligand exchange with simultaneous liquid to gas phase phosphine equilibration.[13]

$$[Ru]\text{-}PMe_3 \underset{k_{-1}}{\overset{k_1}{\rightleftharpoons}} [Ru] + PMe_3 \qquad [Ru] = Cp^*(PMe_3)Ru$$

$$[Ru]\text{-}P(CD_3)_3 \underset{k_{-1}}{\overset{k_1}{\rightleftharpoons}} [Ru] + P(CD_3)_3$$

(Scheme 2)

$$PMe_{3(sol)} \underset{k_{-2}}{\overset{k_2}{\rightleftharpoons}} PMe_{3(gas)}$$

$$P(CD_3)_{3(sol)} \underset{k_{-2}}{\overset{k_2}{\rightleftharpoons}} P(CD_3)_{3(gas)}$$

The assumption made in this method of obtaining dissociation rate constants is that the rates for these processes do *not* change upon isotopic labelling. Support for this assumption comes from finding the anticipated equilibrium constants, K, of 1 for the final equilibrium mixtures, see eq. 3.

$$Cp^*(PMe_3)_2Ru\text{-}X + 2P(CD_3)_3 \overset{K}{\rightleftharpoons} Cp^*(P(CD_3)_3)_2Ru + 2PMe_3 \qquad (3)$$

The fit of the phosphine exchange data obtained for a representative complex, $Cp^*(PMe_3)_2RuCH_2Ph$, to the kinetic model in Scheme 2 is shown in Figure 2. Concentrations of all species in this plot were measured, or obtained by difference. The intermediate complex, $[Cp^*(PMe_3)RuCH_2Ph]$, has never been observed in any of our experiments.

Four rate constants were calculated: k_1, k_{-1}, k_2, k_{-2}. As expected, since intermediates are never observed, k_{-1} is not well defined; satisfactory fits to the data are observed as long as

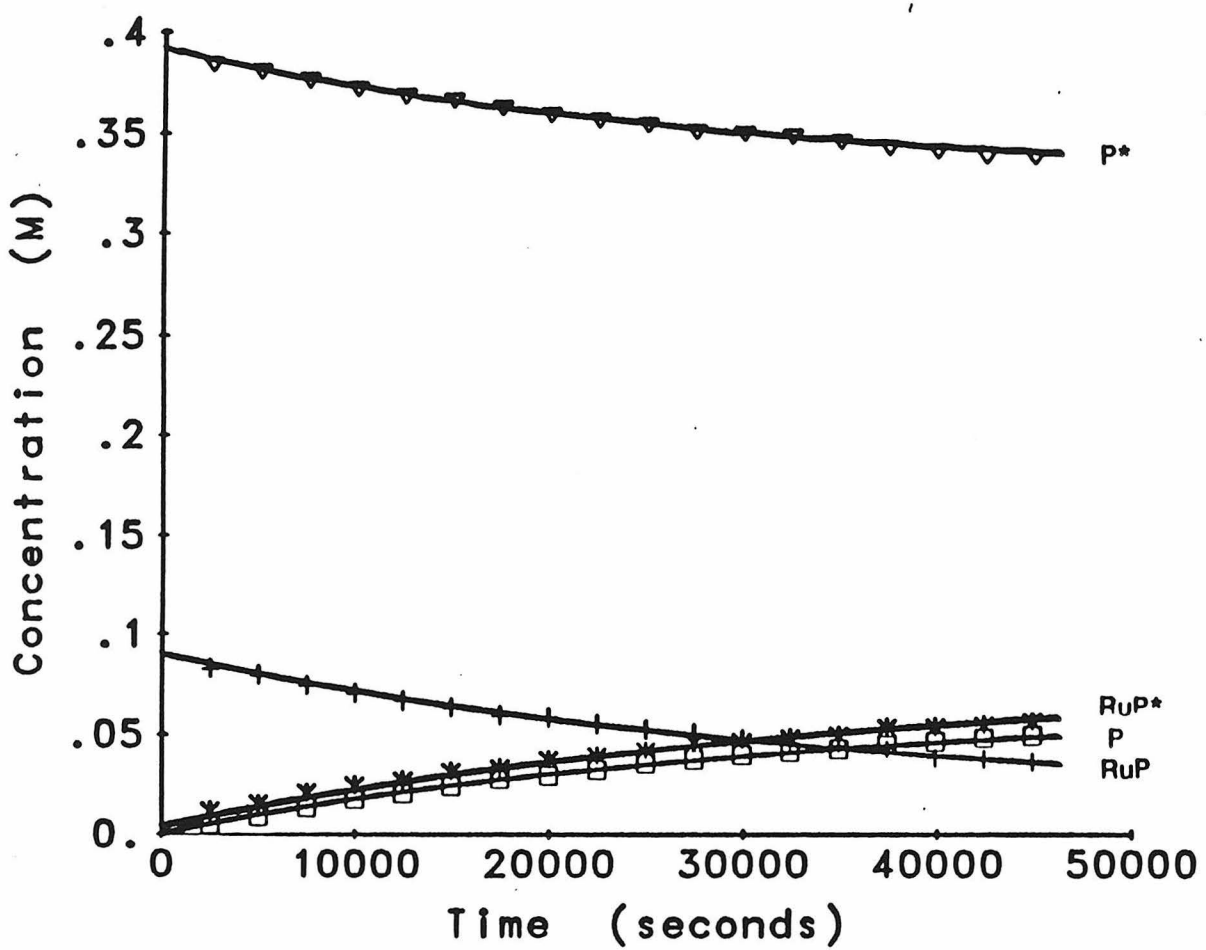

Figure 2. Fit of data for approach of equilibrium of $Cp^*(PMe_3)_2RuCH_2Ph + P(CD_3)_3$ to the kinetic model proposed in Scheme 2. Conditions: Solvent = *o*-xylene-d_{10}; temp(actual) = 86.7°C; $[Cp^*(PMe_3)_2RuCH_2Ph] = 0.047$ M; $[P(CD_3)_3] = 0.345$ M
Species: $P(CD_3)_3$ (▽); $P(CH_3)_3$ (□); Ru-($P(CH_3)_3$) (+); Ru-($P(CD_3)_3$ (✱)
Parameters: $k_1 = 2.38 \times 10^{-5}$ sec^{-1}; $k_{-1} = 2.41$ sec^{-1}; $k_2 = 1.14 \times 10^{-5}$ sec^{-1}; $k_{-2} = 9.02 \times 10^{-5}$ sec^{-1};
average deviation 9.7×10^{-4} M

$k_{-1} >> k_1$.[14] However, the fit of the model to the data shown in Figure 2 is very sensitive to the value of k_1. Unsatisfactory fits are obtained when the optimized rate constant k_1 is fixed at ±2% of that optimal value and all other rates are reoptimized, see Figure 3. This observation suggests the method and the data provide values of k_1 which are accurate to ±2%. Treatment of the early part of these data by the method of initial rates gives the same k_1 value to within *ca.* 10%. This is not surprising as both treatments assume the same dissociative mechanism.

Care must be taken when treating data with a modeling program. As is usual for any iterative, multiparameter program, a global minimum must be found. The initial rate guesses must be varied over the widest possible range to show convergence to the same minimum. In addition, in a system of coupled equilibria, such as those in Scheme 2, care must be taken to avoid program artifacts. The program "GIT" we have used varies k's sequentially, so once the proper difference is found for the forward and reverse rate (consistent with K_{eq}), changing the first rate will not be productive. GIT will readjust it back to the equilibrium value consistent with the second rate. However, as can be seen in figures 2 and 3, with proper care k_1, the rate of interest, can be determined quite accurately.

To obtain activation parameters, at least four ligand exchange experiments were run over a 40°C range. An Eyring plot of a representative data set is shown in Figure 4.[15] An Arrhenius plot of the data yields the same E_a value as can be obtained from the $\Delta H^{\ddagger}$ value obtained from the Eyring treatment. Table 1 lists the activation parameters obtained for all the $Cp^*(PMe_3)_2RuX$ examined. The $\Delta G^{\ddagger}$ values listed have been extrapolated to a common temperature of 100°C.[16]

Discussion

We must stress that it is not possible to determine bond dissociation enthalpies using our measurements. To do so would require the assumption that the rate, k_{-1}, for trapping of $[Cp^*(PMe_3)RuX]$ be the same for all X. We *suggest* that since the activation barrier for

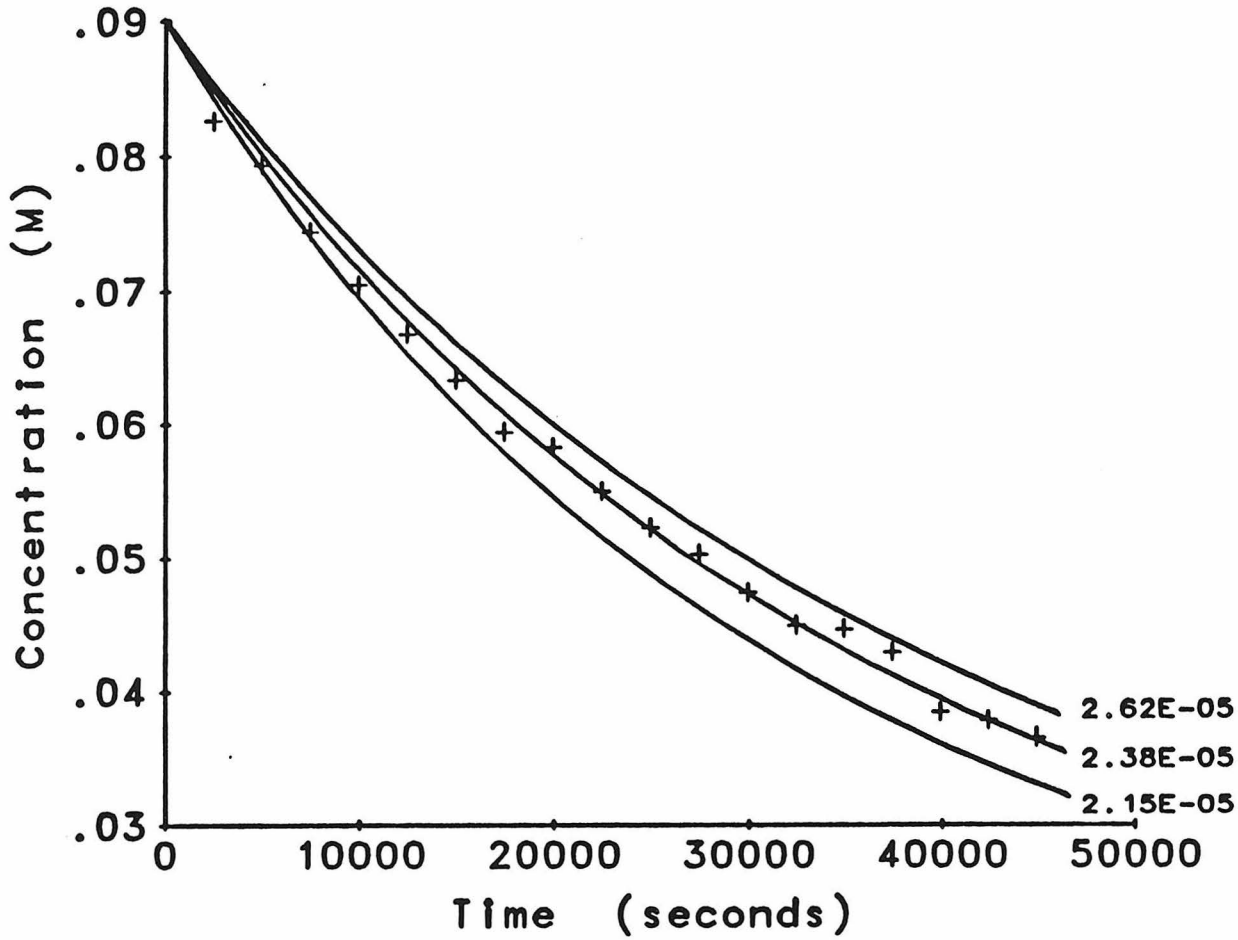

Figure 3. Sensitivity of method to k_{diss} shown for approach to equilibrium of $Cp^*(PMe_3)_2RuCH_2Ph + P(CD_3)_3$, same data as in Figure 2. Center line shows fit of model to disappearance of $[Ru\text{-}(P(CH_3)_3)]$, $k_1 = 2.38 \times 10^{-5}\ sec^{-1}$. This k_1 value altered by ± 2%, and the fit to the same data shown for the reoptimized system.

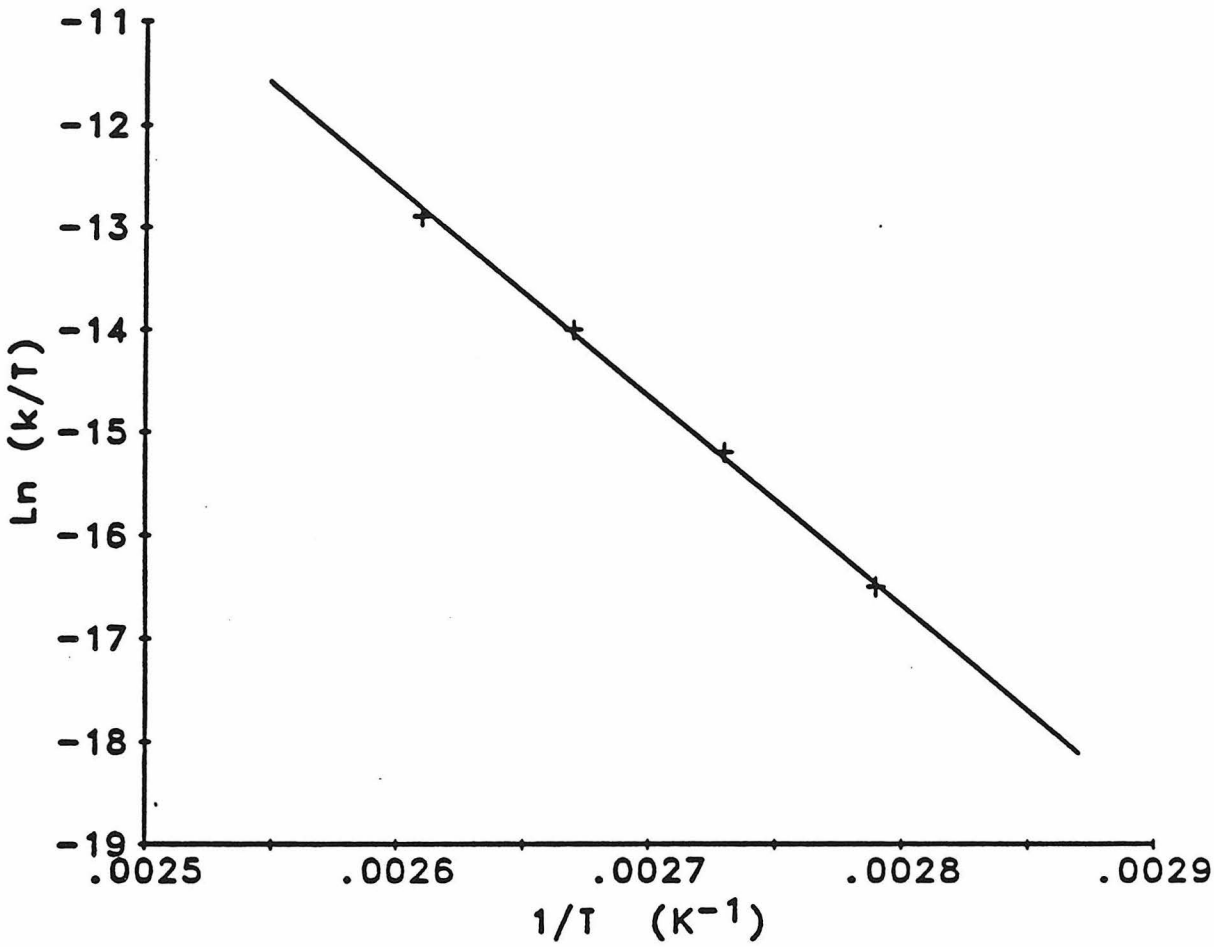

Figure 4. Eyring plot of k_1 values obtained by fitting model in Scheme 2 to data for the approach to equilibrium of $Cp^*(PMe_3)_2RuCH_2Ph + P(CD_3)_3$. See Table 1 for temperature range and k_1 data. Transition state parameters obtained as discussed in ref. 18: $\Delta H^{\ddagger} = 38.2 \pm 2$ kcal•mol^{-1}; $\Delta S^{\ddagger} = 27.7$ e.u.; $\Delta G^{\ddagger}(100°C) = 28.1 \pm 0.2$ kcal•mol^{-1}.

Table 1. Transition State Parameters for Phosphine Loss from $Cp^*(PMe_3)_2RuX$

X	T(°C)[a]	k_1(sec^{-1})[b]	$\Delta H^{\ddagger}$ (kcal/mole)[c]	$\Delta S^{\ddagger}$(e.u.)[d]	$\Delta G^{\ddagger}$(100°C) (kcal/mole)[e]
$CH_2C_6H_5$	110	0.900×10^{-2}	38	27	28
	102	0.305×10^{-3}			
	93	0.906×10^{-4}			
	85	0.241×10^{-4}			
I	94	0.310×10^{-3}	36	23	27
	86	0.109×10^{-3}			
	78	0.327×10^{-4}			
	70	0.909×10^{-5}			
C_6H_5	119	0.229×10^{-3}	37	18	30
	110	0.668×10^{-4}			
	102	0.264×10^{-4}			
	86	0.280×10^{-5}			
CH_3	167	0.931×10^{-2}	40	22	32
	126	0.665×10^{-4}			
	118	0.226×10^{-4}			
	110	0.120×10^{-4}			
	103	0.289×10^{-5}			
$C{\equiv}C\text{-}C_6H_5$	167	0.135×10^{-2}	42	22	34
	134	0.155×10^{-4}			
	126	0.900×10^{-5}			
	118	0.333×10^{-5}			
SH	82	0.157×10^{-2}	33	21	25
	78	0.111×10^{-2}			
	70	0.313×10^{-3}			
	62	0.975×10^{-4}			
$CH_2Si(CH_3)_3$	86	0.151×10^{-2}	34	22	26
	79	0.409×10^{-3}			
	70	0.150×10^{-3}			
	62	0.440×10^{-4}			
OC_6H_6	62	0.280×10^{-2}	33	26	23
	54	0.740×10^{-3}			
	42	0.119×10^{-3}			
	30	0.136×10^{-4}			
NHC_6H_5	62	0.209×10^{-2}	28	12	24
	46	0.298×10^{-3}			
	42	0.198×10^{-3}			
	30	0.204×10^{-4}			
Br	86	0.120×10^{-2}	36	29	25
	74	0.241×10^{-3}			

	62	$0.385X10^{-4}$			
	58	$0.125X10^{-4}$			
CH_2COCH_3	103	$0.116X10^{-2}$	36	23	27
	94	$0.415X10^{-3}$			
	86	$0.143X10^{-3}$			
	78	$0.391X10^{-4}$			
	70	$0.124X10^{-4}$			
$N(C_6H_5)_2$	26	$0.400X10^{-2}$	23	9	20
	13	$0.770X10^{-3}$			
	5	$0.199X10^{-3}$			
	-5	$0.376X10^{-4}$			
Cl	78	$0.324X10^{-3}$	33	19	26
	70	$0.208X10^{-3}$			
	58	$0.186X10^{-4}$			
SC_6H_5	78	$0.294X10^{-3}$	32	17	26
	70	$0.154X10^{-3}$			
	58	$0.246X10^{-4}$			
	46	$0.270X10^{-5}$			
OH	46	$0.230X10^{-2}$	29	19	22
	37	$0.526X10^{-3}$			
	28	$0.130X10^{-3}$			
	15	$0.138X10^{-4}$			

Notes: a) ± 1 °C; **b)** ± 2%; **c)** ± 2 kcal/mole; **d)** ± 10 e. u.; **e)** ± 2 kcal/mole

combination of free phosphine with the 16-electron unsaturated intermediates is likely to be a small and fairly constant amount of energy for a variety of complexes, the observed activation enthalpies will be approximately equal to the true bond dissociation enthalpies, see Figure 5. In this case, the differences in activation enthalpies for two such complexes should be about the same as the difference in Ru-P bond strengths. Support for this premise comes from the large positive free entropies of activation noted for all of these dissociations, indicating the importance of "late" (or product-like) transition states for phosphine loss.[17] This interpretation is also consistent with the observation that $k_{-1} >> k_1$ for all derivatives, *ca.* 10^4-10^6 faster.[14]

This assumption of small activation barriers for recombination is most valid for ligands, X, which have no significant π interactions with the transition metal. The transition state parameters for these compounds can be ordered according to steric bulk, as shown in Table 2. These steric trends are as expected based on previously published studies where phosphine steric requirements were varied.[5] If the assumption of small and constant barriers is made, then this constitutes a series of relative Ru–P bond strengths.

Table 2. Steric Trends - No π Interactions

X	$\Delta H^{\ddagger}$ (kcal/mole)	$\Delta G^{\ddagger}$ (100°C) (kcal/mole)	
C≡CPh	42	34	larger
CH_3	40	32	↓
CH_2Ph	38	28	
Ph	37	30	
CH_2SiMe_3	34	26	

When $Cp^*(PMe_3)_2RuMe$ is used as a benchmark for comparison, changing the sigma substituent to the small, rod-like phenylacetylide ligand strengthens the Ru-P interactions by about 2 kcal/mole. Conversely, when methyl is substituted by a slightly larger ligand, such as

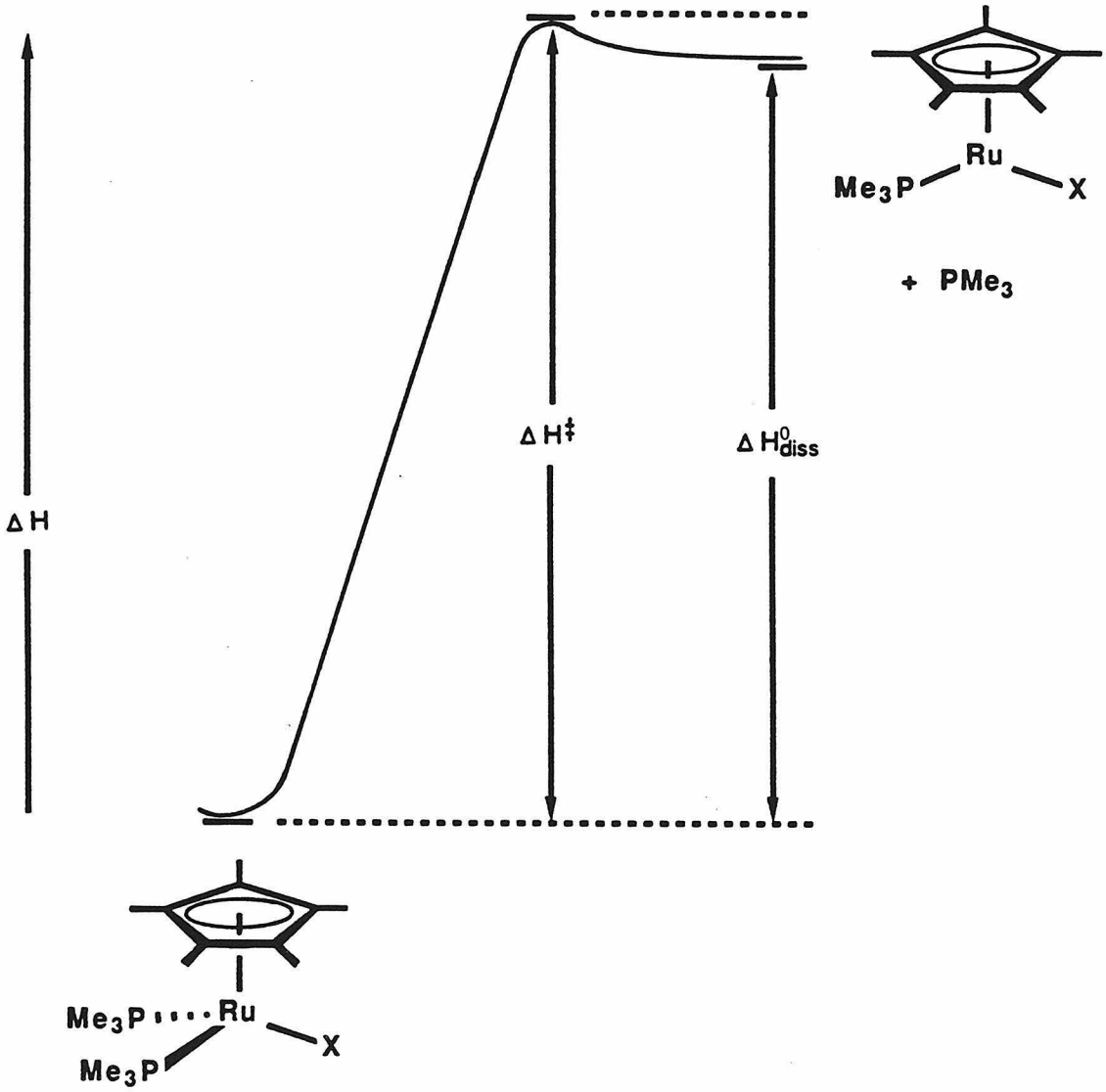

Figure 5. Approximate equivalence of observed activation enthalpy and bond dissociation enthalpy when activation barrier for recombination is small.

benzyl or phenyl, Ru-P interactions weaken by about the same amount. However, when methyl is substituted for something very much larger, CH_2SiMe_3, a *substantial* deviation of more than 6 kcal/mole in the strength of the Ru–P interaction is indicated.[18] These observations suggest the functional group additivity approach to organometallic thermochemistry may be quite appropriate *when substituents of similar sizes are employed. However, our data indicate caution must be exercised when thermodynamic investigations involve ligands of dissimilar sizes.*[19]

The effects of exchanging alkyl substituents for ancillary sigma ligands which contain electron lone pairs, yet which are about the same size, can be seen in Table 3. This π effect can be worth as much as 10 kcal/mole in $Cp^*(PMe_3)_2RuOH$ and $Cp^*(PMe_3)_2RuNHPh$ (*vs* the reference hydrocarbon in each steric series).

The presence of lone electron pairs on the acetone enolate also shows significant (3 kcal/mole) stabilization of the transition state for phosphine dissociation over hydrocarbon derivatives of comparable size. This type of stabilization might approximate the effects of donor solvents on stabilizing the dissociation transition state.

When moving down a triad, as in $Cp^*(PMe_3)_2RuOH$ *vs* $Cp^*(PMe_3)_2RuSH$ and in the series $Cp^*(PMe_3)_2RuX$ (X = Cl, Br, I), changes in transition state stabilizations appear to be only 1-2 kcal/mole, see Table 4. The relatively small energetic differences observed in these cases may, perhaps, be due to the counterbalancing effects of increased steric size and reduced π overlap capabilities of second row main group substituents compared to the first-row main group analogs.

This interpretation assumes that the predominant interaction of ancillary ligand lone pairs is with the transition state, and not with the ground state. Interaction of such lone pairs with the electron-rich and coordinatively saturated ruthenium center appears unlikely.[20] *However, it is not possible to distinguish transition state and ground state effects using these data.* Such

Table 3. Electronic Trends - Similar Sterics

X	$\Delta H^{\ddagger}$ (kcal/mole)	$\Delta G^{\ddagger}$ (100°C) (kcal/mole)
CH_2Ph	38	28
CH_2COCH_3	36	27
OPh	33	23
SPh	32	26
NHPh	28	24
———		
CH_3	40	32
Cl	33	26
SH	33	25
OH	29	22

Table 4. π Overlap Efficiencies

X	$\Delta H^{\ddagger}$ (kcal/mole)	$\Delta G^{\ddagger}$ (100°C) (kcal/mole)
I	36	27
Br	36	25
Cl	33	26

ground state interactions would have to be investigated separately, and are not addressed in this study.

While steric interactions are commonly considered as major factors influencing both dative-[21] and σ-bonded[22] ligand loss, the σ-bonded ligand interaction with the metal center observed in this study has not been previously considered for organometallic complexes. However, such ancillary ligand effects have been studied extensively in coordination complexes.

In octahedral coordination complexes, the sigma *trans* effect has been proposed to be driven by the desire of the *trans* ligand to achieve better orbital overlap in the transition state, *i.e.*, the leaving group shifts out of line with that orbital while the entering group moves in. A π-trans ligand has been proposed to help stabilize the extra electron density on the metal as the new group enters. It is noteworthy that *cis* ligand effects in coordination complexes are quite small.[7] The presence of lone pairs appears to have little effect on such *cis* substitutions, *e.g.*, in *cis*-$(PEt_3)_2Pt(L)Cl$ substitutions the rates vary by less than a factor of three for L = Me^- >C_6H_5->Cl^-.[23]

Conjugate base effects have been observed in the hydrolysis of complexes such as $[(NH_3)_5CoCl]^{2+}$. Halide substitution has been shown to occur by initial deprotonation by OH^- to give an amido complex, $[(NH_3)_4(NH_2)CoCl]^+$, followed by rapid Cl^- loss and trapping by L. The lability of Cl^- is ascribed to the strong labilizing influence of the predominantly *trans* NH_2^- ligand. This could be due to strong π-donation in the pentacoordinate intermediate, $[H_2N{=}Co(NH_3)_4]^{2+}$.[24] Such an effect would appear be similar to that observed for $Cp^*(PMe_3)_2RuX$ complexes with lone pairs. However, evidence in optically resolved amine complexes has been reported which would suggest that this labilization is due to a strong sigma *trans* effect.[25] In addition, loss of negatively charged ligand from a singly charged complex would be easier on electrostatic grounds than loss from a doubly charged complex.

The *cis* sigma ligand in the pseudo-octahedral $Cp^*(PMe_3)_2RuX$ system provides an electronic perturbation on the transition state as large as that induced by steric effects. This observed transition state stabilization appears to have a precedent in organic chemistry. Neighboring groups have been shown to cause large rate increases in the solvolysis of compounds such as alkyl tosylates and halides. The neighboring group displaces the leaving group and stabilizes the resultant carbonium ion, the intermediate is then trapped by solvent. Such effects can lead to rate enhancements of 4-10 orders of magnitude.[26]

Neighboring group participation has been invoked previously in the oxidative addition and reductive elimination reactions of square-planar platinum[27] and iridium[28] complexes. Rate enhancements up to *ca.* 250 fold were observed for complexes containing *o*-methoxyphenyldimethylphosphine and arsine compared to unsubstituted phenyldimethylphosphine and arsine. An interaction a lone pair on the the ligand methoxy group with the transition metal center in the transition state was proposed to explain this difference.

The interaction observed in the $Cp^*(PMe_3)_2RuX$ ligand exchange parameters gives a rate increase of *ca.* six orders of magnitude going from $Cp^*(PMe_3)_2RuOH$ to $Cp^*(PMe_3)_2RuCH_3$. This effect is comparable to that found in organic systems. Even more interesting, though, is that this effect is as important as the commonly considered steric effect in accelerating ligand loss in these compounds. As a great number of ligand loss mechanisms proceed *via* thermally driven reactions, *i.e.*, exothermic reactions with product-like transition states, this effect may be more prevalent than previously realized.

Conclusions

In summary, activation parameters for PMe_3 dissociation in organoruthenium complexes, $Cp^*(PMe_3)_2RuX$, have been obtained as a function of varying X. This has allowed an assessment of both steric and electronic effects on the transition state for this process. A late

transition state is proposed in which the metal center interacts with lone pairs on the σ-bonded ligand. This neighboring group effect is found to increase rates by *ca.* six orders of magnitude for systems of comparable steric size and provides quantitative evidence for the general perception that both sterics and electronics can play an important role in dative ligand dynamics. In addition, the effectiveness of steric congestion in weakening Ru-P bonds suggests great care must be exercised when applying the functional group additivity assumption to thermochemical investigations in organometallic systems.

Experimental

General Considerations: All syntheses and chemical manipulations were carried out in a Vacuum Atmospheres HE-453 drybox equipped with either nitrogen purge or oxygen/water scrubbing recirculation "Dri-Train" or by high vacuum and Schlenk techniques.

Benzene-d_6, and toluene-d_8 were purified by vacuum distillation from sodium followed by storage in the drybox over activated (450xC, 2 hrs) 4 Å molecular sieves. *O*–xylene-d_{10}, mesitylene-d_{12} and tetralin-d_{18} were pre-dried in the drybox over activated molecular sieves but were not distilled from sodium. CD_3I and $^{13}CH_3I$ were used as obtained from Merck. PMe_2Cl was used as obtained from Strem and P(O-*p*-tolyl)$_3$ was used as obtained from Kodak. Dibutyl ether was used as obtained from Aldrich.

NMR spectra were recorded on Nicolet NT-series spectrometers operating at 300 and 360 MHz proton frequencies, respectively. Variable temperature measurements were conducted in NMR probes calibrated with a chromel-alumel thermocouple which was, in turn, calibrated at 100°C and 0°C with water. Physical measurements were acquired using Wilmad #507-TR screw-capped NMR tubes with teflon lined neoprene septa. Tubes were loaded in the drybox using a Mettler AE160 balance (+0.1 mg). The phosphine and syringes used were cooled to prevent losses during transfer. Total volume in the tube was calculated from the solution height in these calibrated tubes using the relationship: volume (μL) = height (mm) X 14.00 +

5.55, which was determined by a least squares fit of volume vs height data involving Hamilton microliter syringes. T_1s data were acquired with Nicolet (GE) spin-inversion/recovery pulse sequences and data analysis software. A combination of timed kinetic and NOE-suppressed (decoupler on during acquisition, off during recycle) pulse sequences were used to acquire NOE suppressed kinetics information on ligand exchange. A synthetic mixture of $Cp^*(PMe_3)_2RuSH$, $Cp^*(P(CD_3)_3)_2RuSH$, PMe_3 and $P(CD_3)_3$ was used to check the pulse sequence to confirm negligible NOE differences. Spectra were acquired using 90° pulses with 60 second pulse delays (approximately 5 T_1s between pulses). Data were collected using aromatic deuterated solvents as described above. Benzene-d_6 was used from 20 to 60°C while toluene-d_8 was used from 60 to 90°C. *O*-xylene-d_{10} was employed from 90 to 120°C and mesitylene-d_{12} was the solvent of choice from 120 to 140°C. Above 140°C decalin-d_{18} was used. The temperature ranges used to study the individual compounds are listed in Table 1.

Concentration vs time data were analyzed by fitting the data to the dissociative kinetic model of this exchange shown in eq 4 using GIT software on a Vax 8650. This software is an iterative program based on the original HAVECHEM[29] programs. Eyring analysis of the kinetics data was done using ARH2 software[16] on a Vax 8650. This version fits a logarithmic function to the data to avoid artifacts sometimes realized in linear fits of log data. RS/1 software was used to format the data into the expected inputs for these programs.

Synthesis of $^{13}CH_3PMe_2$: This complex was prepared in the drybox. Freshly prepared $^{13}CH_3MgI$ was prepared by dissolving Mg into a dibutyl ether solution containing $^{13}CH_3I$. This solution was added to a cold dibutyl ether solution of PMe_2Cl and stirred for 30 minutes as the solution warmed to ambient temperature. The resulting phosphine was distilled twice to remove all traces of butyl ether.

Synthesis of $(CD_3)_3P$: This perdeuterophosphine was prepared by adding a freshly prepared solution of CD_3MgI to tri-*p*-tolyl phosphite in dibutyl ether. The mixture was stirred for an hour

at 25°C and then the resulting phosphine was distilled at atmospheric pressure. The crude phosphine was redistilled to remove all traces of impurities.

Phosphine Exchange Kinetics: In the drybox a screw-capped Wilmad #507-TR 5 mm NMR tube was charged with 15-20 mgs $Cp^*(PMe_3)_2RuX$. Benzene-d_6 (approximately 600 μL) was added by pipette and the tube was capped and reweighed. The entire assembly was cooled in a drybox freezer, along with a 100 μL syringe and the $P(CD_3)_3$. After 30 minutes these items were removed from the freezer. The tube weight was rechecked and then $P(CD_3)_3$ was added, by syringe, and the tube was reweighed. The total solution volume in the tube was determined by height. The tube was placed in a pre-equilibrated 40°C NMR probe and shimmed as thermal equilibrium was attained (approximately 15 minutes). Spectra were acquired and the concentrations of species (Ru-PMe_3, Ru-$P(CD_3)_3$, PMe_3(soln), and $P(CD_3)_3$(soln)) were determined over the same region of each spectrum by an automated series of GR and DR integration routines on the Nicolet spectrometers. The time of each spectrum was similarly recorded along with the data by the internal clock on the spectrometer. This concentration vs time data was simulated with GIT software to obtain the phosphine dissociation rate constant. Dissociation rates of all the ruthenium complexes at a variety of temperatures were measured by this same method.

References

1) Bryndza, H. E.; Fong, L. K.; Paciello, R. A.; Tam, W.; and Bercaw, J. E. *J. Am. Chem. Soc.*, **1987**, *109*, 1444.

2) Tilley, T. D.; Togni, A., Paciello, R. A.; Bercaw, J. E.; and Grubbs, R. H. manuscript in preparation

3) Merola, J. and Bercaw, J. E. unpublished results

4) Bray, R. G.; Bercaw, J. E.; Gray, H. B.; Hopkins, M. D.; Paciello, R. A. *Organometallics*, **1987**, *6*, 922

5) For an overview see: Tolman, C. A. *Chem. Rev.*, **1977**, *77*, 313

6) Martinho Simoes, J. A.; Beauchamp, J. L. *Chem. Rev. in press*

7) See, for example: Langford, C. H. and Gray, H. B. "Ligand Substitution Processes", W. A. Benjamin, Inc., Reading, Massachusetts, **1966**

8) a) Egger, J. W. *J. Organomet. Chem.*, **1970**, *24*, 501: b) Vaska, L.; Werneke, M. F. *Trans. N. Y. Acad. Sci., Ser. 2*, **1971**, *33*, 70: c) Tolman, C. A. *J. Am. Chem. Soc.*, **1974**, *96*, 2780: d) Halpern, J.; Ng, F. T. T.; Rempel, G. L., *Ibid.*, **1979**, *101*, 7124: e) Nappa, M. J.; Santi, R.; Diefenbach, S. P.; Halpern, J. *Ibid.*, **1982**, *104*, 619: f) Ng, F. T. T.; Rempel, G. L.; Halpern, J. *Ibid.*, **1982**, *104*, 621: g) Tsou, T.–T.; Loots, M.; Halpern, J. *Ibid.*, **1982**, *104*, 623: h) Drago, R. S.; Miller, J. G.; Hoselton, M. A.; Farris, R. D.; Desmond, M. J. *Ibid.*, **1983**, *105*, 444: i) Jones, W. D.; Feher, F. J. *Ibid.*, **1984**, *106*, 1650: j) Janowicz, A. H.; Periana, R. A.; Buchanan, J. M.; Kovac, C. A.; Stryker, J. M.; Wax, M. J.; Bergman, R. G. *Pure & Appl. Chem.* **1984**, *56*, 13: k) Jones, W. D.; Feher, F. J. *J. Am. Chem. Soc.* **1985**, *107*, 620: l) Bergman, R. G. *Science* **1984**, *223*, 902: m) Bruno, J. W.; Marks, T. J.; Morss, L. R. *J. Am. Chem. Soc.* **1983**, *105*, 6824: n) Bryndza, H. E.; Fultz, W. C.; Tam, W. *Organometallics* **1985**, *4*, 939: o) Buchanan, J. M.; Stryker, J. M.; Bergman, R. G. *J. Am. Chem. Soc.*, **1986**, *108*, 1537

9) Sometimes called the "Benson Approximation" in reference to the successful approach to organic thermochemistry outlined in Benson, S. W. "Thermochemical Kinetics, 2nd Ed.", **1976**, Wiley-Interscience, New York

10) a) See ref. 1: b) Tilly, T. D.; Grubbs, R. H.; Bercaw, J. E. *Organometallics*, **1984**, *3*, 274

11) The concentrations of labelled free $P(CD_3)_3$ cannot be determined in this system by simple integration and estimates of this quantity by difference suffer from not taking into account the rates (or final levels) of phosphine leaving the solution for the gas phase. Neither can the assumption that this effect will be constant for all systems studied be made; obtaining activation parameters for even one derivative requires rate studies at a variety of temperatures. The $PMe_{3(soln)} \rightleftharpoons PMe_{3(gas)}$ equilibrium

clearly depends on temperature (*vide infra*). These limitations require the accurate determination of all important solution phase concentrations by ^{31}P NMR.

12) A combination of standard Nicolet KINET and 1PDNA pulse sequences were used.

13) GIT developed as an gear integration package from Havchem by Dr. F. J. Weigert at DuPont CR&D.

14) As long as the k_{-1} values were at least 10^4-10^6 faster than the dissociation rate the data are adequately explained by the kinetic model. This is reasonable since, while the concentration of the intermediate is never measured, the inability to observe such species indicates they are extremely short lived in the presence of phosphine.

15) As is usual for an Eyring treatment, κ was assumed equal to 1. For a discussion of the Eyring equation and a comparison to use of the Arrhenius equation see: Sandstrom, J. "Dynamic NMR Spectroscopy", Academic Press, London, 1982, chapt. 7

16) Eyring treatment was done using a program developed locally at DuPont by R. Farlee and D.C. Roe. The data were fit by using a logarithmic function on the actual data to avoid weighting the data.

17) Lowry, T. H.; Richardson, K. S. "Mechanism and Theory in Organic Chemistry, Second Ed." Harper and Row, New York, **1981**, 197

18) Although there may be differences in ground state or transition state hyperconjugative stabilizations due to the different alkyl and hydride ligands, the similarities of Ru-P bond strengths in the ruthenium benzyl, phenyl, methyl and phenylacetylide complexes suggests any such differences are insignificant compared to the magnitude of changes made by steric differences.

19) This observations suggests, for example, the apparent thermodynamic stability of L_nM-H bonds, relative to L_nM–CH_3 linkages, noted in a number of studies may be due, in large part, to other bonds in those hydrides becoming stronger than in the methyl analogs. In effect the hydride complexes may be more thermodynamically stable than alkyls but this is not necessarily due to M-H being particularly strong.

20) It could be proposed that such an interaction might occur if backbonding to empty PMe_3 d–orbitals takes place. Such $d\pi$-$d\pi$ backbonding, while important for PF_3 and possibly $P(OR)_3$ derivatives, does not appear to be an important interaction for alkyl phosphines, PR_3, in general, and should be especially insignificant in these *cis* complexes. Collman, J. P.; Hegedus, L. S. "Principles and Applications of Organotransition Metal Chemistry" University Science Books, Mill Valley California, **1980**, p. 54

21) Tolman, C. A. *Chem. Rev.*, **1977**, *77*, 313

22) Halpern, J. *Inorg. Chim. Acta*, **1985**, *100*, 41

23) Basolo, F.; Chatt, J.; Gray, H. B.; Pearson, R. G.; Shaw, B. L. *J. Chem. Soc.*, **1961**, 2207

24) Basolo, F.; Pearson, R. G. "Mechanisms of Inorganic Reactions", Wiley, New York, **1958**, chapt. 3

25) Buckingham, D. A.; Marzilli, P. A.; Sargeson, A. M. *Inorg. Chem.*, **1969**, *8*, 1595

26) Carey, F. A.; Sundberg , R. J. "Advanced Organic Chemistry" Plenum, New York, **1977**, vol. A,pg 229

27) Constable, A. G.; Langrick, C. R.; Shabanzadeh, B.; Shaw, B. L. *Inorg. Chim. Acta*, **1982**, *65*, L151

28) Miller, E. M.; Shaw, B. L. *J. C. S. Dalton*, **1974**, 480

29) Stabler, R. N.; Chesnick *J. Int. J. Chem. Kinet.*, **1978**, *10*, 461